USING MULTILEVEL SAMPLERS TO ASSESS ETHANOL FLUSHING AND ENHANCED BIOREMEDIATION AT FORMER SAGES DRYCLEANERS

BY

GORDON HITCHINGS BROWN

A THESIS PRESENTED TO THE GRADUATE SCHOOL
OF THE UNIVERSITY OF FLORIDA IN PARTIAL FULFILLMENT
OF THE REQUIREMENTS FOR THE DEGREE OF
MASTER OF SCIENCE

UNIVERSITY OF FLORIDA

2006

ACKNOWLEDGEMENTS

This research effort was funded by The Strategic Environmental Research and Development Program (SERDP). This program is the Department of Defense's (DoD) environmental science and technology program, planned and executed in full partnership with the Department of Energy and the Environmental Protection Agency. The views and conclusions contained herein are those of the author and should not be interpreted as representing the U.S. Government agencies.

The faculty and staff of the University of Florida's Department of Environmental Engineering Sciences have been instrumental in the completion of this project. There were many people responsible for the field sampling and laboratory analysis, including Randy Sillan, Gloria Sillan, Irene Poyer, and M. Zhou. The data analysis process was assisted by Jaehyun Cho. Christina Akly provided help with figures and formatting.

For their expertise, support, and encouragement, the author would like to acknowledge his committee co-chairs, Mike Annable and Jim Jawitz. Their patience, open door policies, and guidance were invaluable in this effort. Also, Joe Delfino was the remaining member of his committee and his sharp editing was highly important. All three committee members' courses related to this research were also invaluable to the author's ability to understand and analyze the data and results.

Finally, I would like to thank my family for all their years of support, encouragement, and relentless exposure to nature and science while I was growing up.

TABLE OF CONTENTS

LIST OF TABLES

LIST OF FIGURES

ABBREVIATIONS

PCE	perchloroethylene, tetrachloroethene, or perc
TCE	trichloroethylene or trichloroethene
DCE	dichloroethene
VC	vinyl chloride
DNAPL	dense non-aqueous phase liquid
NAPL	non-aqueous phase liquid
VOC	volatile organic chemical
bgs	below ground surface
MLS	multi-level sampling well
RW	recovery or extraction well
IW	injection well
PITT	partitioning interwell tracer test
BTC	breakthrough curve
ISB	in situ bioremediation
SERB	solvent extraction residual biotreatment
MCL	maximum contaminant limit
RBCA	risk-based corrective action
CDF	cumulative distribution function
FNR	fractional NAPL removal
ENR	estimated NAPL removal
FFR	fractional flux reduction
IFT	interfacial tension

Abstract of Thesis Presented to the Graduate School
of the University of Florida in Partial Fulfillment of the
Requirements for the Degree of Master of Science

USING MULTILEVEL SAMPLERS TO ASSESS ETHANOL FLUSHING
AND ENHANCED BIOREMEDIATION AT FORMER SAGES DRYCLEANERS

By

Gordon Hitchings Brown

August 2006

Chair: Michael D. Annable
Cochair: James W. Jawitz
Major Department: Environmental Engineering Sciences

As a result of dry cleaning operations, there are hundreds of sites where the subsurface aquifer has been contaminated by perchloroethylene (PCE), the dry cleaning agent. One of the more challenging problems facing environmental scientists and engineers today is locating PCE source areas and cleaning up these sites to reduce the risk of contaminated groundwater reaching water supplies. The high specific gravity, low solubility, and recalcitrance make PCE highly persistent in the environment. Without some remedial action, many of these sites would serve as a source of dissolved groundwater contamination for decades. The Sages former drycleaning site in Jacksonville, FL, was the test ground for a pilot scale in-situ alcohol flushing test in 1998. The sandy aquifer was contaminated with PCE, found as a separate phase in discrete layers in the subsurface.

A network of multilevel sampling wells (MLS) was installed in the source area to collect liquid samples before, during and for six years after the pilot test. The depth level sampling of MLS allows three dimensional spatial analyses. Multilevel samples were able to determine the initial and post-remedial PCE architecture at the site. This information will help the site manager

target residual PCE for future corrective action. Site characterization determined that hydraulic conductivity decreased with depth. Thus, ethanol flushing encountered the difficulty getting high concentrations to the deep, low flow zones. Furthermore, once remedial fluids penetrated the lower depths, they were difficult to recover in the pumping rate and time frame of this test.

The remedial performance was evaluated through comparison of pre and post-remedial groundwater samples and partitioning tracer tests. The ethanol flushing test was effective at removing significant levels of subsurface PCE and favorably reduced the contaminant flux at most MLS locations.

One of the benefits of using ethanol as the remedial fluid was the fostering of microbial reductive dechlorination of residual PCE. Ethanol served as an electron donor in biodegradation. From long term transect monitoring, the mass discharge of the source zone and downgradient control plane were determined. Once higher levels of unrecovered ethanol were carried away by natural gradient flow, microbial activity spiked up until four years after the 1998 event. Then, dechlorination declined rapidly as all the ethanol was exhausted by microbes or removed by groundwater flow. While residual PCE dissolution was microbially enhanced, significant PCE remained in the source zone at the end of this study. Therefore, another combined effort took place at the conclusion of this study in 2004 with a second full scale ethanol flushing.

The combination of enhanced solubililization and residual source biotreatment was effective at removing significant PCE mass, reducing PCE flux, and fostering bioremediation in the source zone and plume. This combined technology will serve to decrease source strength and longevity for sites meeting the proper criteria. Clean up and site closure will occur much faster than natural gradient dissolution and plume control via a pump-and-treat system.

CHAPTER 1
INTRODUCTION AND BACKGROUND

1.1 Project Introduction

The Sages former drycleaning site in Jacksonville, FL was the test ground for a pilot scale in-situ alcohol flushing test in 1998. The groundwater at the site was contaminated with the drycleaning chemical perchloroethene, (PCE), also called tetrachloroethylene and perc. PCE was found in discrete layers in the sandy aquifer. Four previous studies have been published about the Sages site. The first two papers studied the NAPL removal effectiveness of the 1998 alcohol flushing test [*Sillan*, 1999; *Jawitz et al*., 2000]. Next, the bioremediation of residual PCE stimulated by the unrecovered ethanol was studied by the US EPA in the three years after the pilot test [*Mravik et al*., 2003; *Sewell et al*., 2006].

This thesis presents the analysis of data from multilevel sampling wells installed in the PCE source zone and up to ten meters downgradient. These wells consist of bundles of smaller stainless steel tubes each installed to a different depth, allowing the collection of discrete vertical liquid samples normally diluted in standard well screen intervals. In the remedial zone, the spatial distribution of initial groundwater concentrations of PCE, partitioning interwell tracer tests, ethanol flushing, and post-remedial groundwater concentrations of PCE and ethanol were obtained by sampling the multilevel well depths. After the ethanol flushing test, long term monitoring commenced in the source zone and the additional downgradient multilevel wells. Semi-annual sampling was conducted to monitor contaminant concentrations and to estimate contaminant mass discharges out of the site over the six-year period from 1998-2004.

Much of the data presented in this thesis was collected in the period prior to this author's contributions. Field sampling continued in 2003 and 2004 while the author analyzed the results

of all the previous data. The termination of this study occurred when the second phase of remediation, a full scale ethanol flushing, was initiated in July 2004.

1.2 Motivation for the Project

The Sages site is currently abandoned but was operational from 1968-1973 and from 1979-1989. The suspected source of PCE, a dense non-aqueous phase liquid (DNAPL), was a floor drain at the site [*Levine-Fricke Recon (LFR)*, 1997; *Sillan*, 1999; *Jawitz et al*., 2000]. The high specific gravity of PCE caused it to flow downward by gravity drainage, through the highly sandy media. The subsurface region containing PCE was subject to groundwater flow, generating a dissolved contaminant plume flowing downgradient. The area containing free phase PCE is referred to as the source zone, consisting of PCE pools collecting on lenses of finer grained materials and residual PCE entrapped by the capillary forces in the subsurface media. The source zone was approximately 7.3 m long by 2.7 m wide and existed from 7.9 to 9.6 m below the ground surface (bgs) [*LFR*, 1997; *Sillan*, 1999; *Jawitz et al*., 2000]. Although hydraulic conductivity estimates are high in the mostly sandy media, the hydraulic gradient is very small such that local groundwater velocity is very slow. The low solubility of PCE combined with the low groundwater velocity would generate a contaminated groundwater plume for decades or centuries if depletion of entrapped and pooled DNAPL was strictly by natural gradient dissolution [*Kueper et al*., 1993; *Lemke et al*., 2004].

In 1998, the Florida Department of Environmental Protection (FDEP), Levine Fricke, Inc. (LFR), and the University of Florida conducted a pilot-scale ethanol flushing test to evaluate the enhanced removal of PCE at Sages field site. A mixture of 95% food grade ethanol and 5% water was injected into the subsurface and recovered through a hydraulically controlled remedial

flow field. The project also served as a pilot test of solvent extraction residual biotreatment (SERB) technology [*Mravik et al*., 2003; *Sewell et al*., 2006].

Recently, scientists and engineers have defined a need for data and analyses of DNAPL source zone depletion technologies and the resultant changes in site mass flux and mass discharge [*USEPA*, 2003; *Stroo et al*., 2003; *NRC*, 2005]. The research presented in this thesis evaluates the multilevel well samples taken during the pilot remediation and the six-year period after the flushing until 2004. The primary goals of this work are to define the DNAPL architecture in the source zone before and after the flushing test, to assess the remedial performance in terms of NAPL removal and flux reduction, and to evaluate the groundwater plume response in terms of the mass discharge changes over time after the remedial test.

1.3 Multilevel Sampling

The use of multi-level sampling (MLS) wells for groundwater study delivers a vertical resolution of the subsurface fluids that traditional wells dilute or integrate over their screened interval. Bundled MLS piezometers consists of a cluster of small stainless or Teflon tubes inserted into the ground at designed intervals to pump small groundwater samples at each respective depth [*Pickens et al*., 1978; *Lerner and Teutsch*, 1995]. There is a sand filter on the in-ground end of each tube to prevent clogging. MLS wells have been used at contaminated sites for various groundwater monitoring purposes including natural dissolution, plume development, and remedial assessment [*Lerner and Teutsch*, 1995; *Sillan et al*., 1997; *Broholm et al*., 1999; *Jawitz et al*., 2000; *Rivett et al*., 2001; *Gauilbeault et al*., 2005; *Rivett and Feenstra*, 2005; *Zhang et al*., 2006]. Additionally, MLS have been employed to elucidate the spatial distribution of NAPL from partitioning tracer tests at several field sites [*Rao et al*., 2000].

At the Sages site, bundled MLS wells were employed to add a vertical component to remediation and monitoring studies for three dimensional analyses. A month prior to the August 1998 ethanol flood, MLS 1-7 were installed in the source zone, each coupled to a respective RW. During sampling, each MLS well tube was pumped and purged to 40 mL before the sample was collected. The samples were analyzed by gas chromotagraphy for alcohol tracers, ethanol, and volatile organic chemicals (VOCs). The map below in Figure 1-1, displays the locations of the MLS wells at the Sages site in Florida State Plane Coordinate System units.

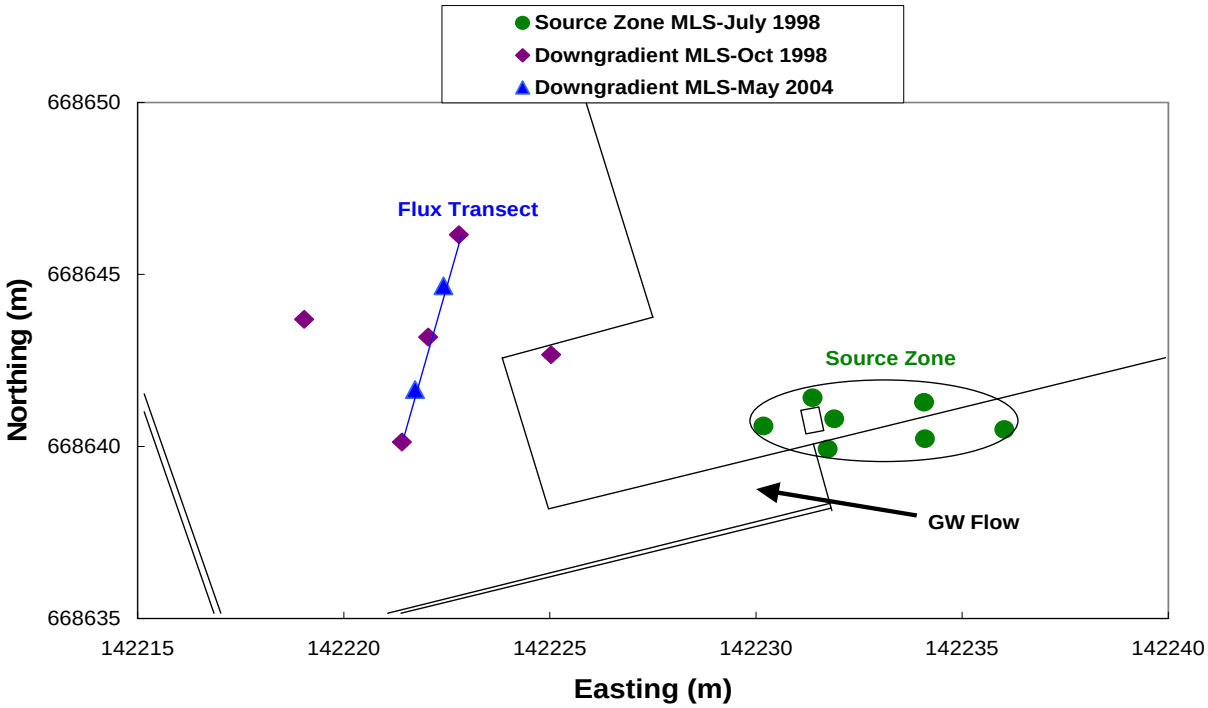

Figure 1-1. Map view of Sages site multilevel sampling wells (units are Florida State Plane Coordinate System). The gray area is the suspected source zone.

For the tracer tests and the ethanol flood, only the seven source zone multilevel wells (MLS 1-7) were in place to collect samples. After the flushing test, five additional multilevel wells (MLS 8-12) were installed downgradient of the source area to monitor the contaminant

plume, including a transect of wells perpendicular to the natural gradient flow (MLS 9-11). Finally in 2004, two additional MLS wells (13 & 14) were installed in the downgradient transect, between the central and outer wells.

1.4 The DNAPL Problem

As a result of many industrial, military, and commercial practices, there are thousands of sites of subsurface contamination by the chemicals used at these places. One of the more challenging problems facing environmental engineers and scientist today is finding and cleaning up these sites to reduce the risk of contaminated groundwater reaching water supplies. DNAPLs often exist as a separate liquid phase in groundwater. Due to their high specific gravity (>1.2), they flow downward by gravity drainage when spilled or released into soil and groundwater [*McKay and Cherry*, 1989; *Broholm et al*., 1999]. They tend to collect on less permeable layers spreading out until meeting courser media to continue downward flow in fingers rather than a uniform front [*Illangasekare et al*., 1995].

To assess a DNAPL contaminated site, the architecture of the source must be identified [*Sale and McWhorter*, 2001; *Rao et al*., 2002]. This refers to the geometry of the source in terms of shapes, sizes, and interconnections of the spatial distribution and DNAPL content in the subsurface. Generally, a DNAPL site is described as a source zone and a dissolved plume [*Rao et al*., 2002; *NRC*, 2005]. The region of the site with separate phase DNAPL is termed the source zone. This is further separated into the areas of entrapped residual saturation, or ganglia, and pools of accumulated DNAPL on confining units [*McKay and Cherry*, 1989; *Kueper et al*., 1993; *NRC*, 2005]. Pooling can lead to diffusion into the aquitard [*Parker et al*., 2004]. Entrapped residual DNAPL is held in pore spaces by capillary forces or as films coating the media [*Bradford et al*., 2003].

As groundwater flows through a source zone, small amounts of DNAPL are dissolved and carried away in a plume of contaminated water. Advection and dispersion forces tend to dilute and spread this plume as it moves away from the source area. However, the low solubility of most DNAPLs makes them highly persistent and the DNAPL acts as a reservoir for sustaining dissolved plumes. Thus, media heterogeneities, sorption to subsurface media, and diffusion into low permeable layers makes DNAPL source zones highly complex and unique at each site.

Another difficulty of DNAPL cleanup efforts is finding the source of groundwater contamination. Although sufficient technologies exist to delineate a source zone, some sites will require extensive sampling due to the spatial distribution of free phase DNAPL in the subsurface [*EPA*, 2003]. Since deposits can be highly localized, multiple methods should be used to locate the source of dissolved contamination. Therefore, it is important to perform accurate, detailed site characterization including hydrogeology, source delineation, and biogeochemistry to best assess site risk and to develop to the proper treatment regimen for the specific site [*NRC*, 2005].

Unfortunately, due to their low solubility and recalcitrance many of the sites contaminated with these compounds will persist for decades or centuries. Although conventional pump-and-treat measures can contain the dissolved plume and slightly enhance DNAPL dissolution, there would be great cost to implement and maintain this type of treatment for the long timescales required [*McKay and Cherry*, 1989; *NRC*, 2005]. Thus, innovative methods to remove DNAPLs have been devised and tested over the past two decades, including enhancements of aqueous solubility, mobility, volatility, and biodegradation. Many of these new technologies are highly successful at removing DNAPL mass from the subsurface. However, due to the complex entrapment architecture of field sites, complete removal of free phase and residual DNAPL has been thus far not possible [*Soga et al*., 2004]. Consequently, remediation at

very few sites has been unable to remove sufficient mass to restore the entire site to drinking water standards [*NRC*, 2005]. Although most DNAPL sites currently have pump-and-treat systems in place to contain contaminant plumes, only a small fraction of sites have attempted aggressive source remediation [*NRC*, 2005].

1.5 Natural Dissolution of DNAPLs

Understanding the dissolution of nonpolar compounds in groundwater is vital to predict the persistence of a DNAPL source zone. The saturated equilibrium concentration (C_{iw}^{sat}) of chemical (i) in water is related to its activity coefficient (γ_{iw}^{sat}) by Eq.1-1 [*Schwarzenbach et al*., 2002].

$$C_{iw}^{sat} = \frac{1}{\overline{V}_w \cdot \gamma_{iw}^{sat}} \tag{1-1}$$

The chemical solubility is inversely proportional to the product of the activity coefficient of the chemical of interest and the molar volume of water ($\overline{V}_w$) which is constant. Most of the nonpolar organic compounds like PCE have high activity coefficients and so they are highly insoluble [*MacKay et al*., 1991].

Natural gradient dissolution of PCE and other DNAPLs has been studied extensively over the past 3 decades. Many laboratory physical models and computer models have attempted to describe DNAPL dissolution [*MacKay et al*., 1985; *MacKay et al*., 1991; *Unger et al*., 1998; *Sahloul et al*., 2002; *Bradford et al*., 2003; *Parker and Park*, 2004]. However, field conditions are considerably more heterogeneous than lab or model conditions, making the process extremely complex.

Researchers at the University of Waterloo have conducted recent field studies of controlled releases of multicomponent DNAPLs into the Borden aquifer to better understand

deposition morphology and dissolution behavior in natural media [*Broholm et al*., 1999; *Frind et al*., 1999; *Rivett et al*., 2001; *Broholm et al*., 2005; *Rivett and Feenstra*, 2005]. Rivett and Feenstra [2005] monitored the dissolution and plume development of an emplaced multicomponent DNAPL source in a natural sandy aquifer. Both source mass and source strength were monitored over a three year period by soil coring and a downgradient multilevel sampling well transect. Dissolution fingering and groundwater flow bypass resulted in 77% of the source mass remaining after 3 years and they predicted source longevity of 25 years. Pooling and entrapment in low permeable media fostered lower hydraulic conductivity zones, leading to groundwater flow bypassing. The study predicted that as pores are cleaned out by dissolution, additional bypassing will follow these new DNAPL free paths [*Rivett and Feenstra*, 2005].

This process is called aging. Over time, many groundwater flow paths are cleaned out by dissolution. The flow paths still containing higher residual or pooled DNAPL will divert groundwater flow around these zones, making them diffusion limited [*NRC*, 2005]. The aging process may reduce plume concentration but may also increase source longevity since groundwater preferentially flows through cleaner, higher conductivity paths. As Sages began operation as a drycleaning facility in 1968, the single component PCE spills may have occurred many years ago. The low groundwater velocity has limited the natural dissolution of subsurface PCE. However, many flow paths may have been cleaned out by dissolution over time, making Sages an aged DNAPL site.

Because PCE is very slowly solubilized by groundwater flow, scientists and engineers have been researching means to enhance the dissolution process. One of these methods is in situ alcohol flushing.

1.6 Cosolvency and Alcohol Flushing

It has been demonstrated that adding a cosolvent to an oil-water system will increase the aqueous solubility of the oil [*Nkedi-Kizza et al*., 1987; *Banerjee and Yalkowsky*, 1988]. An alcohol will decrease the polarity of the water, allowing the nonpolar organic compound to dissolve more readily [*Augustijn et al*., 1997]. The relationship of the cosolvent in the aqueous phase to the solubility of the hydrophobic compound was described by Rao et al. [1990].

$$\log S_{imix} = \log S_{iw} + \beta_i \cdot \sigma_i \cdot f_c \qquad (1\text{-}2)$$

The log of the solubility of component *i* in the cosolvent-water mixture (S_{imix}) is equal to the sum of the log of the aqueous solubility of *i* (S_{iw}) and the product of the water-cosolvent interaction (β_i), the cosolvency power of the solvent for *i* (σ_i), and the volume fraction of cosolvent (f_c). For most completely miscible organic solvents (CMOS), β = 1.0.

The cosolvency power (σ_i) is defined by Eq.1-3, where S_{ic} is the solubility of *i* in pure cosolvent [*Rao et al*., 1990].

$$\sigma_i = \log\left(\frac{S_{ic}}{S_{iw}}\right) \qquad (1\text{-}3)$$

This is the most important parameter in cosolvency theory. There is a well validated linear relationship between the interfacial free energy of the cosolvent and the molecular surface area of the hydrophobic organic compound [*Banerjee and Yalkowsky*, 1988]. Thus, the solubility of solute *i* increases with decreasing solvent polarity.

Due to costs and duration for conventional pump-and-treat systems for plume control at DNAPL sites, enhanced dissolution techniques are desirable. One of these methods is cosolvent flushing, in particular using alcohols as the solubility enhancement agent. This has been called a variety of terms like cosolvent flooding, enhanced pump-and-treatment, enhanced dissolution,

but for this paper it will be referred to as in-situ alcohol flushing or ethanol flooding. Alcohol flushing has been demonstrated to be an effective method for enhancing the removal of DNAPLs from sand in laboratory tests and from the subsurface in sandy aquifers [*Augustijn et al*., 1994; *Imhoff et al*., 1995; *Augustijn et al*., 1997; *Rao et al*., 1997; *Sillan et al*., 1998; *Jawitz at al*., 2000; *Falta et al*., 2000; *Brooks et al*., 2003].

There is always a risk of mobilization when using alcohols as the cosolvent for in-situ flushing [*Lunn and Kueper*, 1999; *Padgett and Hayden*, 1999]. Ethanol was chosen by LFR [1998] from ternary phase diagrams because it exponentially increases PCE solubility but provides a lower risk of PCE mobilization [*Falta*, 1998]. Shorter chain alcohols tend not to lower the interfacial tension (IFT) associated with entrapped DNAPL, reducing the binding capillary forces. Thus, the risk of IFT reduction and downward mobilization of DNAPL during flushing is reduced when employing ethanol as the solubilization enhancing agent [*Lunn and Kueper*, 1999].

1.7 Site Characterization

The hydrogeology of the Sages site was characterized by soil cores, pumping tests, water table levels, and an electromagnetic borehole flowmeter test. The results will be summarized here but extensive studies at the site have been performed and published [*LFR*, 1997, 1998a, 1998b; *Sillan*, 1999; *Jawitz et al*., 2000; *Mravik et al*., 2003]. The water table is approximately 3 m bgs, and the natural hydraulic gradient is 0.0025. The media was characterized to be fine to very fine sand down to 9 m bgs. In the lower zone, from 9 m to 10.7 m, very fine to silty sand was observed down to the discontinuous clay layer at 10.7 m bgs. Hydraulic conductivities were estimated at 6 m/day in the upper region and 3 m/day in the lower. Combined with the low

hydraulic gradient, groundwater velocity is very slow, from 0.0075 to 0.015 m/day (see Eq. 1-12).

The standard methods for source zone characterization include soil coring, direct push methods, geophysical methods, downhole methods, and tracer tests [*NRC,* 2005]. An effective method of estimating the mass of DNAPLs in a source zone is the partitioning interwell tracer test (PITT) [*Jin et al.,* 1995*; Annable at al.,* 1998]. At the Sages site, the PCE source zone was characterized through soil coring, cone penetrometer tests, and partitioning interwell tracer tests.

In the site evaluation process, it was deemed that Sages was not a good candidate for natural attenuation of chlorinated solvents [*LFR*, 1997]. Based on the criteria put forth by Weidemeier et al. [1996], the biodegradation potential of the groundwater at Sages was considered inadequate for natural attenuation. The LFR survey concluded that reductive dechlorination was not favored by aerobic conditions, low levels of dechlorination daughter products, and lack of sulfate reduction and methane production [*Sewell et al*., 2006]. Thus, a coupled site restoration method was developed to aggressively remove source PCE mass, while facilitating subsurface microbial processes. The US EPA continued to monitor the site following the 1998 ethanol flood for three years at monitoring wells throughout the site. Its assessment is available in Mravik et al. [2003], and Sewell et al. [2006].

1.8 Partitioning Tracer Tests

The development and implementation of a subsurface chromatographic means to determine DNAPL mass and volume is highly advantageous. The partitioning interwell tracer test (PITT) method is well established and described in both laboratory tests [*Jin et al.,* 1995; *Cho and Annable*, 2005] and field tests [*Annable et al*., 1998; *Jawitz et al*., 1998; *Dwarakanath et al*., 1999; *Setarge et al*., 1999, *Rao et al*., 2000; *Brooks et al*., 2002]. Around or across a

suspected source zone, a hydraulic flow field is established using injection wells (IWs) and recovery wells (RWs) [*Annable et al*., 1998]. A suite of alcohol tracers, including a non-partitioning tracer and a number of partitioning tracers, is injected and recovered [*Jin et al*., 1995]. As the tracers flow through the swept volume, the partitioning tracers are delayed or retarded versus the non-partitioning tracer arrival at the RWs. The breakthrough curves are analyzed by the method of moments to yield the mean arrival time of each tracer. From the difference in the mean arrival times of the partitioning and conservative tracers, the saturation of NAPL can be estimated for the region interrogated by the tracers [*Jin et al*., 1995; *Annable et al*., 1998]. Assumptions made for a PITT include: (1) the NAPL is essentially insoluble and is the only sorbent of partitioning tracers; (2) NAPL is present in low saturations such that it has a negligible effect on non-partitioning tracers; (3) equilibrium, linear, reversible partitioning occurs; and (4) dispersion is negligible over the short time frame of the tracer test [*Jin et al.,* 1995; *Annable et al*., 1998; *Enfield et al*., 2005].

The ratio of the concentration of the partitioning tracer in the NAPL phase (C_p) to the concentration of the tracer in the aqueous phase (C_w) is the NAPL – water partition coefficient (K_{Nw}).

$$K_{Nw} = \frac{C_p}{C_w} \tag{1-4}$$

The retardation factor (R) is the ratio of the mean arrival times of the partitioning tracer (τ_p) to the non-partitioning tracer (τ_n).

$$R = \frac{\tau_p}{\tau_n} \tag{1-5}$$

The selection of the tracers is based on each being nontoxic, nondegrading, having low volatility, and being easily quantifiable [*Annable et al*., 1998]. The K_{Nw} values determine the amount of

time the partitioning tracer will spend in the subsurface. Tracers should be chosen to provide adequate retardation, but not so that the test is unreasonably long. The recommended retardation factor is between 1.2 and 4 [*Jin et al*., 1995].

The mean arrival times are calculated from the method of moments [*Jin et al*., 1995; *Annable et al*., 1998; *Jawitz et al*., 2003; *Jawitz*, 2004]. The injection pulse is maintained at constant concentration, and the MLS or RWs are sampled frequently. The resultant break through curves (BTCs) are then be plotted and analyzed by the method of moments. The *N*th absolute moment (M_N) of a distribution is described by:

$$M_N = \int_0^\infty t_N C(t) dt \tag{1-6}$$

The first normalized moment (μ_1) is determined by dividing M_1 by M_o.

$$\mu_1 = \frac{\int_0^\infty tC(t)dt}{\int_0^\infty C(t)dt} \tag{1-7}$$

One half of the tracer pulse duration (t_o) is subtracted from the first normalized moment to get the *i*th tracer mean arrival time, τ_i.

$$\tau_i = \mu_1 - \frac{t_0}{2} \tag{1-8}$$

The average NAPL saturation (S_N) in the swept volume is then calculated from the difference in the mean arrival times of the non-partitioning and partitioning tracers.

$$S_N = \frac{\left(t_p - t_n\right)}{\left[t_p - t_n\left(K_{Nw} - 1\right)\right]} \tag{1-9}$$

The effective pore volume (V_e) for each RW is determined from the mean arrival time of the non-partitioning tracer and the RW extraction rate, Q_i.

$$V_e = Q_i t_n \tag{1-10}$$

The NAPL saturation and the effective pore volume are used to calculate the volume of NAPL (V_N) in the area swept by the tracers.

$$V_N = \frac{S_N V_e}{1 - S_N} \tag{1-11}$$

Summing up the NAPL volumes from the RWs will determine the total volume of NAPL in the region swept by all the tracers. For the field test, RW pre and post-remedial PCE saturations were determined using this method [*Sillan*, 1999; *Jawitz et al*., 2000]. However, since MLS tubes are not continuously pumped, the effective pore volume cannot be exactly determined, thus volume of the NAPL for the tracer swept zone for the MLS was not determined in this work.

The site hydrogeology and DNAPL architecture can cause errors in PITT estimation of DNAPL content. Media heterogeneity and the resultant non-uniform DNAPL distribution are expected at field sites. This results in hydraulic constraints in tracers accessing DNAPL which causes underestimation of free phase DNAPL saturation [*Rao et al*., 2000]. These limitations can be overcome by sufficient tracer injection volume and adequate test time to fully record tracer tailing [*Meinardus et al*., 2002]

The administration of a post-remedial PITT allows the determination of the amount and location of DNAPL remaining [*Jin et al*., 1995] and thus when compared to the pre-PITT, and assessment of remedial performance [*Jin et al*., 1995; *Annable et al*., 1998]. At Sages, the pre and post-remedial PITTs allowed the evaluation of ethanol flushing for aggressive source removal [*Sillan*, 1999; *Jawitz et al*., 2000]. However, the comparison of source depletion and subsequent concentration response was not previously published. The results of pre and post flushing PCE saturations for both RW and MLS wells affords the calculation of NAPL reduction. This can be compared to aqueous concentration changes, another metric for remedial

performance. From the results of NAPL removal and concentration changes, the site can be compared to other alcohol flushing remedial actions.

1.9 Bioremediation

At sites with the required conditions, monitored natural attenuation of DNAPLs may be an alternative to other remediation methods [*USEPA*, 1999]. However, when these requirements are not met, other means of controlling, removing, or destroying the source may be appropriate. Although enhanced volatilization, solubilization, and mobilization are methods of removal, bioremediation is the destruction of DNAPL by microbes in the subsurface [*NRC*, 2005]. In-situ bioremediation (ISB) of DNAPL source zones refers to the stimulation or augmentation of biological processes to accelerate contaminant mass removal or to control downgradient plume migration [*ITRC*, 2005]. This can be achieved by biostimulation, providing the conditions to promote colonization of indigenous reductive dechlorinating bacteria, or by bioaugmentation, the introduction of microbes capable of destroying chlorinated solvents [*ITRC*, 2005]. Although several recent studies have demonstrated the ability of biological species to survive in the high concentration of source zones, combined source removal and residual treatment is recommended for PCE saturated source zones [*Yang and McCarty*, 2000, 2002; *NRC*, 2005]. The long term monitoring of ISB sites is called enhanced monitored natural attenuation [*ITRC*, 2005].

Proper choice of remediation technology can facilitate the depletion of significant source mass and it can also enhance the sites natural ability to attenuate the residual contamination [*Rao et al*., 2002; *NRC*, 2005]. Dissolution is limited at sites with very low groundwater velocities because the aqueous phase reaches equilibrium with the NAPL phase, hindering further dissolution [*Chu et al*., 2004]. It has been demonstrated that DNAPL biodegradation can also enhance dissolution of chlorinated solvents [*Cope and Hughes*, 2001; *Yang and McCarty*, 2000,

2002]. Biological enhancement of PCE solubility occurs by biological transformation of dissolved PCE to its more soluble daughter products, TCE and DCE. At the NAPL water boundary, this allows additional PCE mass transfer to the aqueous phase [*Carr et al*., 2000]. This has the advantage of decreasing source zone longevity [*Yang and McCarty*, 2000]. Increased dissolution creates greater aqueous phase DNAPL, thus greater accessibility for microbial use [*Carr et al*., 2000].

1.10 Solvent Extraction Residual Biotreatment

During standard bioremediation methods, the biostimulation or bioaumentation agents are delivered to the source or plume to provide the necessary requirements for biodegradation. Mixing and contact with DNAPL are the limiting processes. Source zone depletion only occurs at the DNAPL-water interface, so the agents must be delivered to this region if this is the goal. One of the distinct advantages of the solvent extraction residual biotreatment (SERB) technology is that the mixing and contact of biotreatment agents with contaminants is achieved directly during the flushing event [*Mravik et al*., 2003]. The limitation of all flushing technologies is that the remedial fluids primarily flow through zones of higher hydraulic conductivity. Thus, even in the SERB method, there will be lack of contact in lower permeable zones where DNAPL tends to accumulate [*Sewell et a*l., 2006]. The mixed areas will stimulate bioremediation as the flushing agent can act as the electron donor and the DNAPL can act as the electron acceptor. If electron donors, electron acceptors and dechlorinating microbes are present, the environment may be suitable for reductive dechlorination to occur [*Sewell et al*., 2006].

As a result of this pilot alcohol flushing test, some ethanol was not able to be recovered at the RWs. This residual ethanol serves as an electron donor and PCE will be the electron acceptor. Of the 34 kL of ethanol injected into the source zone, 92% was recovered leaving a

residual ethanol of 2.72 kL in the subsurface [*Mravik et al*., 2003]. The post flushing groundwater samples indicate increasing byproducts of reductive dehalogenation of PCE over time, demonstrating enhanced natural attenuation of residual PCE [*Mravik et al*., 2003; *Sewell et al*., 2006].

1.11 Mass Flux and Mass Discharge

Although quantifying the source mass or volume is important in determining the size of the source and the best method for remediation, the amount of mass leaving the source in dissolved form may be more important [*Feenstra et al*., 1996]. The risk to a downgradient well has less to do with the mass of the source and more to do with the hydrogeologic conditions at the site. A site with little or no groundwater flow maybe of little risk to receptors downgradient, however an area with high flow through a contaminated site, may create an extensive plume of dissolved contaminants stretching for miles [*Einarson and McKay*, 2001].

The assessment of contaminant source strength is completed by calculating the mass leaving the source area in dissolved form [*EPA*, 2003]. The groundwater flux (q_i) is also called the Darcy flux, and is a measure of the flow per unit area of a region. It is calculated from the product of the saturated hydraulic conductivity (K_s) and the hydraulic gradient (j) [*USEPA*, 2003; *Basu et al*., 2006].

$$q_i = -K_s j \tag{1-12}$$

The hydraulic gradient is the change in head (dh) per change in distance (dl). By measuring or estimating the groundwater flux, the contaminant flux can be calculated when combined with the concentration in the respective groundwater samples The contaminant mass flux (J_i) is the product of the water flux and concentration of the contaminant in that water $\left[M / L^2 T \right]$ [*USEPA*, 2003; *Falta et al*., 2005; *Guilbeault et al*., 2005; *Basu et al*., 2006;].

$$J_i = q_i C_i \qquad (1\text{-}13)$$

Both the water flux and mass flux require a cross sectional area (i), or control plane. This is best illustrated in Figure 1-2.

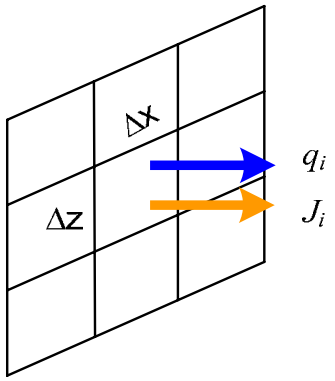

Figure 1-2. Water flux (q_i) and contaminant flux (J_i) across a control plane. ΔX and ΔZ are the cross sectional distances and the cross sectional area A_i is the product of these two lengths.

In the field, there have been a number of new technologies developed recently for assessing in-situ mass flux. One of these is the University of Florida passive flux meter (PFM) [*Hatfield et al.,* 2004; *Annable et al*., 2005; *Basu et al.,* 2006]. This downhole device allows the simultaneous measurement of groundwater flux and contaminant flux across a control plane of wells. Another new method for flux measurement is the integral groundwater investigation method (IGIM) or integral pump test [*Bockelmann et al*, 2001; *Bockelmann et al*, 2003; *Bauer et al*., 2004; *Jarso et al*., 2005]. A modification of this method has been utilized by Guilbeault et al. [2005] at several sites to simultaneously pump a control plane of wells continuously, capturing the entire contaminant plume, and affording an estimation of mass flux.

Finally, we can determine the mass discharge for the source area, a full measure of the source zone strength. This is the mass leaving the source area per unit time. The product of the total cross sectional area with the contaminant mass flux (J_i) is the mass discharge (M_d) [*USEPA*, 2003].

$$M_d = \sum J_i A_i = \int_A J_i dA \qquad (1\text{-}14)$$

This can be also thought of as the spatial integration of contaminant flux across the control plane [*Basu et al*., 2006]. The units of contaminant mass discharge are mass per time [M/T].

Stroo et al. [2003] identified the need for field data of mass discharge at sites undergoing source removal. Estimates of the mass discharge across the source zone and downgradient transects will be evaluated over a six-year period following the 1998 ethanol flood and presented in Chapter 3 of this thesis.

1.12 Benefits of DNAPL Source Depletion

Mass flux may be more important than the actual mass in the source zone [*Rao et al*., 2002; *USEPA*, 2003; *NRC*, 2005]. Through a contaminant source region of very slow groundwater velocity, the mass flux maybe very small due to the low Darcy flux. However, a small mass of residual PCE can produce a long plume of contaminated groundwater in a region of high groundwater velocity. Large reductions in mass discharge from remedial efforts should produce significant decreases in concentrations reaching downgradient receptors, and decrease site longevity [*Rao et al*., 2002]. In the past decade several alcohol flushing field tests have demonstrated the ability to reduce a field source zone DNAPL mass [*Rao et al*., 1997*; Jawitz et al*., 1998; *Sillan*, 1999; *Jawitz et al*., 2000*; Falta et al*., 1999*; Brooks et al*., 2003]. Although aggressive source removal rarely will achieve total site groundwater concentrations below maximum contaminant limits (MCLs), contaminant flux reductions have been demonstrated. This has spawned considerable debate on the benefits of source depletion [*Sale and McWhorter*, 2001; *Rao et al*., 2002; *Rao and Jawitz*, 2003]. Due to a shift in consideration to the downgradient receptors of a contaminant source's plume, risk based corrective action (RBCA)

was developed to provide the framework for assessing downgradient risks to people and the environment [*ASTM*, 2002].

Recently several researchers have altered focus to the RBCA framework, studying the effects of DNAPL source depletion on contaminant mass flux [*Lemke et al*., 2004; *Annable et al.,* 2005; *Guilbeault et al*., 2005; *Jawitz et al.,* 2005; *Wood et al*., 2005; *Fure et al.,* 2006*; Newman et al.,* 2006]. Because traditional plume control methods tend to be costly due to the high insolubility of DNAPLs, leading to long term maintenance and operation expenses [*MacKay and Cherry*, 1989; *Mayer et al.*, 2002], aggressive source zone depletion measures are attractive. While active remediation rarely achieves source zone clean up to regulatory limits, the benefits of reduction in source mass have been predicted in models through decreases in mass flux, source longevity, and associated maintenance costs [*Rao et al*., 2002; *Falta et al*., 2005; *Jawitz et al*., 2005]. In 2-D heterogeneous physical models, aqueous dissolution experiments determined that NAPL architecture was the primary control of the mass depletion, flux response relationship [*Fure et al*., 2006]. Although simple uniform flow field models have predicted that most of the mass needs to be removed to result in significant flux reduction, field sites are not this simple [*Sale and McWhorter*, 2001]. Even small natural heterogeneities in media result in much greater heterogeneity in the groundwater velocity field [*Kueper et al*., 1993]. Further Lagrangian steamtube modeling has demonstrated that as heterogeneity of aquifer properties and the subsequent NAPL heterogenous architecture increase, more favorable flux responses will follow source zone depletion [*Jawitz et al*., 2005]. This type of situation better represents field conditions.

The relationship of mass reduction to flux reduction has been modeled by many researchers recently [*Rao et al*., 2001; *Rao and Jawitz*, 2003; *Parker and Park*, 2004; *Jawitz et al.*, 2005; *Falta et al*., 2005a,b; *Enfield et al*., 2005; *Wood et al*., 2005; *Basu et al.,* 2006]. A modified version of this is described in Eq. 1-15, where fractional mass reduction (1-M/M_0) is plotted against fractional flux reduction (1-C/C_0).

$$\left(1-\frac{C}{C_0}\right)=\left[1-\frac{M}{M_0}\right]^{1/\beta} \tag{1-15}$$

Figure 1-3 presents the relationship described in Eq 1-15.

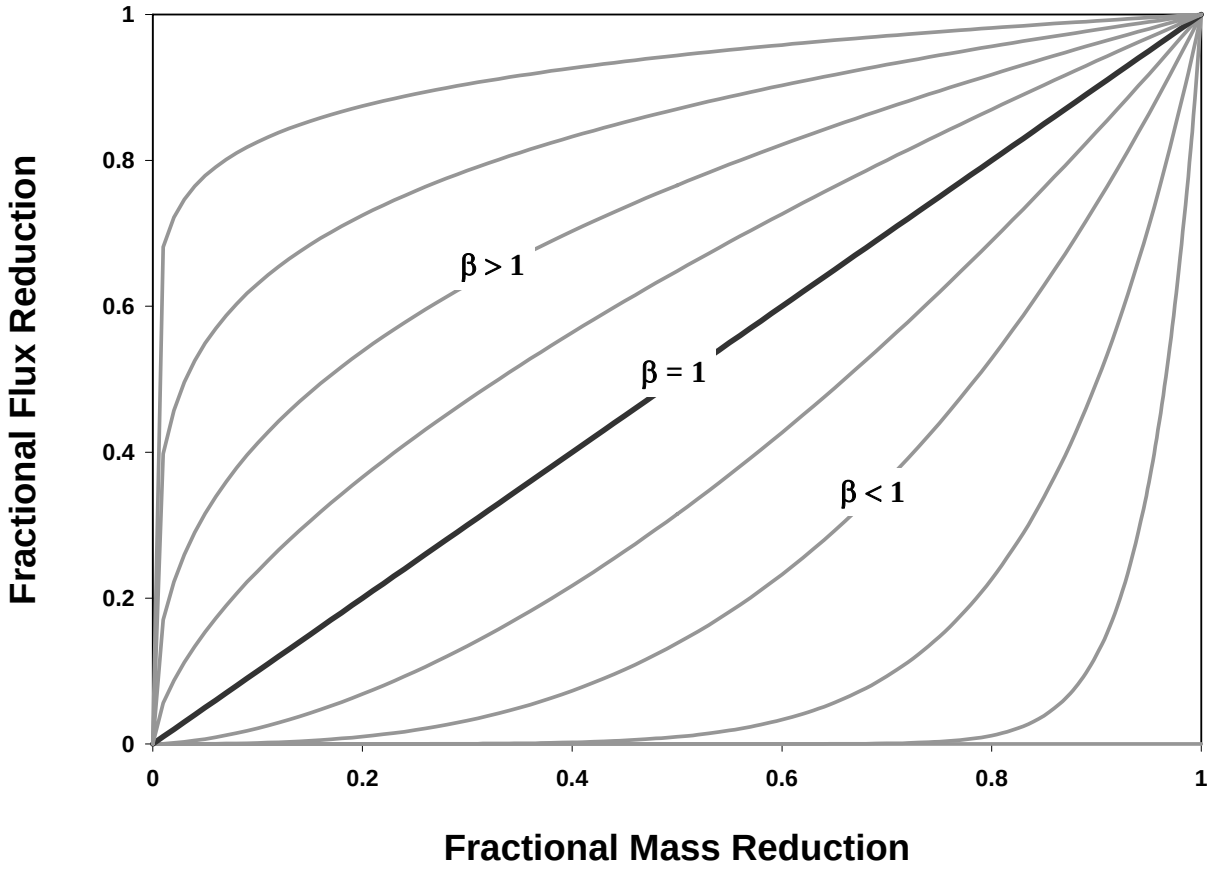

Figure 1-3. Flux reduction to mass reduction relationship. The black line down the middle (β = 1) represents a situation where equal amount of flux reduction is produced from a mass reduction. The lines to the right (β < 1) indicate the conditions where larger amounts of mass must be removed to realize reductions in flux. In the left region (β > 1) smaller mass reductions produce greater flux reduction.

In this figure, conditions where very large mass reductions are required to create significant flux reductions ($\beta << 1$) are considered unfavorable for remediation [*Sale and McWhorter*, 2001]. However, this type of condition has not been demonstrated in alcohol flushing field tests [*Rao et al.,* 1997*; Falta et al,* 1999*; Brooks et al.,* 2004]. Although the initial field tests were performed in highly sandy aquifers, sufficient homogeneity of media has not been found to create such an unfavorable situation.

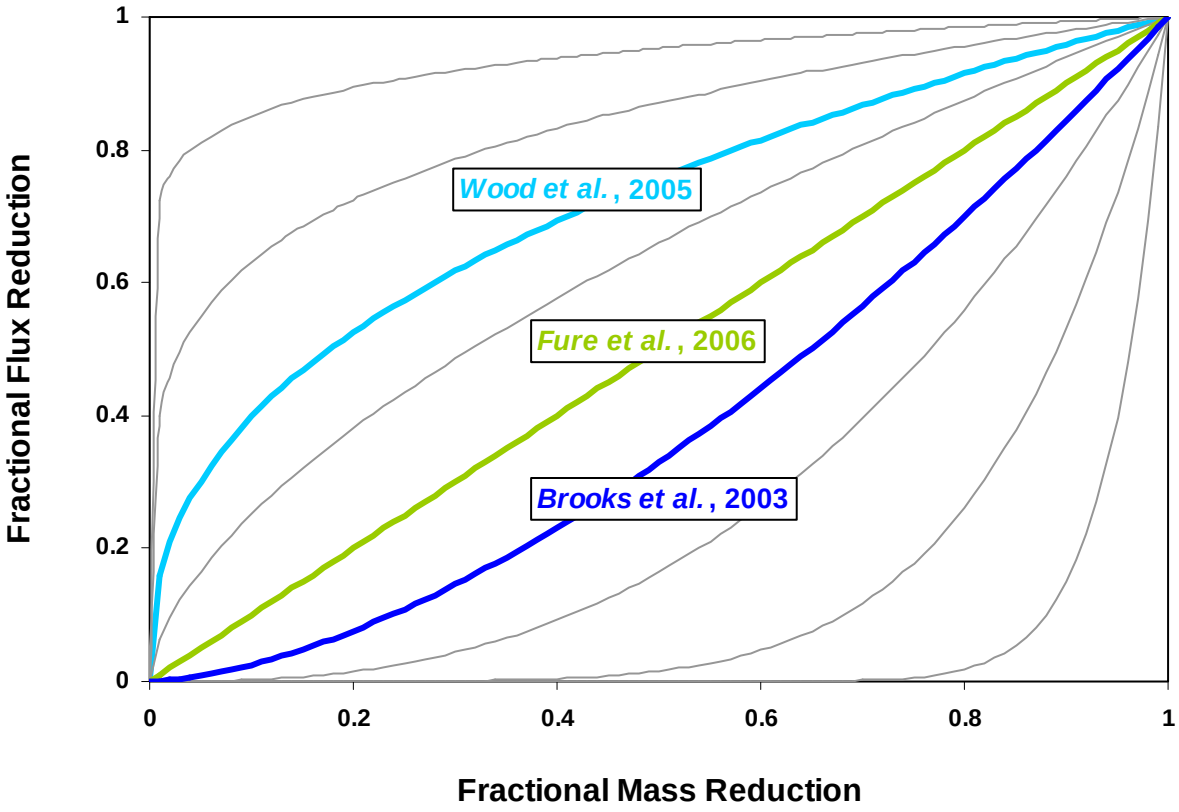

Figure 1-4. Approximate alcohol flushing test results of source zone depletion and subsequent flux reduction [*Brooks et al.*, 2004; *Wood et al*., 2005; *Fure et al*., 2006].

More often, both laboratory and field tests of alcohol flushing has produced relationships from $\beta = 0.5$ to $\beta = 2.5$ as in Figure 1-4. Recent laboratory experiments with 2-D box physical models have confirmed that media heterogeneity leads to near 1:1 mass reduction to flux

reduction relationship ($\beta = 1$) for DCA and TCE [*Fure et al*., 2006]. In a controlled release of PCE at Dover AFB, Brooks et al. [2004] reported favorable mass reduction to flux reduction ratios for the extraction wells after an ethanol flushing field test. Another field test at Hill AFB OU1, in a field test inside a sheet pile test cell, alcohol flushing was performed and the results yielded even more favorable flux response to source removal ($\beta > 1$)[*Wood et al*., 2005].

These results forecast that in-situ alcohol flushing can be successful in both source zone depletion and decreasing contaminant flux. The relationship described above was applied to the ethanol flood results for both RW and MLS wells and will be reported later in this paper.

After thorough site characterization, an understanding of DNAPL dissolution, cosolvency, bioremediation, mass discharge, and the benefits of source depletion, this work can now transition to the analysis of the 1998 ethanol flushing and its long term effects on the Sages site.

CHAPTER 2
REMEDIAL FLOW FIELD

2.1 Flow Field Design

From the site characterization, computer modeling and pumping tests, the design of the remedial system was for hydraulic containment of both extracted contaminant and remedial fluids. Around the perimeter of inferred PCE source zone, six recovery wells were installed. In the middle of the source zone, three injection wells were deployed to deliver the PITT and remedial fluids. The injection wells were screened from 7.6 to 9.9 m bgs, while the recovery wells were screened from 7.9 to 9.6 m bgs. The design was to reduce the risk of downward mobilization of PCE by forcing slight upward gradient flow of remedial fluids [*Lunn and Kueper*, 1999; *Sillan*, 1999; *Jawitz et al*., 2000]. Figure 2-1 shows the locations of the wells in and around the PCE source zone.

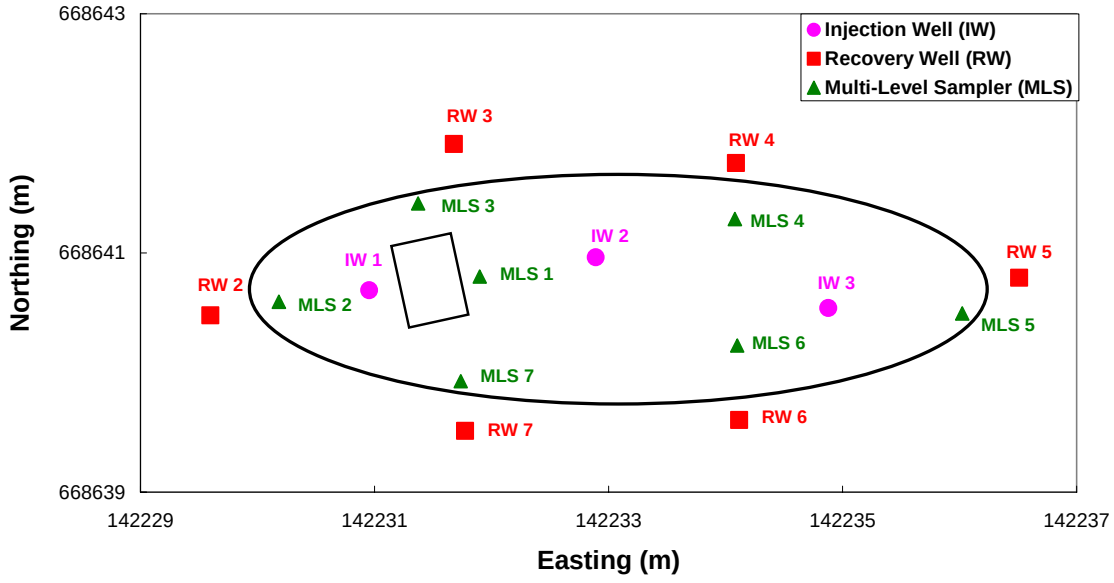

Figure 2-1. Map View of well locations for 1998 remedial flow field (units are Florida State Plane Coordinate System).

To achieve the desired 2:1 extraction to injection rate, the flow rate used for the three injection wells was 5.03 L/min. The central recovery wells (3, 4, 6, 7) were pumped at 5.91 L/min and the outer recovery wells (2, 5) were pumped at 3.4 L/min. This created the induced remedial flow field from the inner injection region of the source zone to the outer recovery wells. These rates were employed for the pre-remedial PITT, the ethanol flood, and the post-remedial PITT.

Referring to Figure 2-2 below, the fluid velocity of each depth at each well was estimated from the distance from the nearest IW to the MLS, and the mean arrival time of the conservative tracer (τ_n) from Eq. 1-12 from the pre-remedial PITT. This delivers an estimation of linear fluid velocity in [L/T] units for each MLS well depth.

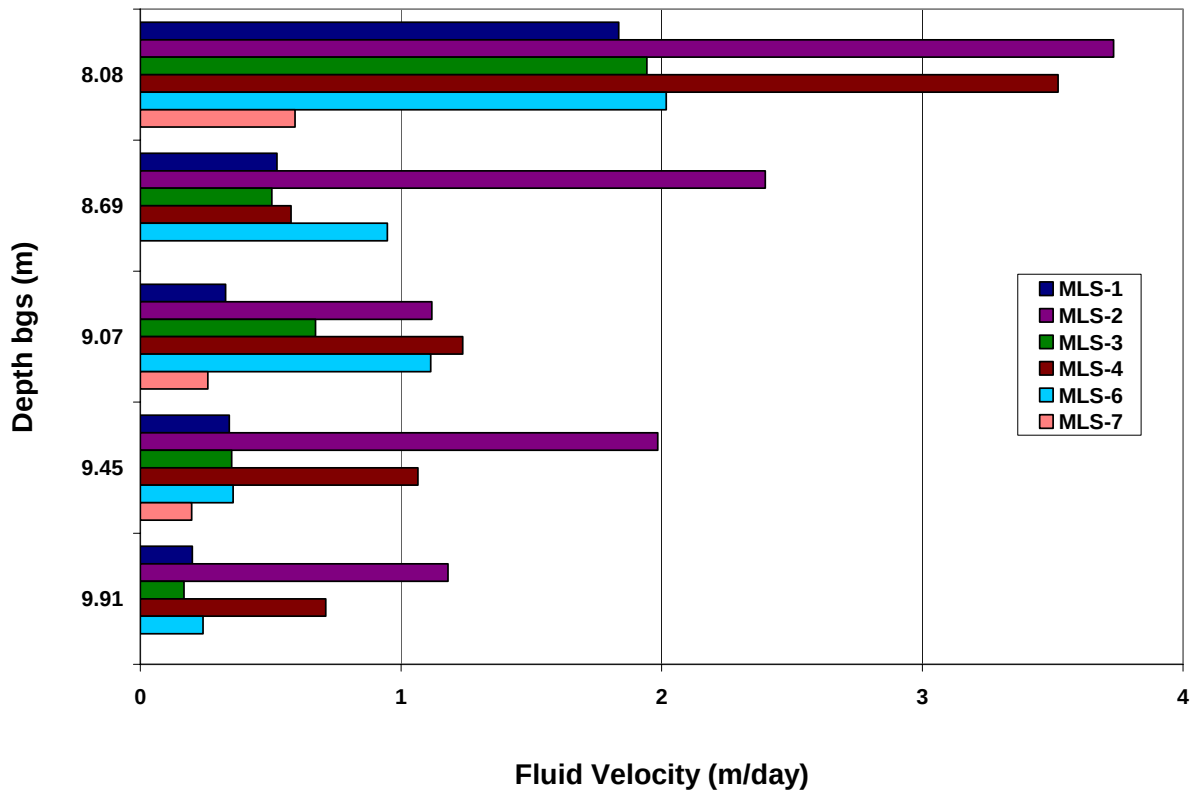

Figure 2-2. Estimated linear fluid velocities of each MLS well at each respective depth during Sages 1998 field test.

The general pattern was that the upper interrogated region (8.08 m bgs) demonstrated higher hydraulic conductivity than the depths below. In the mid-levels there were lower velocities at a depth of 8.69 m bgs in MLS-1, MLS-3, MLS-4, and MLS-6. In every case but MLS-1, fluid velocity increased slightly at the next depth of 9.07 m and then continually decreased to their lowest values at 9.91 m bgs. The low value at MLS-6 at 8.69 m bgs was almost double the value of MLS-1 and MLS-3. This is further evidence of a low permeability layer in the upper middle zone around these wells, which might have caused PCE to collect and spill off to the next finer grained strata. However, at MLS-2 the mid-level lower fluid velocity was observed at 9.07m bgs and the lower depths were slightly higher. At the lowest depth, MLS-6 showed the lowest velocity. This is the region that the highest PCE saturations were observed indicating the presence of finer grained, low permeability media. In all depths of MLS-5 and several depths of MLS-7, sufficient tracers did not arrive at the sampling location to compute mean arrival times, thus an estimated velocity was not determined. MLS-7 displayed the same trend of decreasing fluid velocity with depth.

Previous studies at the Sages site estimated decreasing hydraulic conductivity as depth increased [*Sillan*, 1999; *Jawitz et al*., 2000]. Furthermore, borehole flow meter tests by Mravik et al. [2003] determined hydraulic conductivities of 4 m/d at 8 m bgs, decreasing to less than 1 m/d at 9 m bgs.

2.2 Tracer Selection

The field test included both pre and post-remediation PITTs to identify the NAPL saturation and volume in the suspected source area. In the pre-PITT, methanol (MeOH) was the conservative tracer and n-hexanol (HexOH), 2,4-dimethyl-3-pentanol (DMP), and 2-ethyl-1-hexanol (E-HexOH) were used as the partitioning tracers. In the post ethanol flood PITT,

HexOH was used as the non-partitioning tracer and DMP and E-HexOH were used as partioning tracers. Methanol was not employed as the conservative tracer due to known problems of interference with residual ethanol [*Cho et al*., 2003]. Furthermore, TBA was injected as a conservative tracer, but ethanol analytical interference occurred. Thus, HexOH, with a very low K_{Nw} was used. A summary of the tracer pulse injections, the tracers and their PCE partitioning coefficients is provided in Table 2-1 [*Sillan*, 1999; *Jawitz et al*,. 2000].

Table 2-1. Sages tracers for 1998 PITTs.

Tracer	C_o (mg/L)	K_{Nw}	(t_o) Pulse Duration (hours)
Pre-PITT			
Methanol (MeOH)	2199	0	3.8
n-hexanol (HexOH)	822	5.58	3.8
2,4-dimethyl-3-pentanol (DMP)	436	20.4	3.8
2-ethyl-1-hexanol (E-HexOH)	487	81.23	3.8
Post-PITT			
t-butanol (TBA)	1105	0.17	3.7
n-hexanol (HexOH)	473	5.58	3.7
2,4-dimethyl-3-pentanol (DMP)	354	20.4	3.7
2-ethyl-1-hexanol (E-HexOH)	457	81.23	3.7

2.3 Breakthough Curve Analysis

From the pre and post-flushing PITTs, the S_N was estimated for each MLS well and depth, using the method of moments. For the temporal breakthrough curves (BTCs) where the end of the tail of each tracer did not reach the MLS well, exponential extrapolation was performed to estimate S_N using the method developed by Helms [1997] and utilized by Annable et al. [1998]. This procedure was also employed for all BTCs to reduce fluctuations or noise in the tail regions. Each BTC was then numerically integrated using the trapezoidal rule in the

method of moments to yield mean arrival times for each tracer [*Jin et al*., 1995; *Annable et al*., 1998]. Retardation factors for the MLS pre-PITT ranged from 1.06 to 2.69 and from 1.06 to 1.38 for the post-PITT.

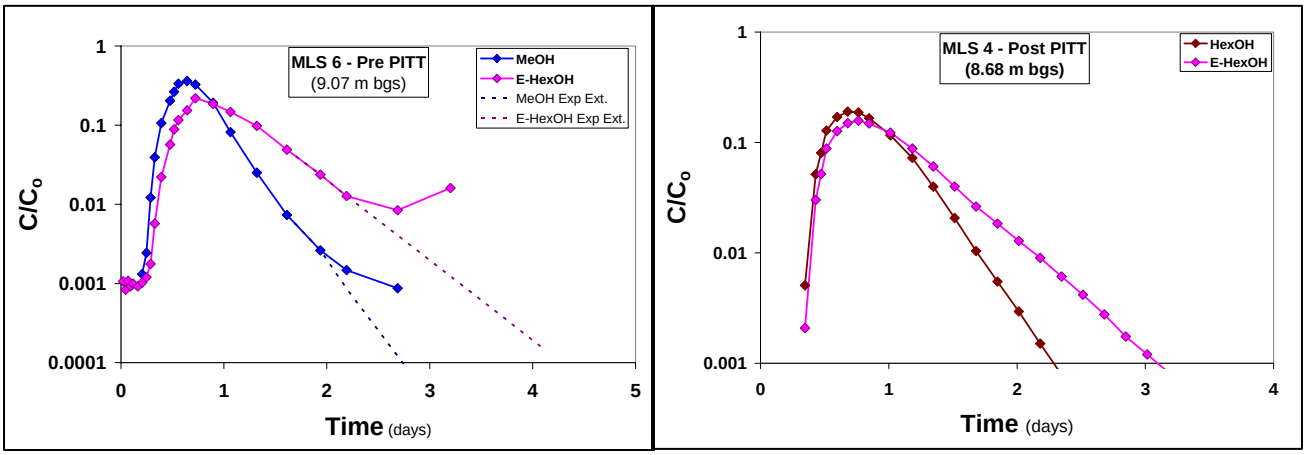

Figure 2-3. Examples of breakthrough curves of tracers during the PITTs at Sages. The tail region of all BTCs were exponentially extrapolated from linear tail segments, including several incomplete tails such as Pre-PITT MLS-6, 9.07 m bgs BTC on the left. The right figure is post-PITT MLS-4, 8.68 m bgs.

The BTCs for wells 2, 3, 4, and 6 were resolved but MLS wells 5 and 7 did not receive enough tracers during the test to determine S_N in those swept regions. Figure 2-3 shows examples of BTCs from the PITTs. The plot on the left is the data from the pre-remedial PITT of MLS-6 at a depth of 9.01 m bgs. Moment analysis returned a conservative tracer (MeOH) mean arrival time of 0.77 days and a partitioning tracer mean arrival time of 1.08 days. The retardation factor was 1.49 and the average PCE saturation in the swept zone was 0.69 %. The graph on the right was the post-remedial PITT results of MLS-4 at a depth of 8.68m bgs. PCE saturations were calculated using Eq.1-9, and the results are presented in Table 2-2.

2.4 Pre-remedial PITT

In the RW analysis of Sages for the pre-flood PITT, there were consistently lower average PCE saturations in the swept zones arriving at RW-3, RW-5, and RW-7 than their

respective MLS wells. In Table 2-2, there are a number of no-value (nv) values where tracers did not arrive at the sampling location. The values with asterisks indicate estimated pre-flood S_N using a method described later. Most of these were observed at the lowest depth, indicating probable lower hydraulic conductivity. One of the disadvantages of PITTs is the inability or difficulty of tracers to arrive at a MLS or RW. Most tracers never reached MLS-5 and MLS-7 in the PITTs. Without at least the conservative tracer reaching the sampling points, the fluid flow velocity or PCE saturations. However, both RW-5 and RW-7 received tracers and recorded initial average PCE saturations greater than 0.5 %, the highest of the RW data set.

Table 2-2. PCE saturations from the pre-flood PITT. No-value (nv) indicates not enough tracers arrived at the well to resolve the PCE saturations. Column 2 is the RW and mean MLS results, the other columns are the specific MLS depth PITT results. Asterisked values were determined in section 2.11.

Well	Pre PCE S_N	8.08 m	8.69 m	9.07 m	9.45 m	9.91 m
RW-2	0.322					
RW-3	0.553					
RW-4	0.236					
RW-5	0.569					
RW-6	0.238					
RW-7	0.584					
	Mean MLS					
MLS-1	0.610	1.342	1.071	0.313	0.217	0.110*
MLS-2	0.373	0.773	0.199	0.675	0.101	0.115
MLS-3	0.801	1.060	0.257	0.461	1.552	0.675*
MLS-4	1.367	0.107	1.146	0.925	2.029	2.628*
MLS-5	nv	nv	nv	nv	nv	nv
MLS-6	1.015	0.135	0.510	0.698	1.686	2.044
MLS-7	nv	0.066	nv	0.181*	0.510*	nv

In the upper zone of MLS-1 and MLS-3, the highest upper source zone saturations were detected. This is closest to the location of the drycleaner floor drain in Figure 2-1. In the mid-depths, MLS-2, MLS-4, and MLS-6 returned the higher average PCE saturations. This indicated PCE moving from the upper zone around MLS-1 and MLS-3 and then collecting in the mid-depths in the wells encircling this region. At the bottom of the sampling zone, the highest PCE saturations were observed in MLS-4 and MLS-6, up to 2.6% indicating pooling in this region.

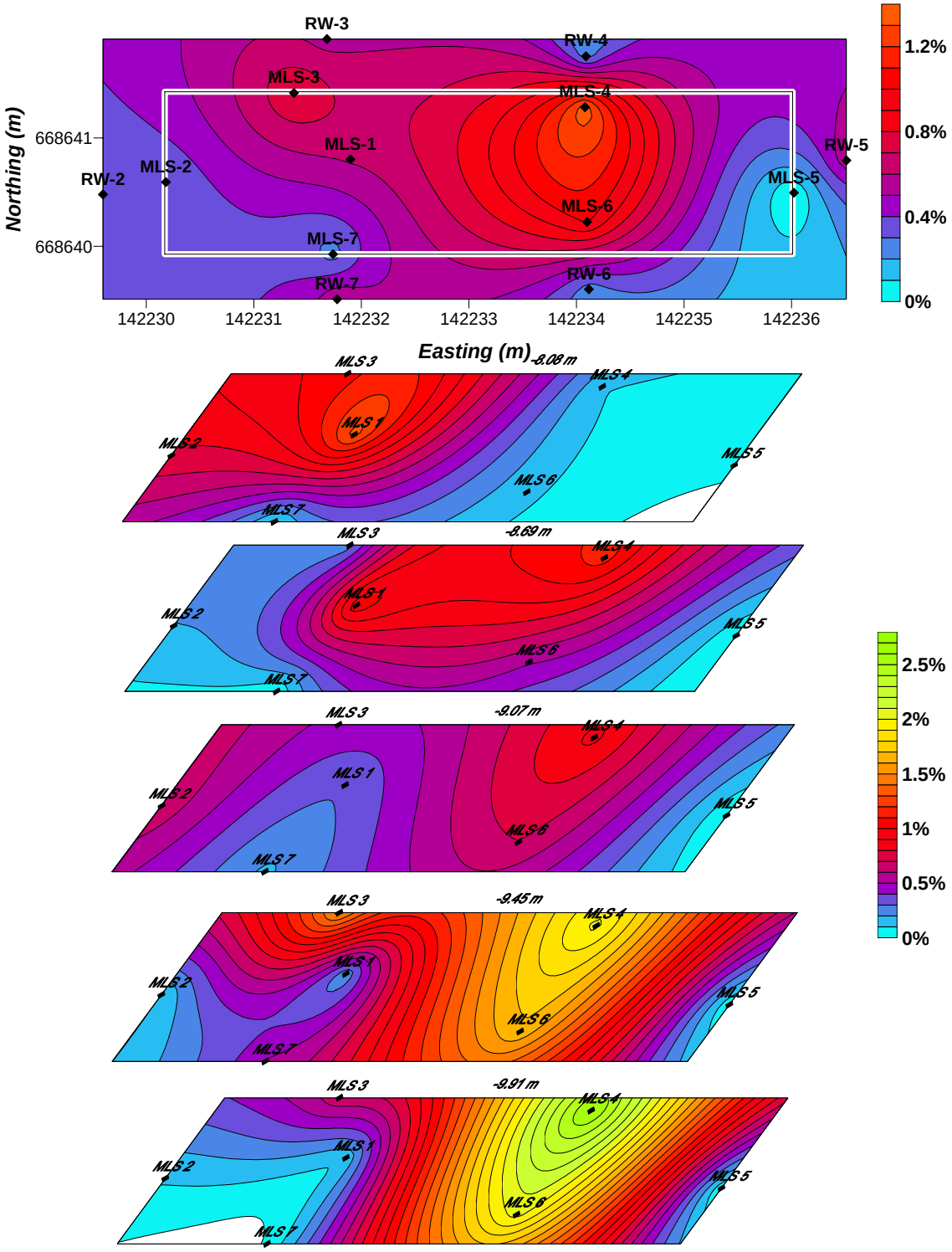

Figure 2-4. Map view of % PCE saturation Surfer visualizations in the source zone from the 1998 pre-remedial PITT at Sages. Top figure is the recovery well and average MLS S_N for each location. Below is S_N from MLS: 8.08, 8.69, 9.07, 9.45, & 9.91 m bgs. White areas are no data.

Spatial views of the initial PITT PCE saturation were generated using the Surfer™ program. Looking at Figure 2-4 below, the top visualization is the entire source zone data in map view, including RW and mean MLS values. The S_N data were plotted as point values and then standard kriging was applied to interpolate between the points. During a PITT, the DNAPL saturation is not actually a point, but an average value for the region swept by the tracers. However, with this limitation in mind, the plots are useful to help visualize the distribution of PCE in the source zone. Within this figure is a smaller area denoted by a white rectangle. This is the MLS well area. The MLS S_N values were plotted for each depth to show the spatial distribution of PCE in the subsurface. The white areas are not regions of zero PCE, but locations where BTCs were incomplete or non-existent due to lack of arrival of tracers. The lower pumping rate of RW-5 and greater distance from IW-3 to MLS-5 resulted in very little tracer capture from the PITT. Thus, no data is reported in the table or visualization. There may or may not have been PCE in this region. Soil cores and initial aqueous concentrations in this region implied very little PCE would be located there. MLS-7 may have clogging or much lower conductivity media.

The MLS PITT results support the soil core analysis from Sillan [1999]. Summarizing Sillan [1999] and Jawitz et al. [2000], it was determined that higher PCE soil saturations were located in the upper zone of MLS-1 and in the lowest zone of MLS-4. Additionally, the soil cores from the three injection wells (IW 1-3) showed the same pattern. The upper zone of IW-1 was highly saturated, the upper region and the lower middle and lowest zones of IW-2 were highly saturated and the lowest region of IW-3 was highly saturated. MLS-3, MLS-2, and MLS-7 soil core analysis also found some PCE present but at an order of magnitude lower than the ones stated above. From the PITT, there were higher PCE saturations in the upper areas of the

aquifer around MLS-1 and MLS-3. Moving east to MLS-4 and MLS-6, the highest PITT PCE saturations were at the lower depths, up to 2.6%.

For the entire data set, there was no significant correlation of initial PCE saturation and the initial estimated fluid velocity for each respective MLS sampling location (R^2=0.05). However, in Figure 2-5, there were significant logarithmic relationships of these parameters in several specific MLS wells. As fluid velocity increased, there was a corresponding reduction in initial PCE S_N. These sampling locations exhibited the highest pre-remedial PCE saturations in the MLS data set.

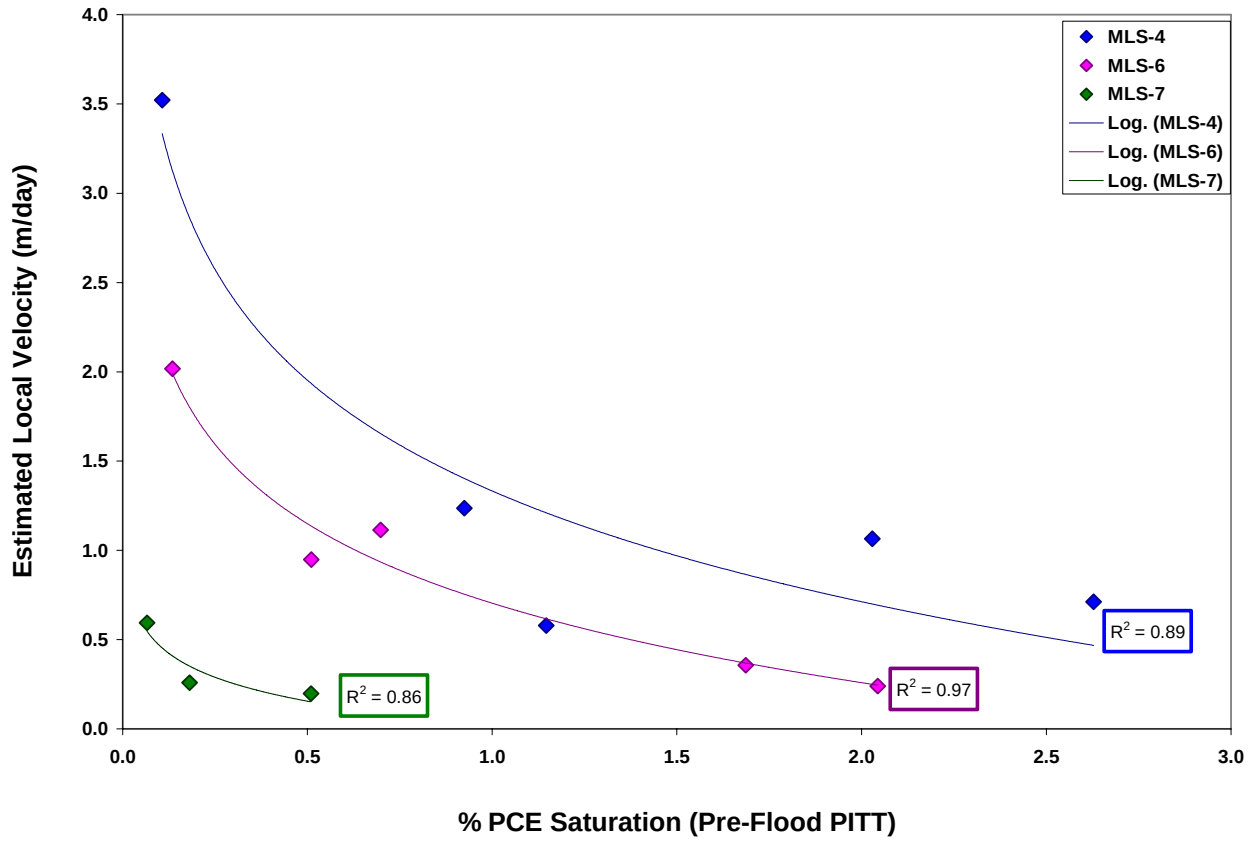

Figure 2-5. Relationship of initial PCE saturation to remedial flow field estimated fluid velocity in the Sages source zone for several MLS wells.

For higher velocity zones, it is likely that PCE experiences greater groundwater flow, resulting in greater removal by natural gradient dissolution. This is evidence of site aging, the reduction of DNAPL saturation in higher conductivity regions. Furthermore, flow bypass has been documented in DNAPL distributions with higher saturations and pools. This behavior is detected in MLS-4 and MLS-6.

2.5 PCE Aqueous Concentration Scaling

Since the process of ethanol flushing enhances the solubility of PCE by cosolvency, any groundwater samples that contain ethanol will be artificially high in PCE. Thus, all samples need to be scaled to the maximum possible PCE concentration, C_{max}. In the absence of ethanol, C_{max} is simply the aqueous solubility limit, 156 mg/L. The maximum PCE solubility as a function of the fraction of ethanol in water was measured by Van Valkenberg [1999] (Figure 2-6)

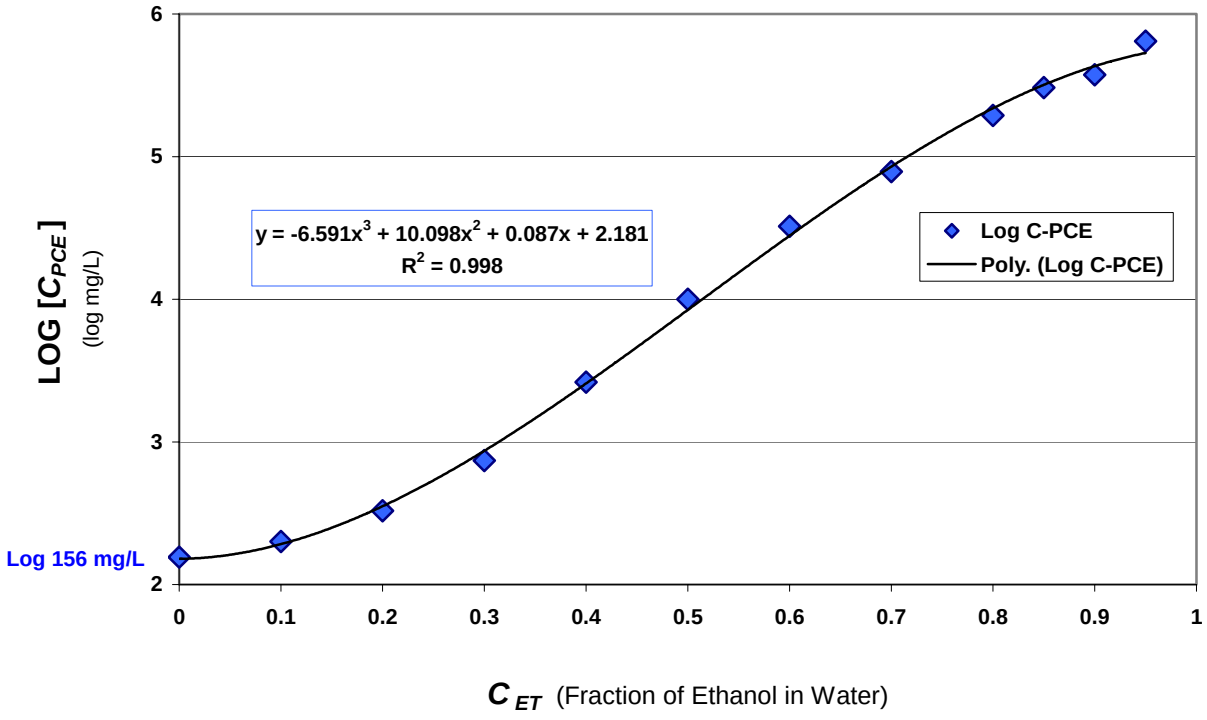

Figure 2-6. Solubility of PCE in ethanol/water mixtures. The data was fit with a polynomial equation.

Because cosolvency is exponential, log-linear fitting has been performed in the past to estimate PCE maximum solubility in ethanol [*Van Valkenburg*, 1999; *Ladaa et al*., 2001]. The data shown in Figure 2-6 are not perfectly linear, but a third-order polynomial was found to fit the data well. Substituting the measured fractional ethanol concentration (C_{ET}) of a sample in for x in Eq. 2-1, yields the logarithm of maximum possible PCE concentration (LOG [C_{max}]).

$$LOG[C_{max}] = -6.591x^3 + 10.098x^2 + 0.087x + 2.181 \qquad (2\text{-}1)$$

PCE solubility is then calculated from the antilog. Finally, the scaled PCE concentration, C_{GW}, for any groundwater sample is determined by Eq 2-2:

$$C_{GW} = \frac{C_{meas}}{C_{max}} \qquad (2\text{-}2)$$

These equations were used to calculate PCE maximum solubility for the remedial flow field post-flushing groundwater samples containing detectable ethanol. During the remediation at Sages, the RWs continued water injection after the ethanol flood until all RWs recorded ethanol concentrations less than 1%. However, after water flooding, residual ethanol was detected at concentrations up to 18 % at MLS locations in portions of the remedial flow field. For both the pre and post-flushing aqueous PCE analysis, the method above was employed so that all the data were scaled from 0 to 1.

2.6 Initial Aqueous Concentrations

During site characterization, groundwater samples were taken from wells at the site and analyzed for a suite of contaminants including PCE, TCE, DCE and VC. The lack of natural attenuation resulted in primarily PCE in the aqueous samples [LFR, 1997]. Before the ethanol flood, the MLS wells in the source zone were installed, developed and sampled. Once the remedial flow field was initiated, the MLS were sampled and again during the water flooding at the end of the pre-remedial PITT. The groundwater velocities and directions are very different

for natural gradient conditions versus the hydraulic flow field created for the flushing test. The samples considered in this Chapter are all under the influence of the remedial flow-field. All initial flow field aqueous concentrations are scaled to the maximum PCE water concentration of 156 mg/L. The results are summarized in Table 2-3.

Table 2-3. Sages scaled PCE concentrations from the pre-flood flow field sampling. MLS sampling depths are meters below ground surface.

Well	Pre C_{PCE}	8.08 m	8.69 m	9.07 m	9.45 m	9.91 m
RW-2	0.411					
RW-3	0.296					
RW-4	0.109					
RW-5	0.007					
RW-6	0.151					
RW-7	0.110					
	Mean MLS					
MLS-1	0.393	0.445	0.397	0.655	0.173	0.298
MLS-2	0.423	0.700	0.533	0.667	0.173	0.040
MLS-3	0.540	0.293	0.619	0.608	0.540	0.642
MLS-4	0.316	0.012	0.371	0.313	0.464	0.419
MLS-5	0.067	0.007	0.115	0.176	0.032	0.003
MLS-6	0.465	0.108	0.422	0.600	0.158	1.038
MLS-7	0.400	0.072	0.575	0.318	0.400	0.637

Although RW-2 and the average concentration at MLS-2 observed a similar 0.4 fraction of maximum PCE solubility, the mean MLS scaled concentrations were higher than their respective RWs. This was similar to the PCE saturation results in Table 2-2. Statistically, there was not a strong correlation between S_N values and aqueous PCE concentrations. However, qualitative analysis shows similar distributions of free phase and dissolved PCE. MLS-1, MLS-2, and MLS-3 recorded the highest concentrations in the upper sampling zone. The mid-depth region was dominated by higher PCE concentrations in MLS-1, MLS-2, MLS-3, MLS-6 and MLS-7. The lowest sampling zones showed higher values at MLS-3, MLS-4, MLS-6 and MLS-7. At the lowest depth of MLS-6, where the highest PCE saturations were recorded, the aqueous PCE concentration was also highest.

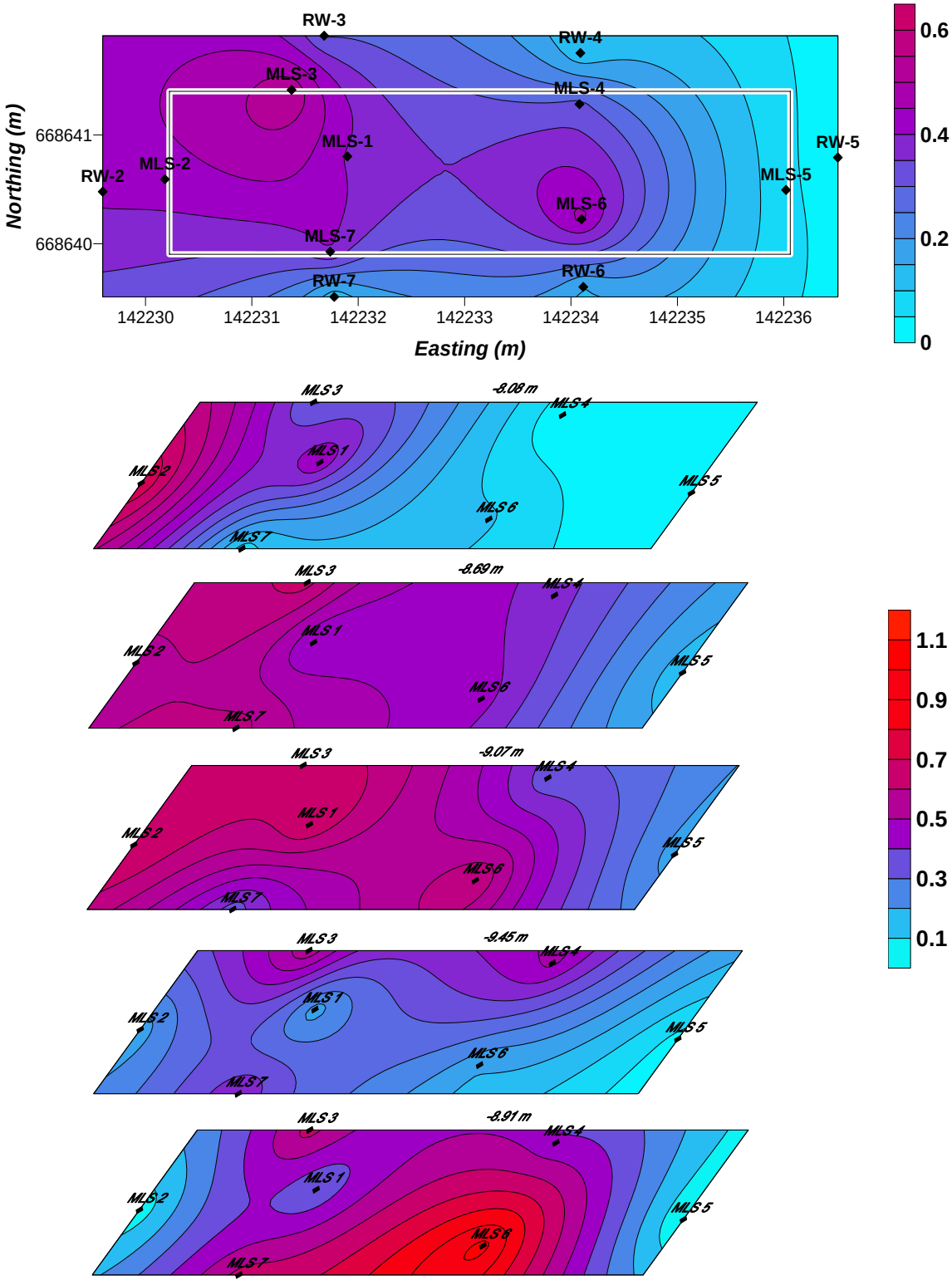

Figure 2-7. Surfer plots of Sages initial source zone maximum solubility scaled aqueous PCE concentrations in map view. Top figure is RW and average MLS values. Lower figures are depth values at 8.08, 8.69, 9.07, 9.45, and 9.91 m bgs.

The Surfer™ visualizations of the data in Table 2-3 are presented in Figure 2-7. The upper plot shows the map view of the source zone initial scaled PCE concentrations including RW and mean MLS data. In the upper plot, it appears that most of the flow field PCE flux was coming out of the MLS-1, MLS-2, MLS-3, and RW-2 region, with a smaller amount emanating from MLS-6 area. However, looking at the depth slices of MLS wells, it was observed that there were some upper zone higher concentrations, but the middle zone throughout the source area was contributing larger concentrations, and the lowest depth around MLS-4, MLS-6, and MLS-7 contained the highest concentrations at the site. This confirms that the zones with the highest PCE concentration contribute the highest aqueous flux, although residual PCE in all regions also contributed. Furthermore, PCE mass removal in the higher PCE saturation regions should yield subsequent decreases in aqueous concentrations.

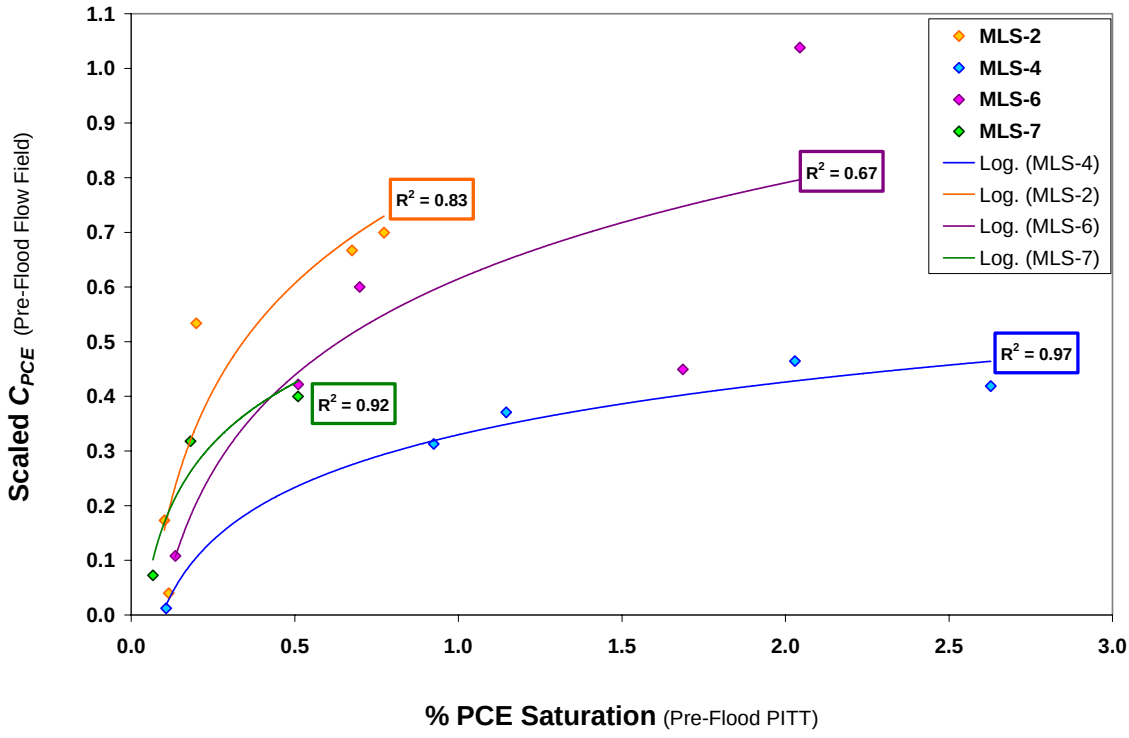

Figures 2-8. Relationship of initial PCE saturation to initial scaled PCE concentration for several MLS wells at Sages.

There was not a strong correlation of initial PCE saturation to the scaled pre-remedial aqueous PCE concentrations (R^2=0.40) for the full MLS data set. However, for several MLS wells there were stronger correlations. Figure 2-8 presents this relationship and illustrates the architecture of the Sages site. Subsurface DNAPL distributions are discontinuous at field sites, collecting on lower permeable layers. For MLS-2, MLS-4, MLS-6 and MLS-7, there were individual trends observed. In general, as the saturation of PCE in the subsurface increased in each well, the scaled PCE concentration in the remedial flow field increased. Although the highest PCE saturations were detected in MLS-4, the PCE concentration response was lower than that of MLS-6 and MLS-2. This may be attributed to greater fluid velocity in MLS-4. With the remedial flow field velocities achieved in MLS-4, equilibrium dissolution may not have been attained. This was likely manifested as reduced concentrations observed at MLS-4.

2.7 Ethanol Flushing Hydrodynamics

The limitation of alcohol flushing technology is the ability of the cosolvent to contact NAPL in the subsurface to enhance NAPL solubility. Ethanol is less dense than water, thus it tends to override lower depths when injected. The remedial design included the use of packers to selectively inject the 95% ethanol/5% water remedial solution to the lowest depth and slowly increase the injection depth upward over the first few hours [*Sillan*, 1999; *Jawitz et al*., 2000]. Ethanol arrival at each MLS well depth was highly variable, as was the concentration of ethanol reaching each zone. It has been established that both media permeability differences and DNAPL heterogeneity will impact the ability of cosolvents to flush each targeted region [*Sillan et al*., 1998]. Table 2-4 presents the peak ethanol concentration (*Pk* C_{ET}), the time to *Pk* C_{ET}, the peak PCE concentration (*Pk* C_{PCE}), and the time to *Pk* C_{PCE}.

Table 2-4. MLS cosolvent hydrodynamics for the 1998 ethanol flushing test at the Sages site.

MLS Well & Depth (m bgs)		*Pk* C_{ET} (mg/L)	*EtOH Tpk* (days)	*Pk* C_{PCE} (mg/L)	*PCE* T_{pk} (days)
MLS-1					
8.08 m		93.10	1.55	4593.69	2.03
8.46 m		80.66	1.55	23400.00	2.74
9.07 m		82.53	2.74	8891.92	3.99
9.45 m		79.26	2.74	2289.62	4.48
9.91 m		29.13	8.50	197.34	6.29
	Mean	**72.94**	**3.90**	**7874.51**	**3.41**
	Std Dev	25.09	1.65	9259.72	2.90
MLS-2					
8.08 m		100.44	2.74	503.17	1.13
8.46 m		99.60	2.23	3.13	1.39
9.07 m		97.29	1.84	6151.90	1.29
9.45 m		97.00	1.39	0.00	0.00
9.91 m		94.37	2.74	2.05	2.74
	Mean	**97.74**	**2.19**	**1332.05**	**1.63**
	Std Dev	2.39	0.58	2703.11	0.74
MLS-3					
8.08 m		95.53	1.84	2809.92	1.39
8.46 m		91.33	3.99	288.55	2.23
9.07 m		92.10	2.23	6666.38	1.84
9.45 m		87.01	4.48	46600.00	3.48
9.91 m		60.59	6.77	25100.00	6.77
	Mean	**85.31**	**3.86**	**16292.97**	**3.14**
	Std Dev	14.15	1.98	19536.41	2.17
MLS-4					
8.08 m		84.59	1.76	2.50	2.10
8.46 m		95.89	2.99	30200.00	1.72
9.07 m		93.31	2.47	15700.00	1.55
9.45 m		96.04	2.74	27200.00	1.55
9.91 m		89.33	3.74	48200.00	2.23
	Mean	**91.83**	**2.74**	**24260.50**	**1.83**
	Std Dev	4.87	0.72	17879.81	0.32
MLS-6					
8.08 m		88.64	2.47	546.02	3.23
8.46 m		91.60	1.84	7826.91	1.29
9.07 m		88.71	1.84	5362.88	1.13
9.45 m		80.43	4.48	2640.12	3.74
9.91 m		82.76	4.25	3106.13	3.74
	Mean	**86.43**	**2.98**	**3896.41**	**2.62**
	Std Dev	4.65	1.29	2785.11	1.31
MLS-7					
8.08 m		59.82	3.99	705.99	3.99
8.46 m		48.48	5.77	3112.63	6.29
9.07 m		63.15	4.80	558.75	4.80
9.45 m		58.51	5.77	2356.45	5.28
9.91 m		10.53	8.50	112.49	7.52
	Mean	**48.10**	**5.77**	**1369.26**	**5.58**
	Std Dev	21.70	1.70	1293.27	1.37

Lower maximum concentrations of ethanol were observed at the MLSs at the lowest depths throughout the remedial flow field. Furthermore, each of these locations received ethanol

later in the flood than the other depths. In most MLS locations, the time of peak PCE concentration was achieved prior to the arrival time of peak ethanol with the exception of the top-most sampling location where there was an observed delay. At MLS-1, peak PCE attainment time was slightly delayed compared to the peak ethanol appearance with only one exception, the lowest depth. The highest removal concentrations were detected in MLS-1, MLS-3, and MLS-4 by almost one order of magnitude.

Cumulative distribution functions (*CDF*s) were generated from the MLS flood results. Figure 2-9 presents the *CDF*s for the maxima of both the percent ethanol and the percent of PCE solubility achieved. This was the same process as the scaling performed on aqueous PCE concentrations in the source zone in sections 2.5, 2.6, and 2.10 except reported as a percent. Beginning with the PCE results, 60% of the MLSs achieved 10% or less of maximum solubility and 90% attained less than 50% of maximum solubility. While only 20% of the MLSs received less than 85% ethanol concentration. These results indicate that high concentrations of ethanol reached most MLS zones, but few achieved high maximum solubility percentages. Although it appears that remedial fluid interrogated the source zone thoroughly, PCE solubilization may be limited by additional factors besides merely the presence of cosolvent. The actual flow path of the remedial fluid in the subsurface is not known. Although high ethanol may reach a MLS, it did not have to contact PCE. As shown in Figure 2-5, higher PCE saturations were observed in regions of lower fluid velocities. This is a result of lower media permeability, resultant PCE pooling, and the dissolution removal of PCE in higher flow zones. Thus, the main limitation of solubility enhancement was demonstrated, the inability to contact and remove all DNAPL. However, this pilot test verified the ability of ethanol to enhance and deplete PCE in well flushed regions. This will be further explored below.

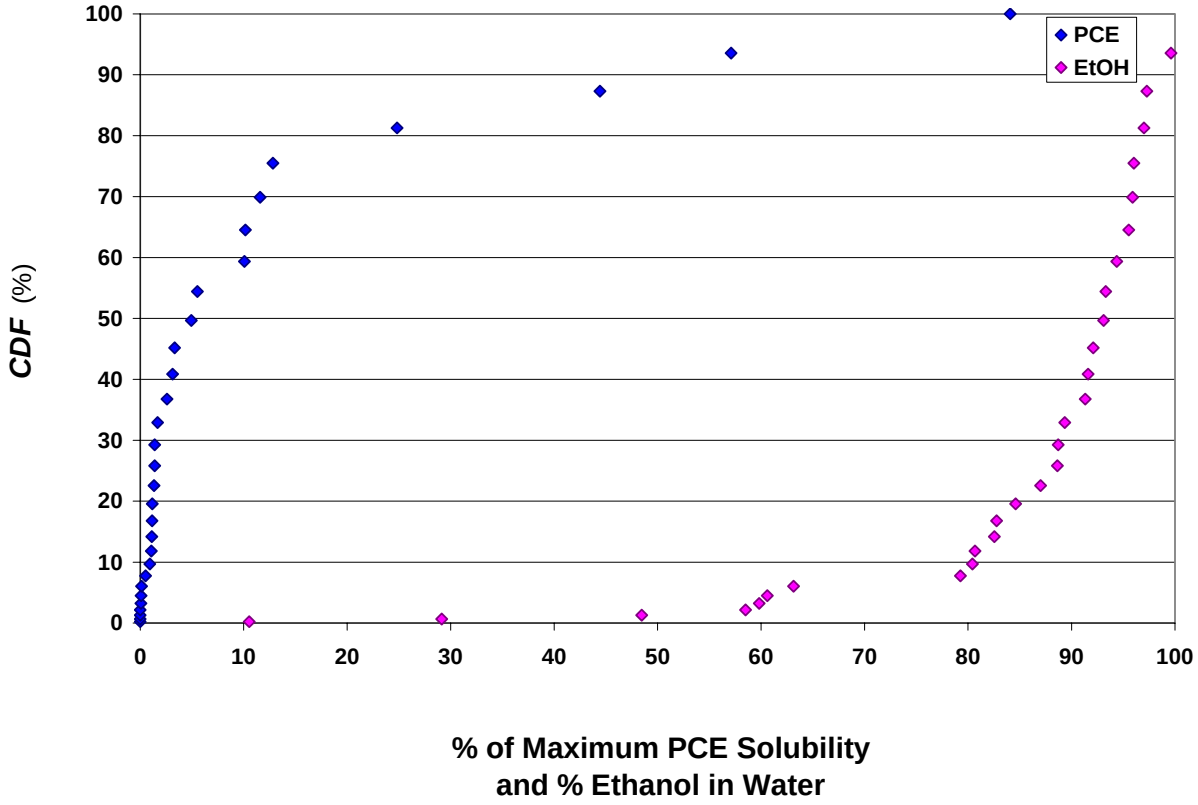

Figure 2-9. Sages 1998 ethanol flood cumulative distribution functions for MLS ethanol and PCE .

2.8 Post Remedial PITT

Following the ethanol flushing pilot test, a post PITT was conducted to determine the residual PCE saturations in the source zone. In this test, all the MLS wells received tracers except most of MLS-5 and the lowest depth of MLS-7. Table 2-5 below summarizes the results of the tracer test. PCE saturations were markedly reduced compared to the pre-remedial PITT. However, in the swept volume between IW-3 and RW-5, the PCE reduction seems to be lower, indicating an inability of remedial fluids to clean out that area, or the mobilization of NAPL into this region. In the upper depths, the highest SN values were observed in MLS-3 and MLS-4. In the mid-depths, PCE was not completely removed from MLS-1, MLS-3, and MLS-4. Finally, at

the bottom of the interrogated region, residual PCE was observed in the swept volume of MLS-7 and MLS-4.

Table 2-5. Percent PCE saturations from the post-flood PITT at Sages. No-value (nv) indicates insufficient tracers arrived at the well to resolve the PCE saturations. Column 2 is the RW and mean MLS results, the other columns are the specific MLS depth PITT results.

Well	Post PCE S_N	8.08 m	8.69 m	9.07 m	9.45 m	9.91 m
RW-2	0.124					
RW-3	0.109					
RW-4	0.146					
RW-5	0.231					
RW-6	0.108					
RW-7	0.146					
	Mean MLS					
MLS-1	0.166	0.154	0.313	0.158	0.112	0.092
MLS-2	0.117	0.096	0.173	0.150	0.074	0.091
MLS-3	0.187	0.207	0.257	0.182	0.137	0.150
MLS-4	0.267	0.103	0.252	0.159	0.195	0.624
MLS-5	nv	nv	0.146	0.072	nv	nv
MLS-6	0.133	0.120	0.170	0.103	0.118	0.154
MLS-7	nv	0.151	nv	0.156	0.464	nv

Post-remedial PITT PCE saturations are presented spatially using Surfer in Figure 2-10, the map view of the entire source zone shows RW and mean MLS results. Overall reductions in PCE saturation were observed throughout the source zone. The lower figures show map view depth slices of the MLS S_N results. There is some residual PCE in the upper swept zones traveling to MLS-1 and MLS-3 and higher residual saturations in the lower swept volumes of MLS-4 and MLS-7. The tracers did not arrive at 9.91 m bgs at MLS-7, but from the 9.45 m visualization, it can be expected that there is PCE there as well. Similar to the RW-5 and MLS-5 situation, not only did tracers not appear at RW-7 and MLS-7 at the lowest depth, but remedial fluids did not thoroughly flush this zone due to inferred lower hydraulic conductivity.

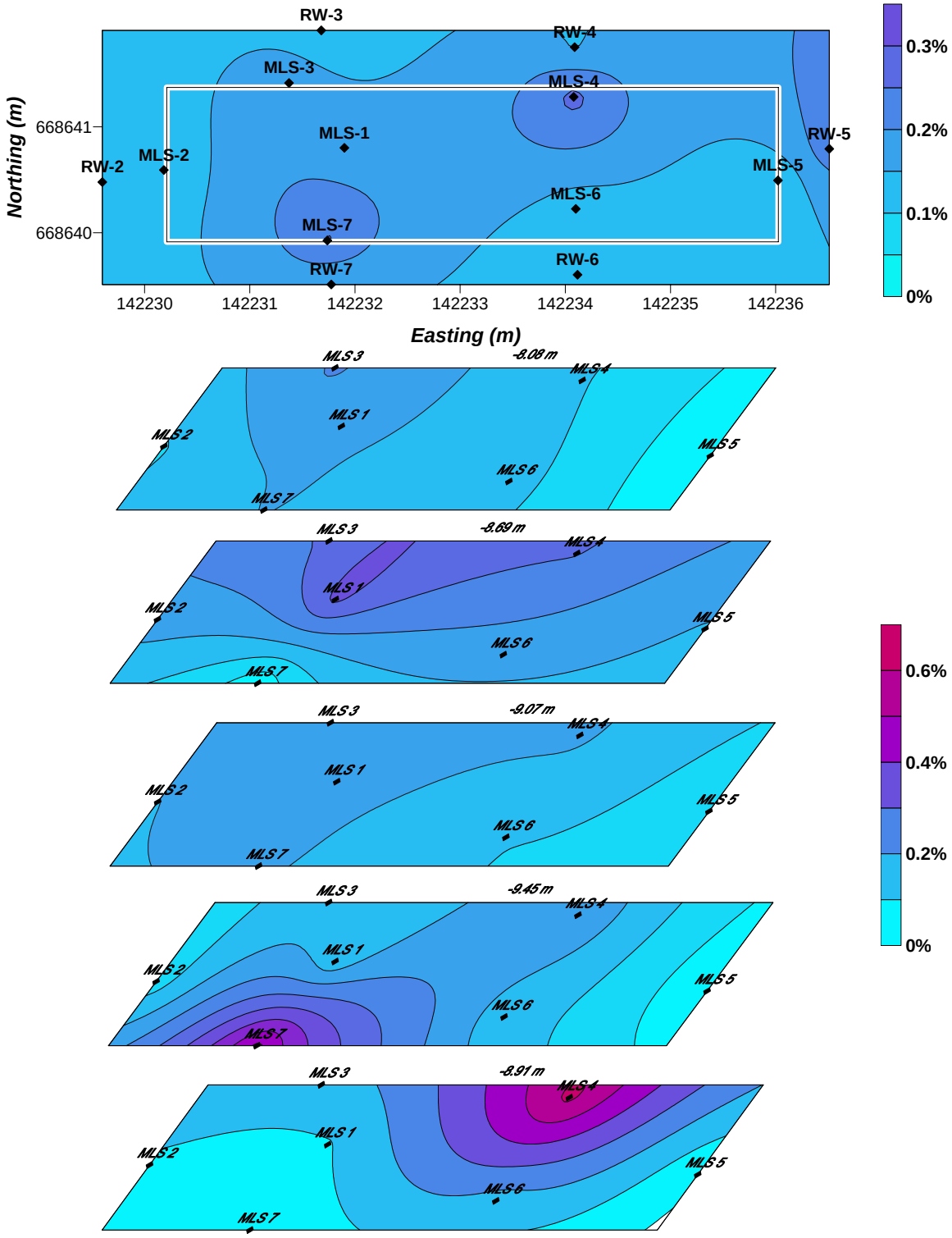

Figure 2-10. Map view of % PCE saturation Surfer visualization of the source zone from post-remedial PITT. On top is the recovery well and mean MLS S_N for each location. Below is S_N from MLS: 8.08, 8.69, 9.07, 9.45, & 9.91 m bgs. White areas are no data.

One of the benefits of MLS PITT resolution is that residual contaminants can be depth identified. There seems to be residual PCE hot spots in the tracer swept zones from IW-1 to MLS-1 and MLS-3 and from IW-3 to MLS-4 for the area between 8.0 and 8.7 m bgs. The greatest residual PCE was detected in the lower swept zones of IW-1 to MLS-7 and IW-3 to MLS-4. This information would allow future corrective action to focus efforts on the areas of highest source zone residual saturation.

2.9 Estimated Mean Arrival Times

After the post-remedial PITT, a comparison of conservative tracer mean arrival times was possible. Figure 2-11 shows the relationship of the pre-remedial non-partitioning tracer (MeOH) to the post (HexOH).

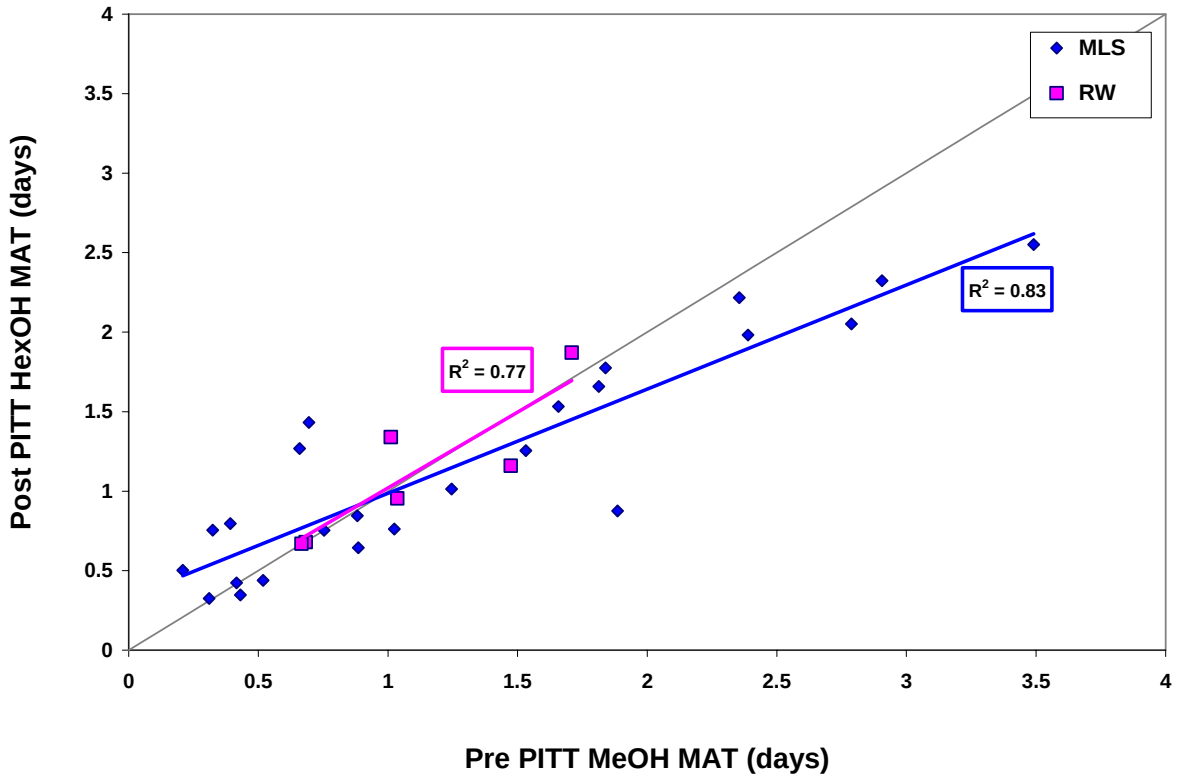

Figure 2-11. Comparison of pre and post remedial conservative tracer mean arrival times at Sages. The blue points are the MLS data and the pink are the RW results. The gray line is $\tau_{pre} = \tau_{post}$.

For the MLSs, the pre-PITT non-partitioning tracer took longer to arrive than the post-PITT tracer at higher velocity locations, yet at the lower velocity locations more of the post-PITT tracers arrived at similar times or earlier than the pre-remedial conservative tracers. Because the low-velocity locations generally had higher NAPL saturations, due to less natural-gradient dissolution, these results may indicate the effect of NAPL removal during remediation on the relative permeability field. The RW non partitioning tracers arrived at more similar times. From the resultant MLS correlation equation, mean arrival times for the conservative tracer could be estimated in the pre-PITT that did not originally resolve.

From the estimated mean arrival times calculated from the correlation in Figure 2-11, estimated fractional NAPL removal, and finally estimated initial PCE saturation was determined. This method is described in Section 2.12.

2.10 Residual Ethanol

As documented by Sillan [1999] and Jawitz et al. [2000], an estimated 2.7 kL of the 34 kL of ethanol injected into the source zone was not recovered during the flood and subsequent water flushing. The allotted residual ethanol for the RWs, mandated by FDEP, was to be less than 1%. Thus, five days of water flooding followed the ethanol flood and all RWs were observed to meet this criteria in Table 2-6.

RW and MLS well detected ethanol concentrations did not agree. MLS wells the recorded ethanol in the post-flood flow field recorded significantly higher results. However, several MLS wells detected no ethanol while there coupled RW received low ethanol concentrations. The highest recorded concentrations were located at MLS-1 and MLS-5. MLS-1 was located in a flow field low flow zone between IW-1 and IW-2, while MLS-5 was coupled

to RW-5 which was a greater distance from IW-3 than MLS-4 or MLS-6 and the extraction rate was lower.

Table 2-6. Percent ethanol remaining in Sages source zone groundwater after flushing. MLS sampling depths are meters below ground surface.

Well	Post C_{ET} (%)	8.08 m (%)	8.69 m (%)	9.07 m (%)	9.45 m (%)	9.91 m (%)
RW-2	0.759					
RW-3	0.881					
RW-4	0.602					
RW-5	0.550					
RW-6	0.473					
RW-7	0.617					
	Mean MLS					
MLS-1	7.790	0.000	4.907	5.957	10.269	17.817
MLS-2	0.000	0.000	0.000	0.000	0.000	0.000
MLS-3	1.379	0.000	0.065	2.068	0.924	3.836
MLS-4	0.000	0.000	0.000	0.000	0.000	0.000
MLS-5	9.066	0.014	5.623	16.71	12.814	10.167
MLS-6	1.597	0.000	0.000	0.011	2.073	5.913
MLS-7	3.098	0.217	4.926	4.728	1.692	3.929

It was observed that the upper zone (8.08 m bgs) had been essentially flushed out of remedial fluids by the five days of post-ethanol injection water flooding. There is up to 6 % unrecovered ethanol in the middle depths at MLS-1, MLS-3, and MLS-7, except in MLS-5 where concentrations were measured to be 16.7%. In the lower depths, higher residual levels of ethanol were observed at MLS-1, MLS-3, MLS-5 and MLS-6, in the range of 3.8 to 17.8%. MLS-7 also contained high concentrations in the mid-depths and the deepest, from 1.7 to 4.9%. MLS-2 and MLS-4 indicated no residual ethanol at any depths.

In Figure 2-11 below, the unrecovered ethanol in the source zone is displayed as a series visualizations. Again, the upper picture is the RW and mean MLS values while the lower map view plots are the values for each respective MLS well and depth. It was observed that residual ethanol concentrations increased with depth in all but MLS-5 where the highest amounts were detected in the middle depth of 9.07 m bgs.

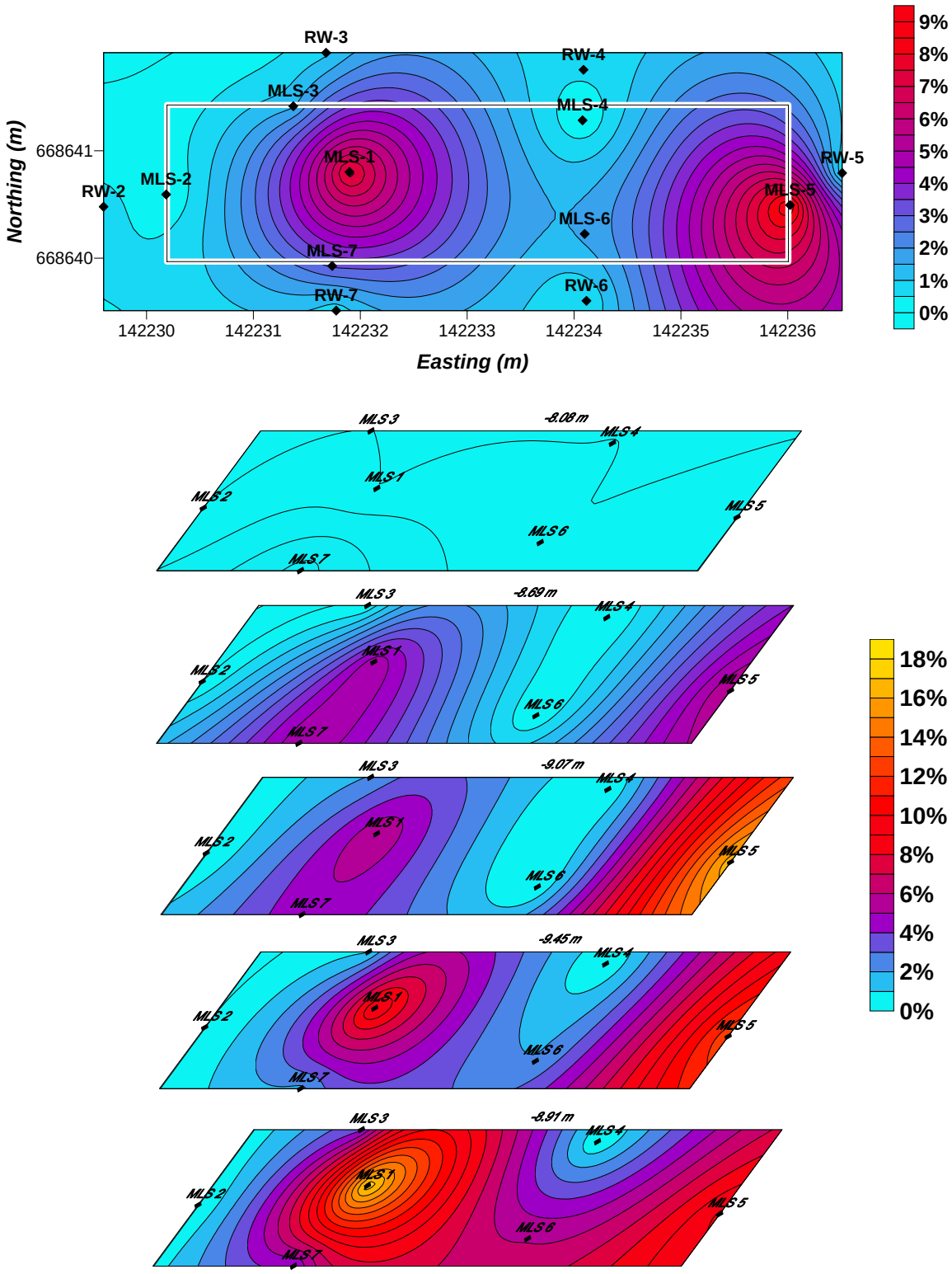

Figure 2-12. Map view Surfer visualizations of % ethanol in the Sages source zone. On top is the recovery well and average MLS values for each well location. Below is the % ethanol in MLS wells at depths of 8.08, 8.69, 9.07, 9.45, & 9.91 m bgs.

Most significant residual ethanol was found in MLS-1, MLS-5, and MLS-7. MLS-2 and MLS-4 appeared to have had most of their remedial fluids recovered throughout their sampling zones.This corresponding increase in concentration with depth parallels the decrease in remedial flow field fluid velocity with depth in Figure 2-2. This relationship is explored in Figure 2-13.

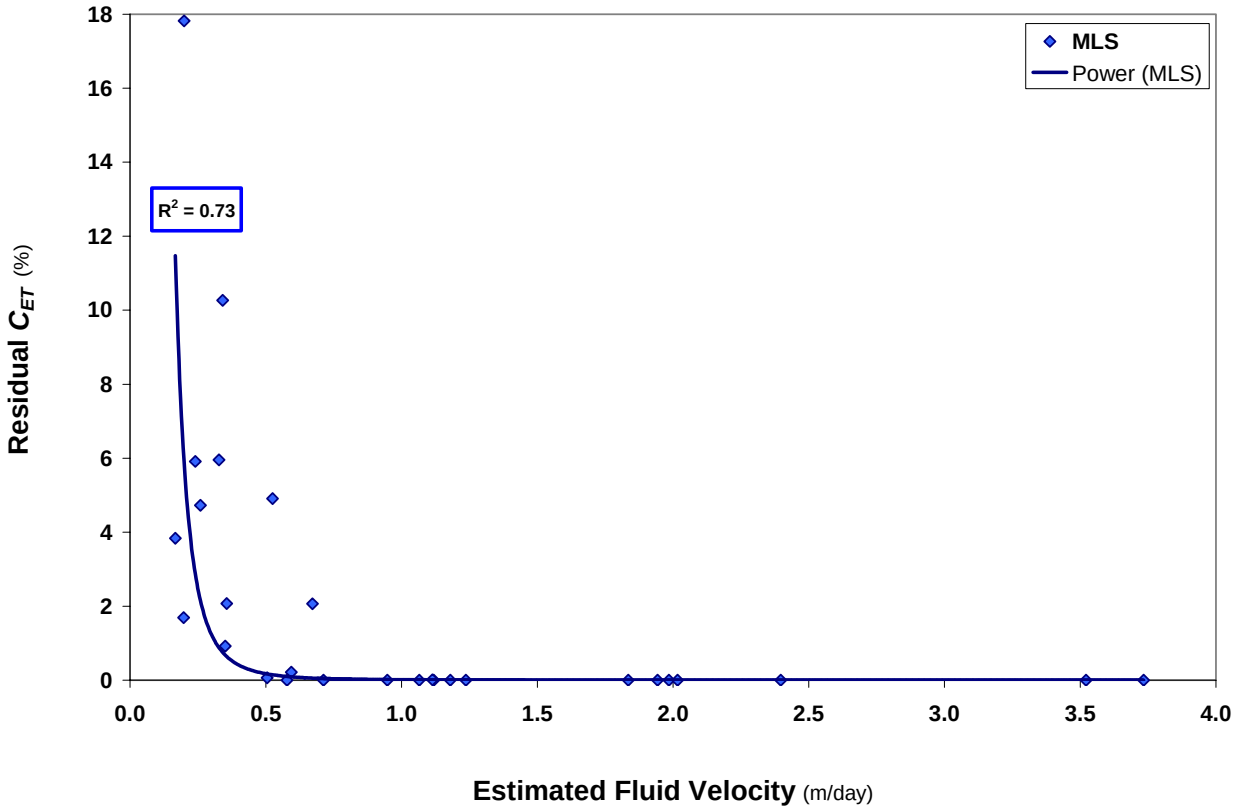

Figure 2-13. Comparison of estimated fluid velocity in remedial flow field to percent residual ethanol concentration at Sages. Fit line is a power function.

The wells and depths with the highest estimated fluid velocities (refer to Figure 2-2), indicate no residual ethanol at any depth including MLS-2, MLS-4, and the upper and middle levels of MLS-6. There appears to be a threshold remedial fluid velocity between 0.5 and 0.8 m/day where below this velocity, ethanol was unable to be completely recovered over the 8 day time period of the 1998 test.

2.11 Post-remedial PCE Concentrations

The ethanol data provided in the previous section was used to scale the post remedial PCE concentrations to the maximum PCE solubility to account for the effect of residual ethanol on PCE solubility enhancement. A summary is provided in Table 2-7 below.

Table 2-7. Scaled PCE concentrations from the post-flood flow field sampling. MLS sampling depths are meters below ground surface.

Well	Post C_{PCE}	8.08 m	8.69 m	9.07 m	9.45 m	9.91 m
RW-2	0.089					
RW-3	0.078					
RW-4	0.043					
RW-5	0.009					
RW-6	0.081					
RW-7	0.140					
	Mean MLS					
MLS-1	0.097	0.003	0.000	0.329	0.009	0.144
MLS-2	0.017	0.066	0.007	0.003	0.005	0.005
MLS-3	0.086	0.010	0.001	0.012	0.013	0.392
MLS-4	0.003	0.000	0.003	0.002	0.002	0.006
MLS-5	0.182	0.000	0.208	0.158	0.350	0.194
MLS-6	0.007	0.001	0.003	0.003	0.008	0.022
MLS-7	0.271	0.030	0.803	0.008	0.046	0.469

In the RW samples, most of the wells showed significant decreases in scaled aqueous PCE concentrations than their respective pre-remedial levels. The exception was RW-5 and RW-7 which increased very slightly. The MLS results also showed decreases in all wells except MLS-5.

The Surfer visualization of the data in Table 2-7 is shown below in Figure 2-14. The top plot is the RW and average MLS values in map view, while the lower slices are the MLS data at their respective depths, also in map view. The upper depth of 8.08 m bgs showed very little soluble PCE. This can be attributed to higher fluid flow rate and very low of residual PCE saturation at this depth.

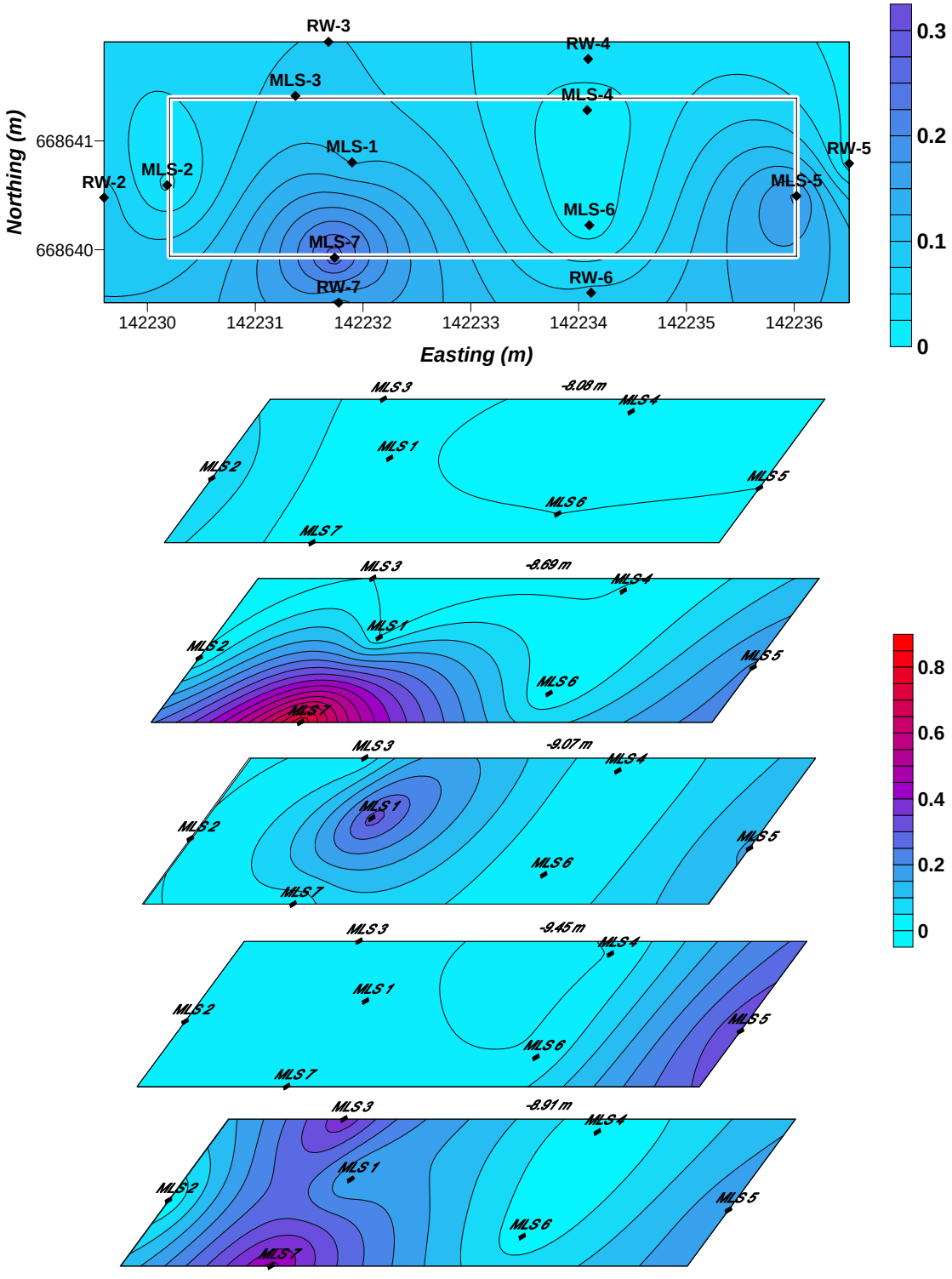

Figure 2-14. Surfer visualizations of Sages post remedial source zone maximum solubility scaled aqueous PCE concentrations in map view. Top figure is RW and mean MLS values. Lower figures are depth values at 8.08, 8.69, 9.07, 9.45, and 9.91 m bgs.

In the upper middle depth of 8.69 m bgs, it was observed that MLS-7 had considerably higher PCE concentrations than the other wells at most other depths, up to a 0.8 fraction of maximum PCE solubility. This was not a recorded hot spot of residual PCE saturation because either blockage or extremely low flow here prevented tracer arrival. It is likely that this level contained high residual PCE. There was about 5% of ethanol remaining in this region, as shown earlier. One level lower (9.07 m bgs), only MLS-1 contained elevated PCE. This was a high initial concentration area, and had about 6% residual ethanol, but only about 0.3 % residual PCE saturation. In the lower depths, MLS-5 was observed to have moderate PCE concentrations (0.35 fraction of C_{max}) at the 9.07m bgs depth, and both MLS-3 and MLS-7 had PCE in the 0.39 to 0.47 fraction of its maximum solubility.

2.12 NAPL Removal

From an initial and post-remedial PITT, the fractional NAPL removal (*FNR*) can be quantified from a modification of Eq. 1-15. Since mass was not able to be directly calculated from MLS data, the pre ($S_{N,i}$) and post ($S_{N,f}$) PCE saturations can be substituted.

$$FNR = \left(1 - \frac{S_{N,f}}{S_{N,i}} \right) \tag{2-3}$$

The summary of FNR calculations are presented in Table 2-8. Two MLS wells reported lower *FNR* than their coupled RWs, RW-2 and MLS-2, and RW-6 and MLS-6. One MLS well demonstrated significantly higher *FNR*, for RW-4 and MLS-4. Neither MLS-5 nor MLS-7 received sufficient tracers to report *FNR* values for all their respective depths, as stated earlier. There was possible evidence of PCE mobilization into the 8.08 m bgs depth of MLS-7, as it was the only MLS recording a negative *FNR* value, due to an increase in post-flood PCE saturation. It is possible that other depths of MLS-7 or MLS-5 may have shown similar results, but that cannot be more than speculated. In most MLS wells and depths, it was observed that PCE

removal decreased with depth increase. This is likely due to low estimated remedial fluid velocity at this depth of this test; that is, the inability of remedial fluids to thoroughly penetrate the lowest MLS depth.

Table 2-8. Fractional NAPL removal from RW and MLS well tracer tests at Sages. MLS sampling depths are meters below ground surface.

Well	*FNR*	8.08 m	8.69 m	9.07 m	9.45 m	9.91 m
RW-2	0.615					
RW-3	0.802					
RW-4	0.380					
RW-5	0.594					
RW-6	0.547					
RW-7	0.750					
	Mean MLS					
MLS-1	0.547	0.885	0.708	0.495	0.481	0.166
MLS-2	0.384	0.800	0.121	0.779	0.016	0.204
MLS-3	0.626	0.804	0.030	0.605	0.912	0.778
MLS-4	0.637	0.037	0.653	0.828	0.904	0.762
MLS-5	nv	nv	nv	nv	nv	nv
MLS-6	0.135	0.667	0.853	0.942	0.749	0.135
MLS-7	nv	-1.287	nv	0.137	0.089	nv

The effect of initial PCE saturation on the resultant *FNR* was evaluated graphically. Figure 2-15 demonstrates that as initial PCE saturation increased, the mass removal effectiveness was also increased for the Sages ethanol flood test. The fit line was generated using the Langmuir Equation with a $1/FRN$ to $1/\%S_N$ linear relationship. The Pearson product correlation coefficient for that plot was 0.90. This correlation identified that for this ethanol flushing test, the remedial flow field removed much of the regions of high PCE saturation in only a few days. Although the lower initial saturation zones achieved some DNAPL removal, the fraction of that removal was smaller than higher pre-S_N wells and depths. In regions of high initial saturation, there may be greater post-remedial PCE than low saturation zones, but the fraction of removal was considerably higher.

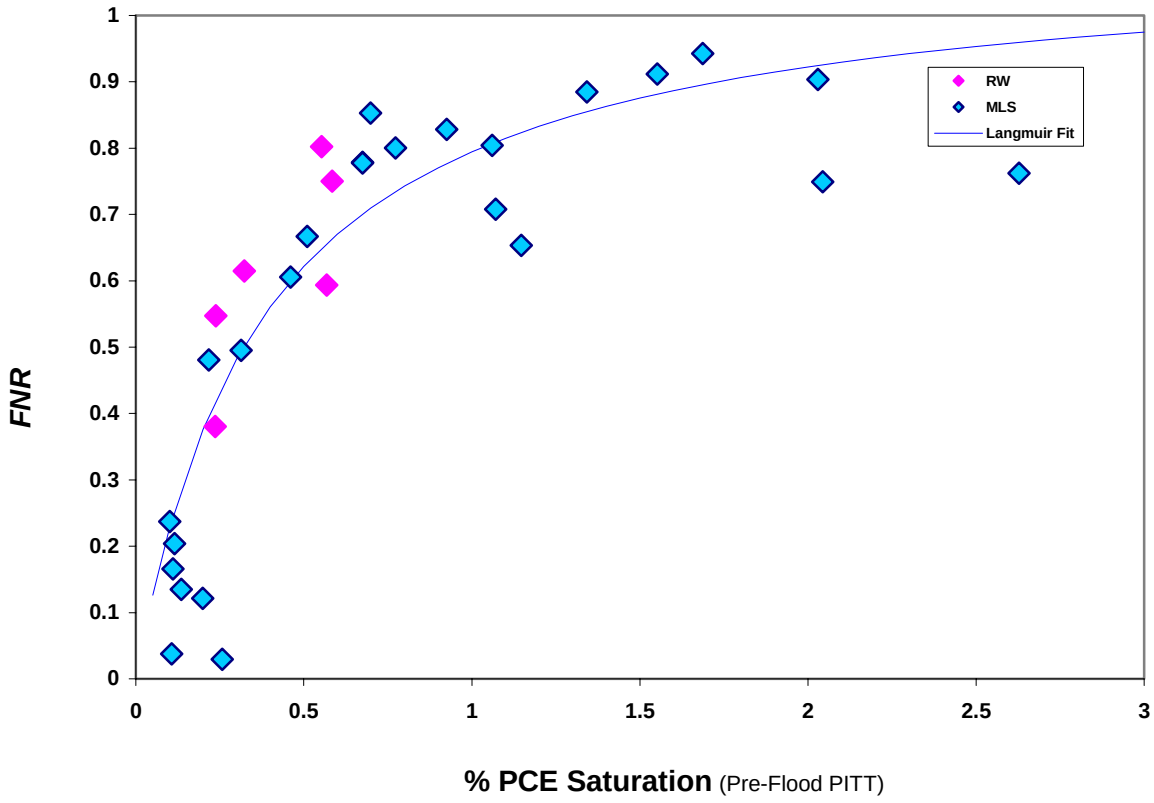

Figure 2-15. Fractional NAPL removal (FNR) as a function of initial PCE saturation from the 1998 ethanol flood at the Sages site.

PCE can be adsorbed to aquifer media, but much more was likely present as a separate phase that was held tightly by capillary forces. Since the goal of this remedial effort was enhancing solubility, the IFT of PCE and water was not intentionally reduced to limit PCE mobilization. Without a significant decrease in IFT, entrapped residual PCE bound by capillary forces cannot be overcome and some residual PCE will remain. The process becomes diffusion limited. Thus lower saturation zones exhibited lower *FNR* at Sages.

Although *FNR* in Figure 2-15 and estimated fluid velocity in Figure 2-5 both separately demonstrated correlations to initial PCE saturation at the Sages site, these two parameters were not correlated.

Estimated NAPL removal (*ENR*) was determined from the amount removed in the flood, the post-remedial saturations, and the mean arrival time of the post-flood conservative tracer. First, each MLS the ethanol flood BTC was numerically integrated using the trapezoidal method, resulting in [(mg/L)*T] units. The density of PCE (ρ_{PCE}) is 1.62 g/cm^3

$$ENR = \left(\frac{\int C_{PCE} dT}{\left(S_{N,f} \bullet \tau_n \bullet \rho_{PCE} \right) + \int C_{PCE} dT} \right) \quad (2\text{-}4)$$

The *ENR* moderately correlated with *FNR* determined directly from the PITT (R^2=0.64). The *ENR* calculations were then employed to back-calculate initial PCE saturation using Eq. 2-3. These results are included in Table 2-2 and indicated with asterisks.

2.13 Flux Reduction

In the remedial induced flow field, groundwater concentration data was scaled to the PCE maximum solubility. By comparing the initial scaled concentrations to the post-remedial scaled concentrations, we can calculate a fractional flux reduction (*FFR*) using the left side of Eq. 1-15. Table 2-9 summarizes the RW and MLS flux reductions as a result of this pilot test.

Table 2-9. Fractional flux reduction (*FFR*) based on scaled PCE concentrations from RW and MLS wells. MLS sampling depths are meters below ground surface.

Well	*FFR*	8.08 m	8.69 m	9.07 m	9.45 m	9.91 m
RW-2	0.785					
RW-3	0.736					
RW-4	0.605					
RW-5	-0.311					
RW-6	0.462					
RW-7	-0.273					
	Mean MLS					
MLS-1	0.682	0.994	0.999	0.411	0.936	0.068
MLS-2	0.948	0.906	0.988	0.996	0.970	0.881
MLS-3	0.823	0.967	0.998	0.977	0.194	0.981
MLS-4	0.989	1.000	0.987	0.989	0.993	0.975
MLS-5	-19.285	1.000	-1.092	-0.333	-14.037	-81.964
MLS-6	0.980	1.000	0.989	0.994	0.954	0.963
MLS-7	0.492	0.862	-0.425	0.968	0.796	0.258

With the exception of RW-5 and RW-7, the RWs demonstrated fractional flux reductions from 0.46 to 0.78. The average MLS values ranged from 0.49 to 0.99 with the exception of MLS-5 which showed large increases in PCE concentration as depth increased. This could be an indication of PCE mobilization into the flow zone between IW-3 and MLS-5/RW-5. Generally, flux reductions decreased with depth increase in the MLS results. However, in MLS-7 the flux increased at 8.69 m bgs. In the mid to lower-middle depths, MLS-1 and MLS-3 showed less reduction in PCE concentration than other wells. For the entire data set, there was a weak correlation between flux reduction and initial PCE saturation, unlike fractional NAPL removal (Figure 2-15). Furthermore, there was no relationship of initial PCE aqueous concentration to *FFR*.

The results of the fractional NAPL removal and fractional flux reductions will be further assessed in Chapter 4 in section 4.3, the benefits of ethanol flushing.

CHAPTER 3
LONG TERM MONITORING

3.1 MLS Monitoring

The multilevel wells were sampled semi-annually for the six-year period following the 1998 ethanol flood pilot test. This included the downgradient MLS installed after the remedial effort, as well as the previously installed source zone MLS. The MLS orthogonal to the mean groundwater flow in the source zone will be referred to as the source zone transect. The MLS perpendicular to groundwater flow ten meters downgradient from the source zone will be designated the downgradient transect. MLS monitoring ceased at the initiation of Phase II flushing in 2004.

Normal groundwater flow was assumed to initiate following the cessation of the pilot test, but not to fully dominate the region until at least four months post-flood, December 1998. All the data in this chapter will be termed natural gradient flow, contrasted to Chapter 2, where all sampling was in the remedial flow field induced by the injection and extraction of the source zone well system.

The long term MLS monitoring was performed to assess the changes in concentration throughout the site over the stated time period. Spatial patterns of the dissolved plume emanating from the source zone will be discussed as well as mass discharge estimates across the transects. The concentrations will be reported as the molar sum concentration due to the initiation of microbial reductive degradation of residual PCE evidenced by increases in PCE biodegradation daughter products. The biological dehalogenation or dehalorespiration of PCE follows the following pathway.

$$PCE \rightarrow TCE \rightarrow DCE \rightarrow VC \rightarrow ethene \qquad (3\text{-}1)$$

The spatial evaluation of contaminant concentrations and the assessment of source strength will be calculated on a molar sum basis to account for all the chlorinated species in the degradation pathway in Eq. 3-1. Each of these chemicals is highly toxic and is a known or suspected carcinogen. Thus, the molar sum of all chlorinated ethenes was calculated for each location and respective sampling time. The concentrations in the groundwater samples were converted to molar concentrations. Each measured concentration in mg/L was divided by its molar mass to give mmol/L or mM units. The molar mass values of PCE, TCE, DCE, and VC used were 165.85, 131.4, 96.95, and 62.5 mg/mmol respectively. The entire suite of chlorinated species was then summed to calculate the molar sum concentration in each sample location to determine the total downgradient risk for any sampling time.

Although the concentration of each species is valuable, the total risk to downgradient receptors was one of the primary focuses of this thesis. Mass flux and mass discharge are increasingly being used as a measure of site risk and as a metric for remedial performance [*EPA*, 2003; *Stroo et al*., 2003; *NRC*, 2005]. At the Sages site, the rate of mass flux across the source zone transect was evaluated for the six-year sampling period. Mass flux rate is also called mass discharge and source strength thus these terms may be interchanged in the following discussion.

Estimating mass discharge required calculating the mean of the molar concentration sum of all the depths and locations in the MLS transect, the Darcy flux, and the cross sectional area of the transect. This method weights all sampling points equally and does not factor in groundwater flow variability. However, with these limitations in mind, this estimation method can elucidate changes in mass discharge across a control plane.

Mass discharge estimates at the Sages site were determined from a modification of Eq 1-14. For this study each sampling node was weighted equally. The mean molar concentration

sum of each transect was calculated and then M_d was the determined from the product of the site estimated Darcy flux and the cross sectional area of each transect.

$$M_d = \bar{C}_{sum} \bullet \bar{q} \bullet A_{xs} \qquad (3\text{-}2)$$

The site characterization estimates for hydraulic conductivity (6 m/year) and hydraulic gradient (0.0025) were used to estimate the site Darcy flux ($\bar{q}$) of 0.015 m/day. The mean mass flux ($\bar{J}$) was calculated using Eq. 1-13, the product of $\bar{C}_{sum}$ and $\bar{q}$. The mass discharge was determined from the product of the mass flux and the cross sectional area of the transect (A_{xs}) using the modified version of Guillbeault et al.[2004] and Kubert and Finkel [2006] in Eq. 3-2.

The cross sectional area interrogated by the MLS sampling in the source zone transect was estimated to be 4 m^2, and 14 m^2 in the downgradient transect. Source zone MLS sampling points defined a length and depth of 1.49 m and 1.83 m respectively. The sampling volume was assumed to extend six inches (0.15 m) on either side and both top and bottom of the MLS transect, thereby giving a cross sectional area of approximately 4 m^2. For the downgradient transect this same approach yielded a control plane cross sectional area estimate of 14 m^2. The results of mass discharge study are presented in sections 3.5 and 3.6.

3.2 Source Zone Residual Ethanol

In Table 3-1, the subsurface ethanol concentrations in the source zone transect are reported. Ethanol was monitored for the first nine months, but then was not assessed again until 2002, nearly four years later. By then, under 1% ethanol was detected at all MLS locations. By 2003, very little ethanol remained in the source zone, 1.6 mg/L or less.

The decrease of ethanol over time provided evidence of microbial use of ethanol and the return of natural gradient groundwater flow. Mravik at al., [2003] reported increases of acetate as ethanol concentrations decreased due to the microbial oxidation of ethanol. Furthermore,

ethanol is non-partitioning and completely miscible, thus it will be slowly carried away by the site groundwater velocity. As ethanol was removed from the source zone by natural gradient flow and microbial degradation, daughter products of PCE dechlorination were detected.

Table 3-1. Measured ethanol concentrations in the source zone transect at Sages.

Well	Depth m bgs	12/1998 (%)	01/1999 (%)	02/2002 (%)	10/2002 (%)	10/2003 (%)
MLS-1	8.08	0.029	0.000	0.0037	0.0006	0.00000
	8.69	0.330	0.152	0.4260	0.1475	0.00014
	9.07	1.449	1.381	0.2486	0.1328	0.00016
	9.45	0.139	0.080	0.0464	0.0004	0.00006
	9.91	3.283	2.243	0.0407	0.0009	0.00001
Mean		**1.046**	**0.771**	**0.1531**	**0.0565**	**0.00007**
Std Dev		1.373	0.999	0.1802	0.0766	0.00007
MLS-3	8.08	0.041	0.352	0.0165	0.0001	0.00000
	8.69	1.185	1.260	0.0882	0.0640	0.00002
	9.07	3.095	4.584	0.0087	0.0133	0.00000
	9.45	2.333	1.299	0.0488	0.0017	0.00000
	9.91	5.650	5.999	0.0459	0.0016	0.00000
Mean		**2.461**	**2.699**	**0.0416**	**0.0161**	**0.00000**
Std Dev		2.126	2.449	0.0314	0.0273	0.00001
MLS-7	8.08	0.332	0.094	0.0000	0.0000	0.00000
	8.69	1.146	0.484	0.0221	0.0005	0.00000
	9.07	1.755	1.833	0.0370	0.0009	0.00000
	9.45	1.496	0.493	0.0680	0.0006	0.00000
	9.91	0.582	0.262	0.3375	0.0002	0.00000
Mean		**1.062**	**0.633**	**0.0929**	**0.0004**	**0.00000**
Std Dev		0.600	0.691	0.1389	0.0003	0.00000

There appeared to be a threshold toxicity of ethanol on the microbial population. Once the ethanol concentration dropped below 1%, there were increases in TCE concentrations in groundwater flowing across the transect. This is consistent with Mravik et al. [2003]. They reported laboratory column degradation of PCE in Sages site materials when the ethanol concentration was less than 1%. In Figure 3-1, the ethanol and TCE concentration is plotted for the December 1998 sampling.

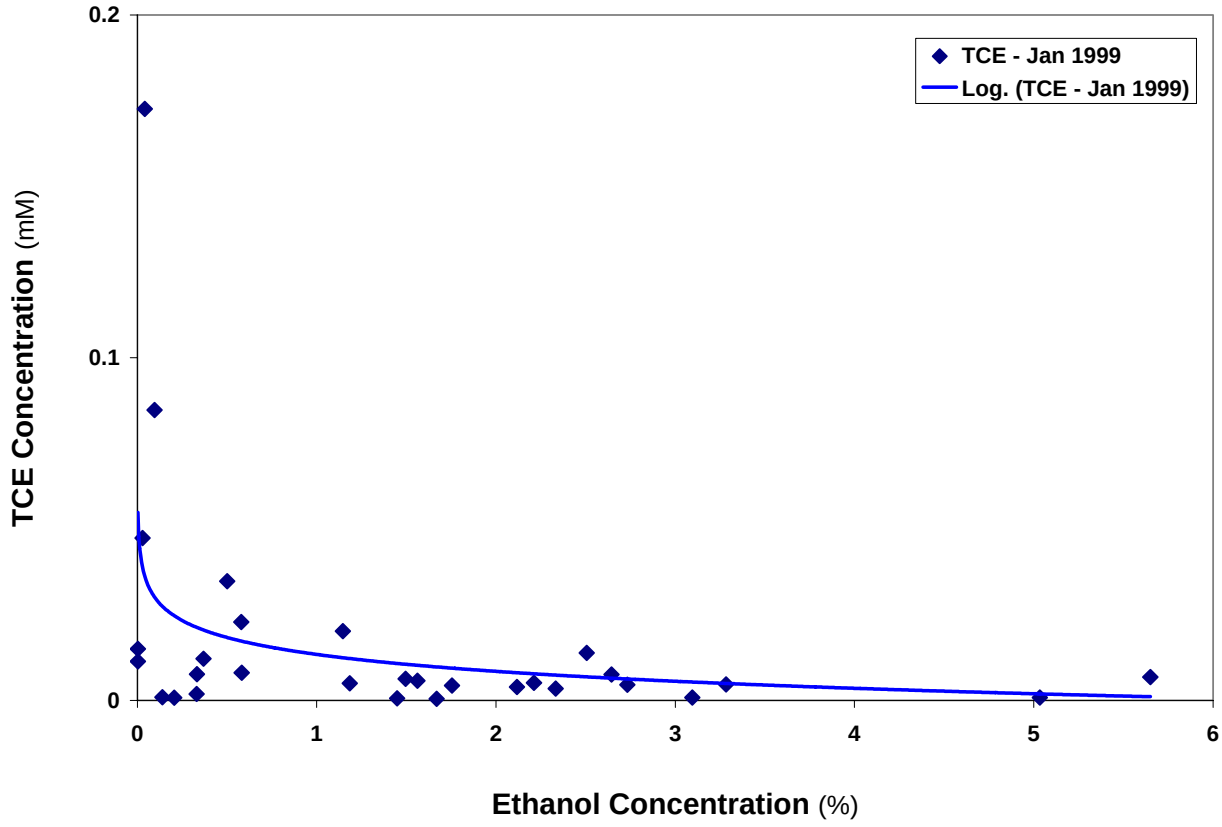

Figure 3-1. December 1998 MLS source zone TCE concentration as a function of ethanol concentration in the subsurface groundwater.

3.3 Source Zone Transect Concentrations

The source zone concentrations were monitored for the six-year period after the flushing pilot test at the MLS wells. Across the source zone transect created by MLS-1, MLS-3, and MLS-7, the concentration of PCE, TCE, DCE, and VC was determined for each well and depth. The data for each of the chlorinated species is available in Appendix C. Table 3-2 presents a summary of the molar sum results, using the method described earlier.

For the first year after the flood, the mean molar sum in each MLS showed little variability. The source zone transect MLS detected a slight increase in molar concentrations in January 1999, 5 months after the flood. By May 2000, the mean concentration molar sum began to increase significantly. In 2002, the concentrations increased markedly and then began to

decrease in 2003. By 2004 further decreases were observed at levels much lower than the initial post flushing concentrations. A paired t-test of the data demonstrated that the molar sum of concentrations in June 2004 were statistically different from the initial molar sum in September 1998. Several plausible explanations for the significant decrease in source zone concentration include, source mass depletion, aging of the source zone, and decrease of microbial activity due to loss of ethanol substrate.

Table 3-2. Sages source zone transect natural gradient concentration. Values are molar sum of all chlorinated species in mM. Transect is MLS-1, MLS-3, MLS-7.

Well	**Depth m bgs**	**12/1998** (mM)	**01/1999** (mM)	**05/1999** (mM)	**05/2000** (mM)	**03/2001** (mM)	**02/2002** (mM)	**10/2002** (mM)	**10/2003** (mM)	**06/2004** (mM)
MLS-1	8.08	0.654	0.649	0.427	0.578	0.336	0.040	0.011	1.147	0.053
	8.69	0.509	0.592	0.393	1.053	0.789	1.037	1.777	1.245	0.594
	9.07	0.600	0.696	0.650	0.926	0.811	0.680	1.332	0.497	0.123
	9.45	0.555	0.596	0.422	0.672	0.246	0.516	0.712	1.165	0.347
	9.91	0.326	0.547	0.388	0.471	0.330	0.933	1.054	0.033	0.306
Mean		**0.529**	**0.616**	**0.456**	**0.740**	**0.502**	**0.641**	**0.977**	**0.817**	**0.285**
Std Dev		0.126	0.058	0.110	0.243	0.274	0.394	0.666	0.532	0.212
MLS-3	8.08	0.340	0.359	0.200	0.556	0.316	0.000	0.005	0.749	0.159
	8.69	0.494	0.490	0.640	1.201	0.742	0.936	1.258	0.575	0.230
	9.07	0.562	0.756	0.802	1.030	0.777	0.743	1.235	0.570	0.403
	9.45	0.513	0.585	0.523	1.057	0.555	0.940	0.909	0.905	0.270
	9.91	0.580	0.685	0.518	1.028	0.648	0.361	1.593	0.053	0.073
Mean		**0.498**	**0.575**	**0.537**	**0.974**	**0.607**	**0.596**	**1.000**	**0.570**	**0.227**
Std Dev		0.095	0.157	0.220	0.245	0.185	0.408	0.607	0.321	0.124
MLS-7	8.08	0.060	0.066	0.110	0.335	0.180	0.111	0.136	0.519	0.117
	8.69	0.710	0.839	0.760	1.222	0.540	1.048	0.833	0.182	0.224
	9.07	0.186	0.218	0.197	0.438	0.572	0.907	1.264	0.253	0.260
	9.45	0.402	0.338	0.200	0.301	0.393	0.683	1.005	0.262	0.142
	9.91	0.672	0.987	0.823	1.105	1.027	0.307	1.899	0.000	0.198
Mean		**0.406**	**0.490**	**0.418**	**0.680**	**0.542**	**0.611**	**1.028**	**0.243**	**0.188**
Std Dev		0.288	0.402	0.343	0.446	0.312	0.396	0.642	0.187	0.059

Surfer^{TM} was used to create visualizations of the source zone transect molar sum of chlorinated species. In Figure 3-2, the concentrations in the cross section listed in Table 3-1 are presented. As before, standard kriging was applied to interpolate between measured data points. The black plus (+) marks indicate the location of each MLS sampling point.

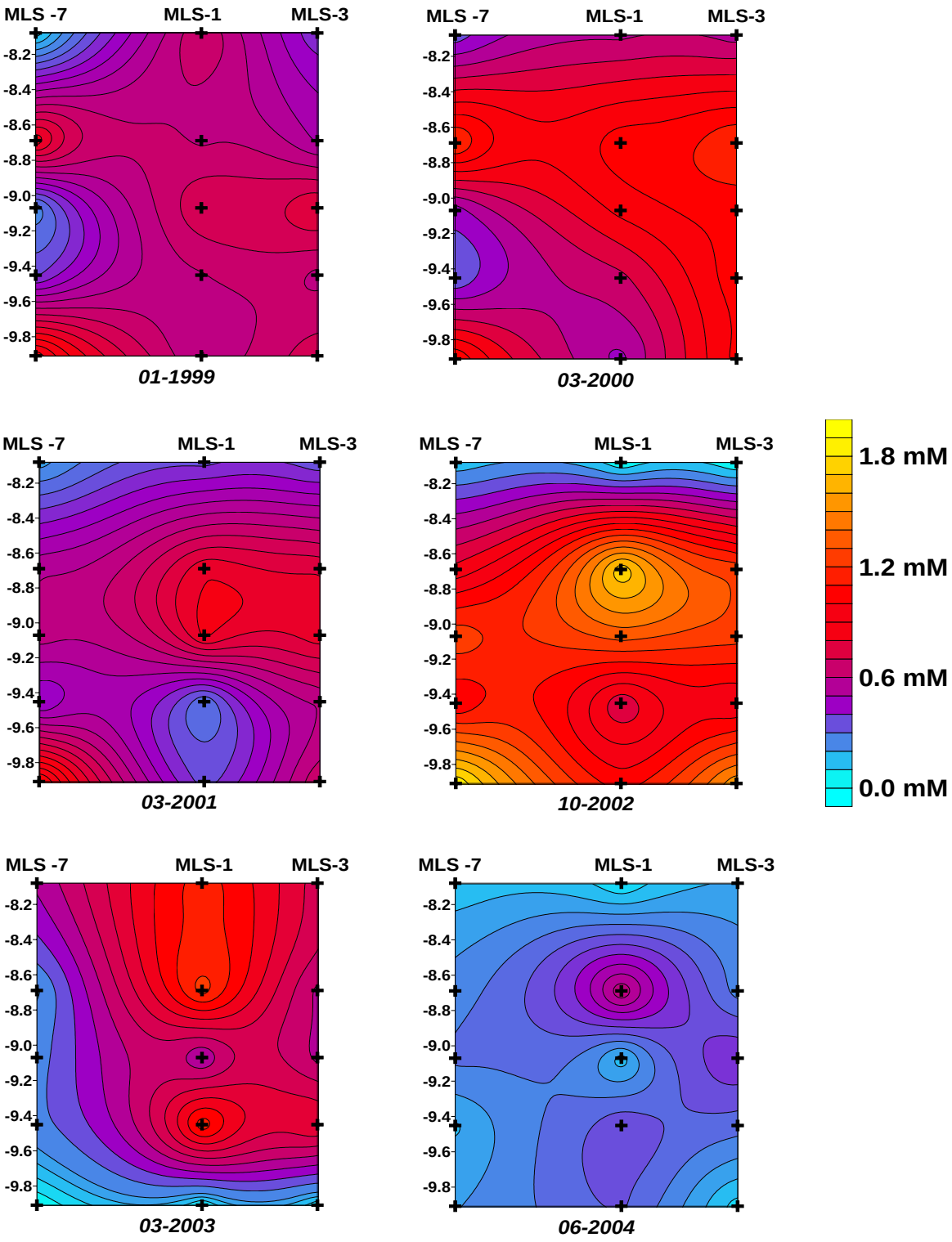

Figure 3-2. Sages source zone transect natural gradient concentrations for 6-year period after the August 1998 ethanol flood. Values are molar sum of chlorinated ethenes (mM). Transect is MLS-7 to MLS-3, 1.49 m across, 8.08 m to 9.91m bgs.

The visualizations show the gradual increase in molar sum concentrations leaving the source zone from 1999 to 2001. The sum peaked in 2002 and then decreased in 2003 until dropping markedly at the end of the sampling period in 2004. For most of the monitoring period, chlorinated ethane concentrations emanated from the mid-depth of MLS-1, the deepest locations of MLS-7 and mid and lower regions of MLS-3. By 2004, the source zone plume was primarily originating from the upper middle zone of MLS-1 and the mid-depth of MLS-3. MLS-7 had essentially ceased as a source.

Mravik et al. [2003] observed a PCE concentration rebound in the RWs and IWs to pre-remedial levels after observing initially low concentrations immediately following the flushing event. The source zone MLS detected a slight increase in molar concentrations in January 1999, five months after the flood. However, the large increase in molar sum concentration detected in 2001 and 2002 was due to the stimulation and reductive dehalogenation of PCE by microbes. Four months following the ethanol flood, December 1998, TCE concentrations increased from non-detect to 0.17 mM. Five months following the flood, January 1999, DCE was detected in several source zone MLS locations.

3.4 Downgradient Transect Concentrations

In addition to monitoring the source zone, the MLS installed downgradient of the source zone were sampled as well. The results of the downgradient control plane analysis are summarized in Table 3-3. The transect consisted of MLS-9, MLS-10, and MLS-11 for the time period from 1998-2003. The molar sum concentration values are lower than the source zone transect due to dilution and dispersion in the 10 m of aquifer between the two control planes. Looking at the mean MLS well results, the transect recorded stable behavior for the first two post remedial-years while recording a slight increase in the center of the transect in 2000. This is an

additional six-month lag compared to the concentration increases detected in the source zone, as expected due to the ten meter downgradient location of the sampling control plane and the low groundwater flow. The higher concentrations were detected throughout the center of the transect at MLS-10, and in the upper region of MLS-9.

Table 3-3. Sages downgradient transect natural gradient concentrations. Values are molar sum of all chlorinated species in mM. Transect is MLS-9, MLS-10, MLS-11.

Well	Depth m bgs	12/1998 (mM)	01/1999 (mM)	05/1999 (mM)	05/2000 (mM)	03/2001 (mM)	02/2002 (mM)	10/2002 (mM)	10/2003 (mM)	06/2004 (mM)
MLS-9	8.08	0.2487	0.3321	0.1325	0.0144	0.0682	0.4730	0.5224	0.0172	0.2264
	8.69	0.2908	0.3424	0.3014	0.3758	0.3553	0.3399	0.4522	0.2790	0.0711
	9.07	0.0360	0.0406	0.0847	0.0139	0.1896	0.1892	0.1187	0.7385	0.0261
	9.45	0.0301	0.0114	0.0168	0.0105	0.0142	0.0295	0.0553	0.2308	0.0268
	9.91	0.0063	0.0025	0.0180	0.0097	0.0650	0.0999	0.1349	0.1573	0.0474
	12.2	0.0059	0.0008	0.0347	0.0037	0.0016	0.0096	0.0083	0.0031	0.0000
Mean		**0.103**	**0.122**	**0.098**	**0.071**	**0.116**	**0.190**	**0.215**	**0.238**	**0.066**
Std Dev		0.130	0.168	0.109	0.149	0.135	0.184	0.217	0.269	0.082
MLS-10	8.08	0.0070	0.0110	0.0062	0.0000	0.0890	0.0410	0.0233	0.2877	0.0004
	8.69	0.1904	0.2140	0.1545	0.2046	0.4228	0.4413	0.4515	0.1516	0.2157
	9.07	0.3861	0.3862	0.3280	0.8048	0.3789	1.0312	0.0149	0.0016	0.0000
	9.45	0.2835	0.1855	0.3198	0.5237	0.4049	0.3772	0.9959	0.0000	0.3330
	9.91	0.1959	0.3883	0.2352	0.4606	0.4518	0.3887	0.8137	0.0320	0.0088
	12.2	0.0019	0.0017	0.0758	0.0109	0.0063	0.0744	0.9836	0.0000	0.0030
Mean		**0.176**	**0.195**	**0.194**	**0.361**	**0.249**	**0.376**	**0.566**	**0.010**	**0.069**
Std Dev		0.168	0.190	0.143	0.348	0.224	0.405	0.505	0.014	0.148
MLS-11	8.08	0.0114	0.0124	0.0127	0.0029	0.0043	0.0060	0.0205	0.0157	0.0002
	8.69	0.0476	0.0765	0.0864	0.1447	0.0718	0.1064	0.0815	0.0086	0.0027
	9.07	0.0790	0.1708	0.1518	0.2466	0.1527	0.1344	0.0000	0.0164	0.0102
	9.45	0.0381	0.1396	0.1761	0.2332	0.1724	0.2121	0.1235	0.0545	0.0314
	9.91	0.1354	0.1426	0.1107	0.1645	0.1079	0.0948	0.0849	0.3002	0.0058
	12.2	0.0011	0.0009	0.0173	0.0016	0.0005	0.0000	0.1363	0.0074	0.0000
Mean		**0.060**	**0.106**	**0.108**	**0.158**	**0.101**	**0.110**	**0.085**	**0.077**	**0.010**
Std Dev		0.050	0.068	0.062	0.098	0.068	0.076	0.053	0.126	0.013

In Figure 3-3, Surfer visualizations are presented. In most of the control plane, increases in detected concentrations were observed until peaking in year four, 2002, at 1.03 mM. Reductions in aqueous chlorinated concentrations were observed from in the peak in 2002 until the end of the sampling period in 2004, concluding at 0.33 mM. These changes will be further examined through mass discharge evaluation in the next section.

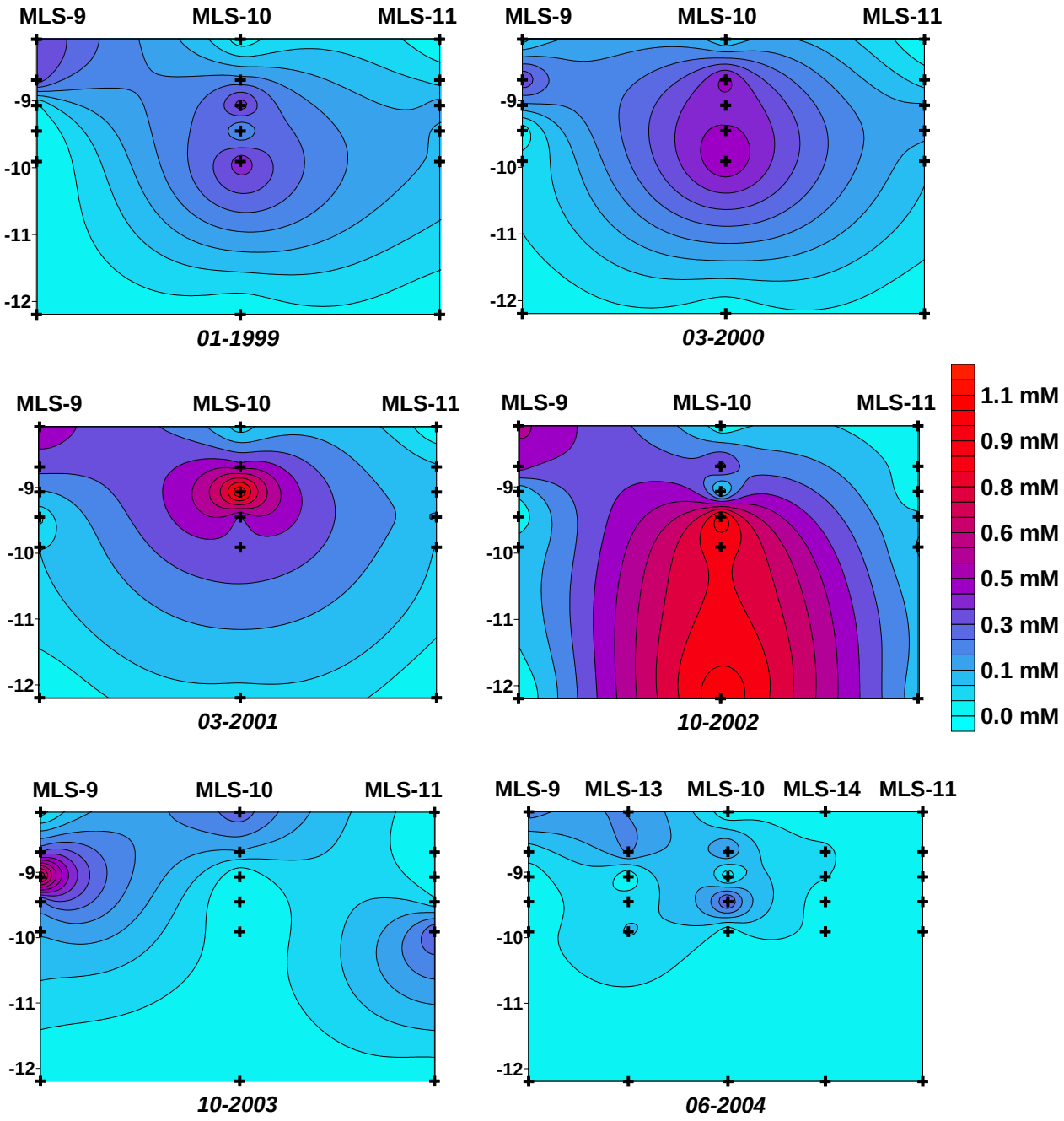

Figure 3-3. Sages downgradient transect natural gradient flux for 6-year period following August 1999 ethanol flood. Values are molar sum of chlorinated species (mM). Transect is MLS-9 to MLS-11, 6.03 m across, from 8.08 m to 12.20 m bgs.

3.5 Source Zone Transect Mass Discharge

The post-remedial mass discharge results from MLS monitoring of the source zone transect is presented in Table 3-4. As aqueous PCE discharge decreased in 1999 and 2000, DCE mass flux rate increased as a result of biological dehalorespiration. This trend continued until 2003. In the last two years of the study period, 2003 and 2004, all discharges decreased except VC. Vinyl chloride analysis recorded non-detect values until 2003 and 2004.

Table 3-4. Sages post-flood source zone transect mass discharge in mmol/day.

	Oct-98 (mmol/d)	Dec-98 (mmol/d)	Jan-99 (mmol/d)	May-99 (mmol/d)	May-00 (mmol/d)	Mar-01 (mmol/d)	Feb-02 (mmol/d)	Oct-02 (mmol/d)	Oct-03 (mmol/d)	Jun-04 (mmol/d)
PCE	12.317	20.818	23.284	20.462	15.671	18.221	10.441	8.397	3.695	0.508
TCE	0.000	2.461	5.324	3.227	19.780	4.056	5.079	4.871	2.141	0.435
DCE	0.000	0.000	0.082	2.709	2.187	12.225	31.715	45.316	20.867	11.134
VC	0.000	0.000	0.000	0.000	0.000	0.000	0.000	0.000	0.150	0.511
Sum	12.317	23.280	28.690	26.398	37.638	34.502	47.234	58.584	26.852	12.588

Maximum and minimum mass discharge values determined in the source zone transect ranged from 0.51 to 23.3 mmol/day for PCE, 0 to 19.8 mmol/day for TCE, 0 to 45.3 mmol/day for DCE, and 0 to 0.5 mmol/day for VC. Source zone source PCE strength rebound was detected in the first six months after the pilot flushing test. This can be attributed to the higher residual ethanol concentrations enhancing PCE solubility until natural gradient flow removed the majority of the ethanol. However, by the end of the first year PCE discharge began to decrease and continued to decrease until the end of the study period with the exception of 2001 when there was a slight PCE discharge spike. Figure 3-4 shows the source zone transect mass discharge over the six-year period after the 1998 ethanol flood.

After the initial post remedial rebound, up to 24 mmol/day, aqueous PCE discharge decreased below 20 mmol/day, eighteen months after the flood event. Simultaneously, DCE discharge increases to 20 mmol/day. The increase in the sum chlorinated ethene mass discharge

compared to the PCE discharge is due to the increased solubility of PCE daughter products down the biodegradation pathway [*Chu et al*., 2004]. By 2002, DCE discharge was dominant indicating increased biodegradation of PCE and TCE. All chlorinated ethane mass discharges decreased in 2003 and 2003, years five and six respectively, except VC. The total discharge reduction could be assumed to be source depletion, but is more likely a function of the biosubstrate losses as ethanol was removed by groundwater flow and microbial use.

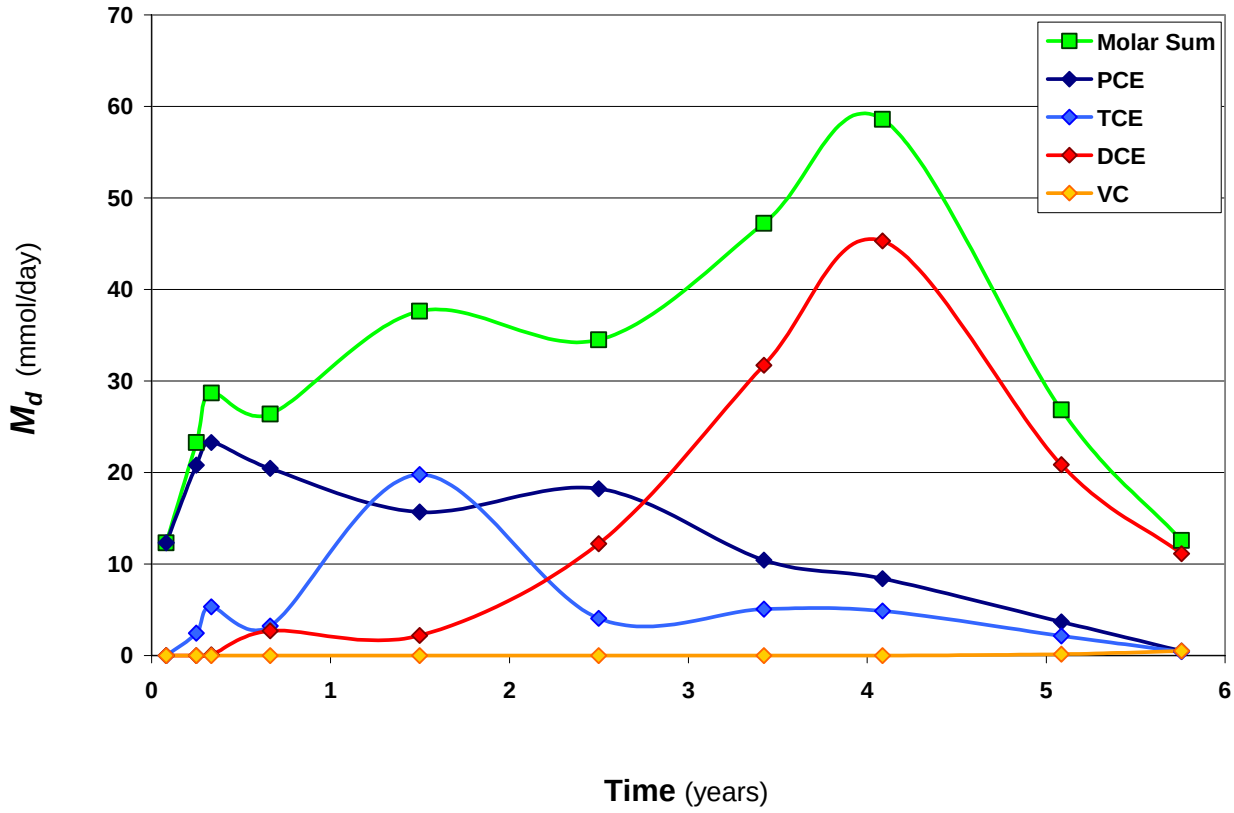

Figure 3-4. Sages source zone mass discharge following August 1998 ethanol flood. Values are in mmol/day.

The PCE curve in Figure 3-4, was numerically integrated using the trapezoid rule to yield the zereoth moment of the curve. This calculated that 4.01 L of PCE crossed the source zone transect indicating microbial enhanced dissolution. This enhancement has been documented in

laboratory studies stated in Section 1.10 [*Cope and Hughes*, 2001; *Yang and McCarty*, 2000, 2002]. At the NAPL-water interface, PCE partitions into the water phase. This makes it available for biodegradation. After reductive dehalogenation, the PCE is transformed to a more soluble daughter species, allowing more PCE to dissolve.

3.6 Downgradient Transect Mass Discharge

At the second control plane, mass discharge was also calculated. Table 3-5 shows the chlorinated species discharge across the transect for the six-year timeframe of this project. The sum discharge was stable until decreases in PCE and the associated increases in DCE were observed in 2000. An short increase in PCE flux rate and a coupled decrease in DCE discharge was detected in 2001. However, PCE decrease and DCE increase rebounded in 2002. In 2003, all mass discharge began decreasing until reaching its lowest level at the cessation of sampling in 2004

Table 3-5. Sages mass discharge across the downgradient MLS transect in the 6-year period following the August 1998 ethanol flushing pilot test. Mass discharge values are in mmol/day units.

	Oct-98 (mmol/d)	Dec-98 (mmol/d)	Jan-99 (mmol/d)	May-99 (mmol/d)	May-00 (mmol/d)	Mar-01 (mmol/d)	Feb-02 (mmol/d)	Oct-02 (mmol/d)	Oct-03 (mmol/d)	Jun-04 (mmol/d)
PCE	30.362	27.487	31.714	26.733	17.454	21.819	17.827	18.531	7.180	2.025
TCE	0.000	1.164	1.278	0.927	0.578	2.165	2.205	2.419	1.388	1.731
DCE	0.000	0.000	0.618	0.557	29.858	9.062	16.937	39.147	23.803	9.263
VC	0.000	0.000	0.000	0.000	0.000	0.000	0.000	0.000	0.252	0.975
Sum	30.362	28.651	33.610	28.217	47.891	33.046	36.969	60.097	32.623	13.994

The magnitudes of the individual chlorinated ethene mass discharges determined in the downgradient MLS transect ranged from 2.03 to 31.71 mmol/day for PCE, 0 to 2.42 for TCE, 0 to 39.15 for DCE, and 0 to 0.98 for VC. The results are comparable to the source zone transect. PCE discharge was estimated to be greater in the downgradient transect than at the source zone,

but the TCE discharge was almost an order of magnitude lower. The magnitude of observed TCE in the downgradient transect compared to the source zone transect was due likely due to reductive dechlorination in the 10 m of aquifer before arriving at the downgradient control plane. VC was observed to be increasing in the final two years. In Figure 3-5, the mass discharge is presented.

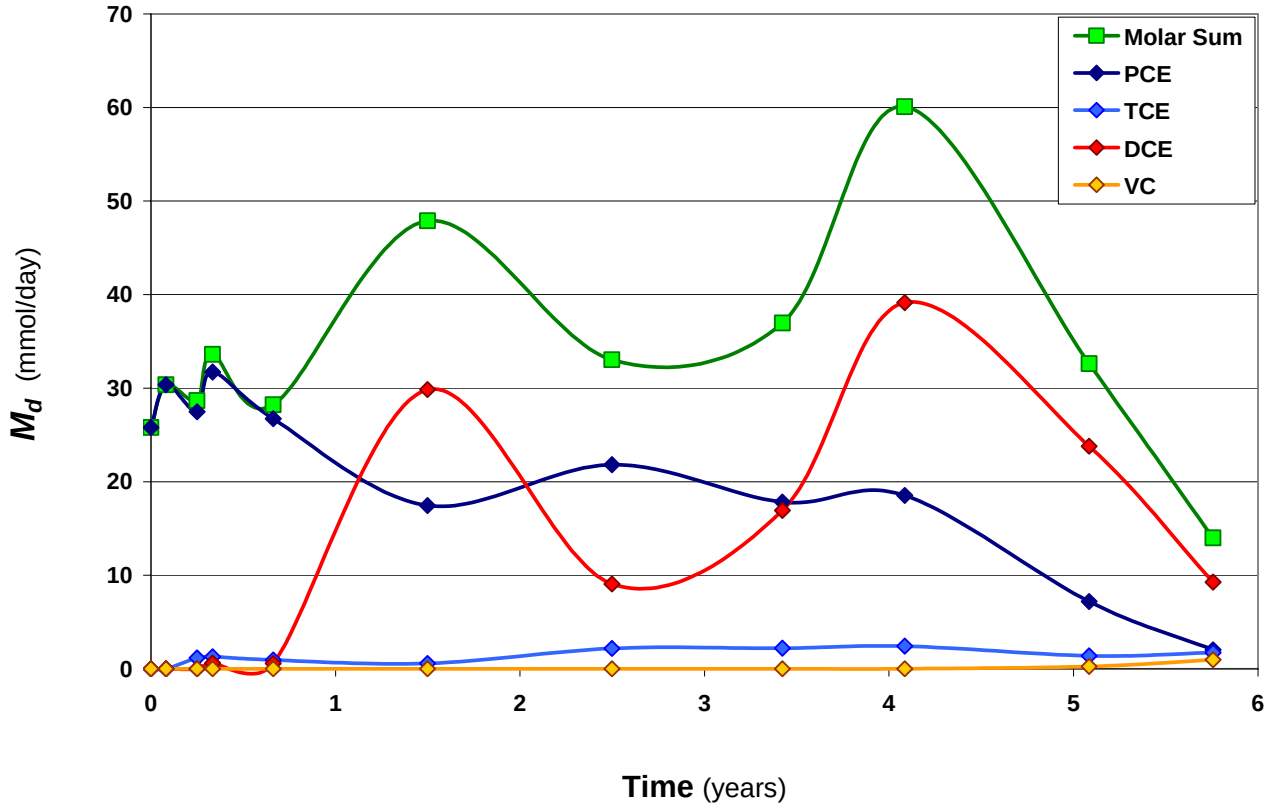

Figures 3-5. Sages downgradient transect mass discharge in mmol/day for the six- year period following the 1998 ethanol flushing event.

Very similar patterns to the source zone mass discharge was observed at the downgradient transect. However, there was an amplification of the fluctuation of mass discharge recorded in the source zone transect in years two and three in the plume response at the downgradient transect. Conversely, in the source zone DCE discharge appeared to be unaffected

by the small PCE discharge increase. By the end of the study period, PCE and DCE flux rate decreased significantly. As these two chlorinated ethenes dominated the sum mass discharge, it decreased as well. As a measure of total risk to downgradient water supplies, the decrease at the end of the study is favorable.

The numerical integration of the PCE curve in Figure 3-5 determined that 2.65 L of PCE reached the downgradient transect over the six-year post-remedial monitoring. The source zone PCE curve integration calculated that 4.01 L removed from the source zone by enhanced microbial dissolution over the same time period. The difference in these values was the enhanced natural attenuation in the 10 m between transects. Thus, 1.36L of PCE was biodegraded over the six years. The average rate of the PCE plume biodegradation over the six-years of this study was determined to be 1.02 g/day.

CHAPTER 4
DISCUSSION

4.1 Inferred Initial PCE Architecture

The characterization of PCE distribution at the Sages site demonstrated the discontinuous architecture of subsurface DNAPL spills. Soil coring performed in the previous studies determined discrete layers of high PCE saturation in the source zone. However, extensive coring would be required to elucidate the NAPL extent that can be determined by exploring the same area with a partitioning tracer test. Employing a network of multilevel sampling wells in the region interrogated by the tracers quickly yields the vertical and horizontal spatial distribution of NAPL.

From the results of the MLS pre-remedial PITT, the Surfer visualizations, and the remedial flow field fluid velocities, the PCE architecture of Sages can be inferred. MLS detected high saturations of PCE in the upper region of the source zone, nearest the drycleaning facility floor drain, at MLS-1. Although upper depth of the source zone (8.08 m bgs) demonstrated the highest fluid velocities in the remedial flow field, it was measured to have hydraulic conductivity nearly an order of magnitude lower than the materials overlying it [Mravik et al., 2003]. As PCE collected on this fine sand, it fanned outward and drained down to the next depth. It seemed to contact finer sands at 8.69 m bgs, evidenced by the marked decrease in remedial fluid velocities at this depth in all MLS wells and high saturations detected at MLS-1 and MLS-4. From this layer, PCE drained to the next low permeable strata at 9.07 m bgs and spread westward to MLS-2 and eastward to MLS-4. The two lowest depths indicated PCE pooling as the average PCE saturations recorded in the swept zone from IW-3 to MLS-4 and MLS-6 were greater than 1.0% [*NRC*, 2005]. The high aqueous PCE concentrations in the middle and lowest depths of MLS-7

indicate significant PCE in this region as well. However, insufficient tracer arrival prevented reliable PCE saturation determination at MLS-7.

4.2 Inferred Final PCE Architecture

The post-remedial PITT, scaled PCE concentrations, and the estimated velocity results allow the estimation of post-flood residual PCE architecture. This type of information can be highly valuable to the site manager for future decisions. The upper depth of the source zone detected very little residual PCE. The next lower depth of 8.69 m bgs indicated residual PCE in the areas of MLS-1, MLS-3, and MLS-4 of up to 0.3%. There was little PCE detected at 9.07m bgs, but continuing downward, significant residual PCE was found in the flow field to MLS-4, up to 0.4%. Finally, at the deepest sampling locations, MLS-7 detected the highest residual source zone PCE, 0.6%. By spatially locating the residual DNAPL, future remedial efforts can be tailored to target these regions.

4.3 Benefits of Ethanol Flushing

In recent years, the relationship of mass reduction to flux reduction has been offered as a method to evaluate site DNAPL heterogeneity and remedial performance. As stated in Chapter 1, there has been increasing amounts of research demonstrating that there is favorable flux response to aggressive mass removal modeling and field tests [*Roa et al*., 2002; *Stroo et al*., 2003; *Lemke et al*., 2004; *Falta et al*., 2005*a*, 2005*b*; *NRC*, 2005; *Wood et al*., 2005; *Fure et al*., 2006]. Modeling, laboratory tests, and field tests have all indicated the ability to reduce source flux as a result of alcohol flushing mass depletion [*Brooks et al*., 2003; *Wood et al*., 2005; *Fure et al*., 2006].

The results of the Sages site 1998 ethanol flood demonstrates this relationship, even though this was merely a technology pilot test, not a full scale remediation. The fractional

NAPL removal (*FNR*) to fractional flux reduction (*FFR*) for the site MLS and RWs is presented in Figure 4-1.

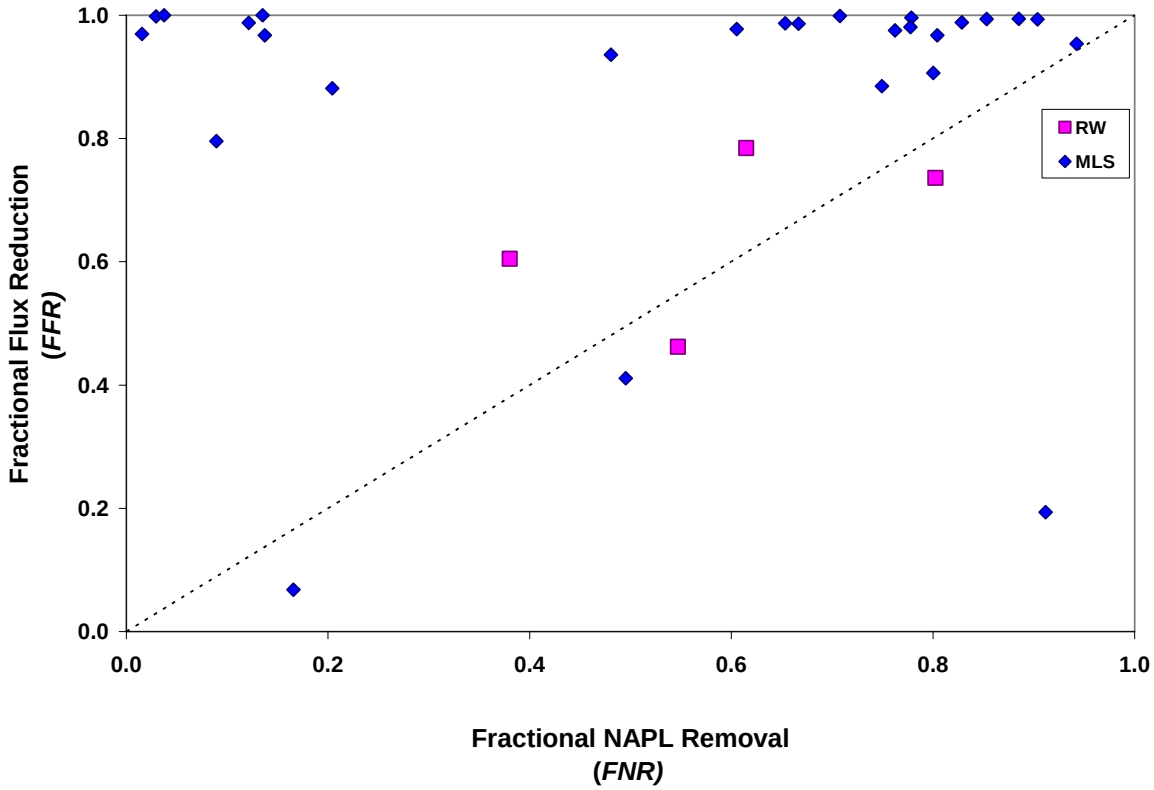

Figure 4-1. Sages 1998 ethanol flushing pilot test fractional NAPL removal to fractional flux reduction relationship.

A favorable flux response to PCE removal was observed for most data points as they were located to the left of the 1:1 line. The RW data shows that four or the six wells straddle the 1:1 relationship line. Brooks et al. [2003] documented this pattern at the Dover AFB site alcohol flushing test, although four of six extraction wells exhibited less than 1:1 behavior, two recorded slightly greater response. For the 1998 Sages flood, there were two RWs that plotted outside the zero to one range of this figure. Both RW-5 and RW-7 produced concentration increases in this test. In the MLS data, most of the depths indicated highly favorable flux reductions to a wide range of fractional NAPL removals. Although there were several flux increases detected in the

MLS results, these were not included because they occurred in MLS-5 and MLS-7. In MLS-5 no *FNR* values were able to be calculated due to insufficient tracer arrival, and at MLS-7 there were only a few results that were based on estimated NAPL removal (*ENR*) described in Section 2.11. There was a single recorded NAPL increase in MLS-7, but this value is off the scale of Figure 4-1 as well.

According to the previous work exploring this relationship, the MLS data distribution on the graph indicates a high level of heterogeneity in PCE distribution. Overall, this data corroborates the modeling and other field tests that have demonstrated aggressive mass removal's favorable impact on mass flux.

Because all MLS and RWs did not experience equal remedial velocity or flow rate, each data point was weighted by the flow rate of remedial fluids sweeping through its region. Each MLS depth *FFR* value was weighted by the fraction of the total estimated fluid velocity for the respective MLS well in Figure 2-2. The weighted MLS velocity *FFR* for each depth was summed to produce a mean weighted *FFR* for each MLS well. The RWs were weighted by the fraction of the total extraction flow rate for the site. The flow rate weighted *FFR* for the RWs were summed to provide a mean flow weighted *FFR* for all RWs. The fractional NAPL removal was then compared to the resultant weighted mean *FFR* values and is presented in Figure 4-2.

The MLS wells displayed highly favorable velocity-weighted flux reductions to their respective PCE removals. Furthermore, the effect of the heterogeneous DNAPL architecture is evident in the high flux to medium NAPL removal. The recovery well flow-weighted average displayed less heterogeneous NAPL morphology and less favorable flux reduction to NAPL removal, due to the integration of liquids arriving at the well.

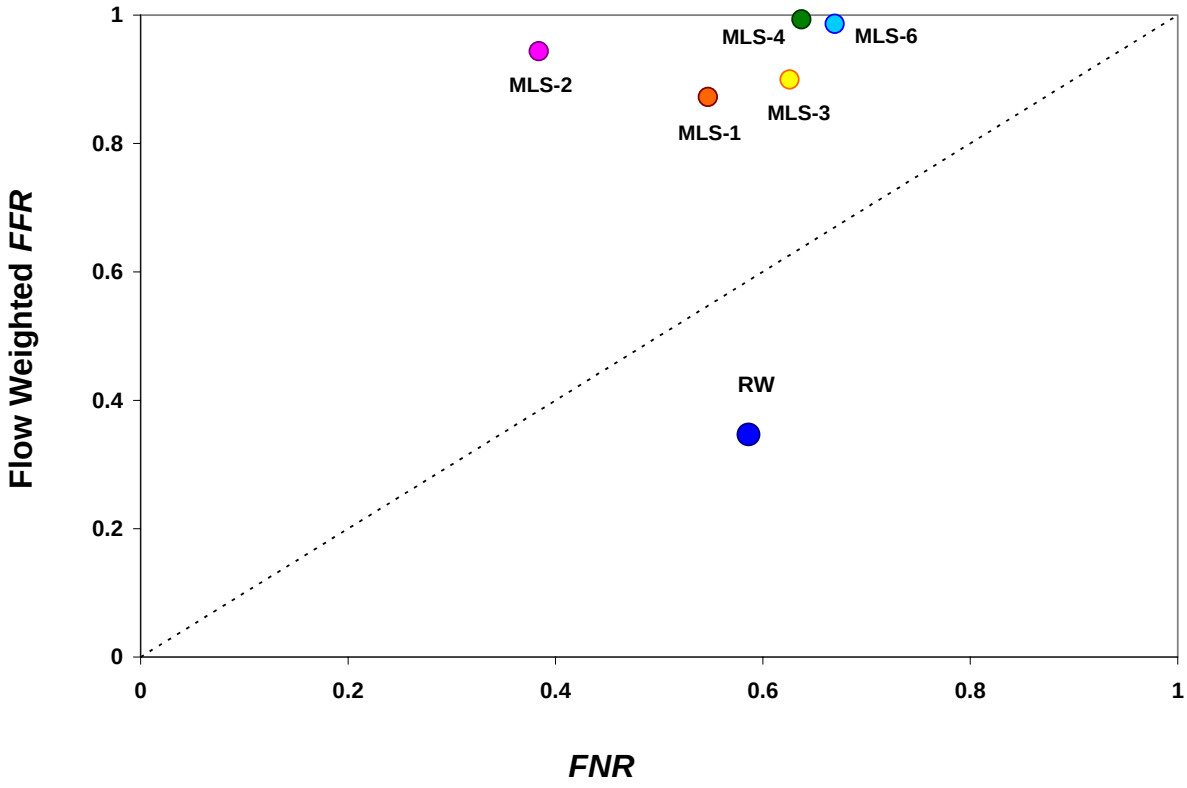

Figure 4-2. Relationship of 1998 Sages flood fractional NAPL removal to flow weighted fractional flux reduction.

For a pilot scale test, ethanol flushing at the Sages site has demonstrated the ability to both remove PCE mass and decrease PCE flux. Modeling by Falta et al. [2005a] showed that without source removal, contaminant plumes are stronger, that is they contain greater dissolved NAPL concentration. Additionally, it was observed in the model that the distance the plume would remain highly concentrated, decreased with source depletion [*Falta, et al*., 2005a].

Further modeling by Falta et al. [2005b], determined that as NAPL heterogeneity increased, the immediate flux reductions were greater after partial source removal. However, it was found that source longevity was also greater for sites with relationships greater than 1:1 ($\beta>1$) compared to sites with 1:1 or less. The magnitude of the plume concentration was reduced in the heterogeneous model results, but the source was depleted less rapidly by natural gradient

dissolution [*Falta et al*., 2005b]. Furthermore, the model demonstrated that low NAPL heterogeneity required greater mass removal to affect significant flux reduction, but source longevity decreased after source depletion. The plume contained much higher concentrations, but the source mass would be depleted more rapidly by natural dissolution [*Falta at al*., 2005b].

Applying this theory to the Sages site, under only natural gradient conditions, the post-remedial PCE distribution will act as a contaminant source for many years. However the longevity and plume distance will decrease as a result of the 1998 flood. Additionally, the site flux will be less concentrated than pre-remedial levels throughout the source life span.

Another favorable outcome of DNAPL site source depletion modeling described the reduction of plume strength and longevity with enhanced plume degradation [Falta et al., 2005b]. This leads to the selection of this site as a pilot study of the SERB technology. Residual PCE may act as a reservoir for dissolved plume formation, but the unrecovered ethanol should foster in situ bioremediation of PCE, reducing plume strength and longevity.

4.4 SERB Activity

The SERB technology clearly demonstrated the ability to stimulate microbial reductive dechlorination of PCE at the Sages site. Had this been a full scale remediation and not a pilot test ethanol flushing technology, the mass recovery and resultant flux reduction in the RWs both would have increased. Furthermore, greater NAPL removal would have decreased site mass discharge and the source longevity. The site showed the common flux rebound that other aggressive source removal projects have recorded. The four-month lag until daughter products were detected can be attributed to microbial population growth and high residual ethanol concentration toxicity. Ethanol concentrations needed to drop below the toxicity threshold of 1% before biologically enhanced dissolution and degradation significantly increased.

Both the collection of PCE during the remediation and the tracer tests concluded that 43 L of the original 69 L of PCE were removed from the source zone, leaving behind 25 L in the aquifer [*Sillan*, 1999; *Jawitz et al*., 2000]. The microbial stimulation and dissolution enhancement of PCE recorded 4.01 L of aqueous phase PCE crossed the source zone transect. The difference of the residual PCE and the dissolution of PCE, leaves 21 L of PCE remaining in the source zone.

There was a marked reduction in chlorinated ethene mass discharge at the end of the study, representing a reduction in risk at the site. However, the source will likely persist for many years requiring continued monitoring and plume control. The cause for the decrease in mass discharge was due to both advective and microbial removal of required substrate for continued dechlorinating microbial activity. Consequently, future injection of ethanol would be required to foster additional bioremediation. Fortunately, the site has proven responsive to ethanol flushing as both an enhanced solubilizing agent and as a treatment for biostimulation. The field sampling of this project terminated with the 2004 Phase II ethanol flushing at the Sages site, conducted by LFR, Inc. and FDEP. This action is consistent with the findings of this thesis. Another full scale flushing should be implemented to remove additional source mass and polish the residual PCE with the SERB technology.

CHAPTER 5
CONCLUSIONS

The primary goals of this work was to: (1) elucidate the architecture of PCE in the source zone at the Sages site, (2) gain additional spatial information about the ethanol flushing test, (3) assess the benefits of this technology to deplete source mass and reduce source flux, and (4) evaluate the mass discharge at the site over the period from 1998 to 2004. The final PCE subsurface distribution was determined by the post-remedial PITT. This information would assist site managers in preparing future corrective action and monitoring. The flushing test displayed the inherent limitations of tracer tests and ethanol flushing. While all the RWs received tracers and remedial fluids, deep zone finer media prevented the arrival of tracers at all deep MLS. The remedial fluids cleaned out more permeable zones, but there was difficulty penetrating the lower zones with high concentrations of ethanol. Furthermore, once remedial fluids interrogated the low flow zones, they were not easily recovered.

This work demonstrated the benefits of this DNAPL source removal technology. Both mass reductions and flux reductions were observed, translating into decreased source strength and longevity compared to natural gradient dissolution with pump-and-treat plume capture. The location of well data in the mass reduction flux reduction relationship displayed moderately to highly heterogeneous PCE morphology.

Additionally, the stimulation of microbial biodegradation was observed. The mass discharge showed the 1% ethanol concentration toxicity threshold of microbes in Sages site materials. When the ethanol concentration was reduced by the return of natural gradient groundwater flow, the microbial response was strong and mass discharge increased. In the ten meters of aquifer between the source zone and the downgradient MLS transect, DCE was not observed to be degraded quickly. Thus, during periods of highly stimulated dechlorination of

PCE and TCE, DCE downgradient risk is increased and plume containment is necessary. By the end of the study, ethanol was no longer observed due to advective and microbial losses. This resulted in sharp decreases in site mass discharge. Although this decrease results in decreased downgradient risk, it is estimated that 21 L of PCE still remain in the source zone at Sages.

If reductive dehalogenating bacteria are present in a sandy aquifer PCE site, they will probably rebound from high concentration ethanol flushing. Before the study the site assessment found these microbes present, but the aquifer was substrate limited. Thus, little daughter products were observed before the 1998 remediation. However, after the flood, microbial dechlorination was greatly stimulated by residual ethanol including enhancing natural dissolution of PCE.

This technology demonstrated the ability to enhance PCE solubility for source removal while concurrently adding a residual biotreatment polishing. If lower residual PCE volumes are determined after an ethanol flood and mass discharge decreases sharply after a few years, the periodic introduction of low concentration ethanol will re-stimulate the microbial biodegradation process. This has several distinct advantages. First, the PCE source will continue to be depleted. Second, microbial activity in the plume will enhance natural attenuation processes, leading to less concentrated and shorter downgradient plumes. Finally, the polishing of residual PCE with ethanol will speed site closure time scales by decreasing site longevity.

LIST OF REFERENCES

American Society for Testing and Materials (ASTM) (2002), Standard Guide for Risk-Based Corrective Action Applied at Petroleum Release Sites, E1739-95.

Annable, M. D., P. S. C. Rao, K. H. Hatfield, W. D. Graham, A. L. Wood, and C. G. Enfield (1998), Partitioning tracers for measuring residual NAPL: Results from a field-scale test, *J. Environ. Eng*., 124(6), 498–503.

Annable, M. D., K. Hatfield, J. Cho, H. Klammer, B. L. Parker, J. A. Cherry, and P. S. C. Rao (2005) Field-Scale Evaluation of the passive flux meter for simultaneous measurement of groundwater and contaminant fluxes, *Environ. Sci. Technol*., 39, 7194-7201.

Augustijn, D. C. M., R. E. Jessup, P. S. C. Rao, and A. L. Wood (1994), Remediation of contaminated soils by solvent flushing, *J. Envir. Eng*., 120(1), 42–57.

Augustijn, D. C. M., L. S. Lee, R. E. Jessup, P. S. C. Rao, M. D. Annable, and A. L. Wood (1997), Remediation of soils and aquifers contaminated with hydrophobic organic chemicals: Theoretical basis for the use of cosolvents, in *Subsurface Restoration Handbook*, C. H. Ward, J. A. Cherry, and M. R. Scalf Eds., Ann Arbor Press, Inc., Chelsea, Mich., pp. 231–270.

Basu, N. B., P. S. C. Rao, I. C. Poyer, M. D. Annable, and K. Hatfield (2006), Flux-based assessment at a manufacturing site contaminated with trichloroethylene, *J. Contam. Hydrol*., 86, 105-127.

Banerjee, S., & S.H. Yalkowsky (1988), Cosolvent-induced solubilization of hydrophobic compounds into water, *Anal*. *Chem*., 60, 2153-2155.

Bauer, S., M. Bayer-Raich, T. Holder, T. Ptak, C. Kolesar, and D. Müller (2004), Quantification of groundwater contamination in an urban area using integral pumping tests, *J. Contam. Hydrol*., 75, 183-213.

Bockelmann, A., T. Ptak, and G. Teutsch (2001), An analytical quantificationof mass fluxes and natural attenuation rate constants at a former gasworks site, *J. Contam. Hydrol*., 53, 429– 453.

Bockelmann, A., D. Zamfirescu, T. Ptak, P. Grathwohl, and G. Teutsch (2003), Quantification of mass fluxes and natural attenuation rates at an industrial site with a limited monitoring network: A case study, *J. Contam. Hydrol*., 60, 97–121.

Broholm, K., S. Feenstra, and J. A. Cherry (2001), Solvent Release into a Sandy Aquifer. 1. Overview of Source Distribution and Dissolution Behavior, *Environ. Sci. Technol.*, 33, 681-690.

Broholm, K., S. Feenstra, and J. A. Cherry (2005), Solvent Release into a Sandy Aquifer 2: Estimation of DNAPL Mass Based on a Multiple-Component Dissolution Model, *Environ. Sci. Technol*., 39, 317-324.

Brooks, M. C., M. D. Annable, P. S. C. Rao, K. Hatfield, J.W. Jawitz, W. R. Wise, A. L. Wood, and C. G. Enfield (2002), Controlled release, blind tests of DNAPL characterization using partitioning tracers, *J. Contam. Hydrol*., 59, 187– 210.

Brooks, M. C., M. D. Annable, P. S. C. Rao, K. Hatfield, J.W. Jawitz, W. R. Wise, A. L. Wood, and C. G. Enfield (2004), Controlled release, blind test of DNAPL remediation by ethanol flushing, *J. Contam. Hydrol*., 69, 281– 297.

Carr, C. S., S. Garg, and J. B. Hughes (2000), Effect of dechlorinating bacteria on the longevity and composition of PCE-containing nonaqueous phase liquids under equilibrium dissolution conditions, *Environ. Sci. Technol*., 34, 1088-1094.

Cho, J., M. D. Annable, and P. S. C. Rao (2003), Residual Alcohol Influence on NAPL Saturation Estimates Based on Partitioning Tracers, *Environ. Sci. Technol*., 37, 1639-1645.

Chu, M., P. K. Kitanidis, and P. L. McCarty (2004), Possible factors controlling the effectiveness of bioenhanced dissolution of non-aqueous phase tetrachloroethene, *Adv. Wtr. Res*., 27, 601–615

Cope, N. and J. B. Hughes (2001), Biologically-enhanced removal of PCE from NAPL source zones, *Environ. Sci. Technol*., 35, 2014-2021.

Dekker, T. J. and L. M. Abriola (2000), The influence of field scale heterogeneity on the infiltration and entrapment of dense nonaqueous phase liquids in saturated formations, *J. Contam. Hydrol*., 42, 187–218.

Einarson, M. D. and D. M. Mackay (2001), Predicting impacts of groundwater contamination, *Environ. Sci. Technol*., 35, 66A–73A.

Enfield, C. G., A. L. Wood, F. P. Espinoza, M. C. Brooks, M. Annable, and P. S. C. Rao (2005), Design of aquifer remediation systems: (1) Describing hydraulic structure and NAPL architecture using tracers, *J. Contam. Hydrol*., 81, 125–147.

Falta, R.W. (1998), Using phase diagram to predict the performance of cosolvent floods for NAPL remediation, *Ground Water Monit. Rem*., 18(3):94-102.

Falta, R. W., C. M. Lee, S. E. Brame, E. Roeder, J. T. Coates, C. Wright, A. L. Wood, and C. G. Enfield (1999), Field test of high molecular weight alcohol flushing for subsurface nonaqueous phase liquid remediation, *Water Resour. Res*., 35(7), 2095–2108.

Falta, R. W., P. S. Rao, and N. Basu (2005a), Assessing the impacts of partial mass depletion in DNAPL source zones I. Analytical modeling of source strength functions and plume response, *J. Contam. Hydrol*., 78, 259– 280.

Falta, R. W., N. Basu, and P. S. Rao (2005a), Assessing the impacts of partial mass depletion in DNAPL source zones II. Coupling source strength functions to plume evolution, *J. Contam. Hydrol*., 79, 45– 66.

Feenstra, S, J. A. Cherry, and B. L. Parker (1996), Conceptual Models for the Behavior of Dense Nonaqueous-Phase Liquids (DNAPLs) in the Subsurface, in *Dense Chlorinated Solvents and Other DNAPLs in Groundwater*; J. F. Pankow, J. A. Cherry, Eds.; Waterloo Press: Portland, OR.

Frind, E. O., J. W. Molson, M. Shirmer, and N. Guiguer (1999), Dissolution and mass transfer of multiple organics under field conditions: The Borden emplaced source, *Water Resour. Res*., 35(3), 683–694.

Guilbeault, M. A., B. L. Parker, and J. A. Cherry (2005), Mass and flux distributions from DNAPL zones in sandy aquifers, *Ground Water*, 43(1), 70–86.

Hatfield, K., M. Annable, J. H. Cho, P. S. C. Rao, and H. Klammler (2004), A direct passive method for measuring water and contaminant fluxes in porous media, *J. Contam. Hydrol*., 75, 155– 181.

Helms, A. D. (1997), Moment estimates for imperfect breakthrough data: Theory and application to a field-scale portioning tracer experiment, M.E.Thesis, University of Florida, Gainesville, Florida.

Illangasekare, T. H., Ramsey, J. L., Jensen, K. H., and M. B., Butts (1995), Experimental study of movement and distribution of dense organic contaminants in heterogeneous aquifers. *J. Contam. Hydrol.,* 20(1–2), 1 – 25.

Imhoff, P. T., S. N. Gleyzer, J. F. McBride, L. A. Vancho, I. Okuda, and C. T. Miller (1995), Cosolvent-enhanced remediation of residual dense nonaqueous phase liquids: experimental investigation, *Environ. Sci. Technol*., 29(8), 1966–1976.

Interstate Technology & Regulatory Council (ITRC) (2005), *Overview of In Situ Bioremediation of Chlorinated Ethene DNAPL Source Zones*. BIODNAPL-1, Washington, D.C.: Interstate Technology & Regulatory Council, Bioremediation of Dense Nonaqueous Phase Liquids (Bio DNAPL) Team.

Jarsjö, J., Bayer-Raich, M., and T. Ptak (2005), Monitoring groundwater contamination and delineating source zones at industrial sites: Uncertainty analyses using integral pumping tests, *J. Contam. Hydrol.,* 79, 107-134.

Jawitz, J. W., M. D. Annable, P. S. C. Rao, and R. D. Rhue (1998), Field implementation of a Winsor Type I surfactant/alcohol mixture for in situ solubilization of a complex LNAPL as a single-phase microemulsion, *Environ. Sci. Technol*., 32(4), 523– 530.

Jawitz, J. W., R. K. Sillan, M. D. Annable, P. S. C. Rao, and K. Warner (2000), In situ alcohol flushing of a DNAPL source zone at a dry cleaner site, *Environ. Sci. Technol*., 34(17), 3722–3729.

Jawitz, J. W., M. D. Annable, G. G. Demmy, and P. S. C. Rao (2003), Estimating non-aqueous phase liquid spatial variability using partitioning tracer higher temporal moments, *Water Resour. Res*., 39(7), 1192.

Jawitz, J. W. (2004), Moments of truncated continuous univariate distributions, *Adv. Water Resour*., 27(3), 269 – 281.

Jin, M., M. Delshad, V. Dwarakanath, D. C. McKinney, G. A. Pope, K. Sepehrnoori, and C. E. Tilburg (1995), Partitioning tracer test for detection, estimation, and remediation performance assessment of subsurface nonaqueous phase liquids, *Water Resour. Res*., 31(5), 1201–1211.

Kübert, M. and M. Finkel (2006), Contaminant mass discharge estimation in groundwater based on multi-level point measurements: A numerical evaluation of expected errors, *J. Contam. Hydrol*., 84, 55-80.

Kueper, B. H., D. Redman, R. C. Starr, S. Reitsma, and M. Mah (1993), A field experiment to study the behavior of tetrachloroethylene below the water-table: Spatial distribution of residual and pooled DNAPL, *Ground Water*, 31(5), 756– 766.

Ladaa, T. I., C. M. Lee, J. T. Coates, and R. W. Falta (2001), Cosolvent effects of alcohols on the Henry's law constant and aqueous solubility of tetrachloroethylene (PCE), *Chemosphere*, 44, 1137-1143.

Lemke, L. D., L. M. Abriola, and J. R. Lang (2004), Influence of hydraulic property correlation on predicted dense nonaqueous phase liquid source zone architecture, mass recovery, and contaminant flux, *Water Resour. Res*., 40(12), 1-18.

Lerner, D. N. and G. Teutsch (1995), Recommendations for level-determined sampling in wells, *J. Hydro*., 171, 355-377.

Levine-Fricke Recon, Inc. (LFR) (1997), Contamination assessment report, former Sages dry cleaner, Report to FDEP, Tallahassee, FL.

LFR (1998a), Pilot test work plan: former Sages drycleaner, LFR Inc., Tallahassee, FL

LFR (1998b), Cosolvent flushing pilot study: former Sages drycleaner, LFR Inc., Tallahassee, FL

.

Lunn, S. R. D., and B. H. Kueper (1999), Risk reduction during chemical flooding: Preconditioning DNAPL density in situ prior to recovery by miscible displacement, *Environ. Sci. Technol.*, 33, 1703-1708.

MacKay, D. M., and J. A. Cherry (1989), Groundwater contamination: Pump-and-treat remediation, *Environ. Sci. Technol*., 23(6), 630–636.

MacKay, D., W. Y. Shiu, A. Maijanen, and S. Feenstra (1991), Dissolution of non-aqueous phase liquids in groundwater, *J. Contam. Hydrol*., 8, 23-42.

Mayer, A. S., C.T. Kelley, and C. T. Miller (2002), Optimal design for problems involving flow and transport phenomena in saturated subsurface systems, *Adv. Water Resour*., 25, 1233–1256.

McWhorter, D. B., and T. C. Sale (2003), Reply to comment by P. S. C. Rao and J. W. Jawitz on ‘‘Steady state mass transfer from single-component dense nonaqueous phase liquids in uniform flow fields’’ by T. C. Sale and D. B. McWhorter, *Water Resour. Res*., 39(3), 1069.

Meinardus, H. W., V. Dwarakanath, J. Ewing, G. J. Hirasaki, R. E. Jackson, M. Jin, J. S. Ginn, J. T. Londergan, C. A. Miller, and G. A. Pope (2002), Performance assessment of NAPL remediation in heterogeneous alluvium, *J. Contam. Hydrol*., 54, 173– 193.

Mravik, S. C., R. K. Sillan, A. L. Wood, and G. W. Sewell (2003), Field evaluation of the solvent extraction residual biotreatment technology, *Environ. Sci. Technol*., 37, 5040–5049.

Nelson, N. T., and M. L. Brusseau (1996), Field study of the partitioning tracer method for detection of dense nonaqueous phase liquid in a trichloroethene-contaminated aquifer, *Environ. Sci. Technol*., 30(9), 2859–2863.

Nkedi-Kizza, P., P. S. C. Rao, and A. G. Hornsby (1987), Influence of organic cosolvents on leaching of hydrophobic organic chemicals through soils, *Environ. Sci. Technol*., 21(11), 1107–1111.

Padgett, P. K., and N. J. Hayden (1999) Mobilization of residual tetrachloroethylene during alcohol flushing of clay-containing porous media, *J. Contam. Hydrol*., 40, 285-296.

Parker, B.L., J. A. Cherry, and S. W. Chapman (2004), Field study of TCE diffusion profiles below DNAPL to assess aquitard integrity, *J. Contam. Hydrol*., 74, 197-230.

Parker, J. C., and E. Park (2004), Modeling field-scale dense nonaqueous phase liquid dissolution kinetics in heterogeneous aquifers, *Water Resour. Res*., 40(5), 1-12.

Pickens, J. F., J. A. Cherry, G. E. Grisak, W. F. Merritt, and B. A. Risto (1978), A multilevel device for groundwater sampling and piezometric monitoring. *Ground Water*, 16(5): 322-327.

Rao, P. S. C., L. S. Lee, and R. Pinal (1990), Cosolvency and sorption of hydrophobic organic chemicals, *Environ. Sci. Technol.*, 24, 647-654

Rao, P. S. C., M. D. Annable, R. K. Sillan, D. P. Dai, K. Hatfield, W. D. Graham, A. L. Wood, and C. G. Enfield (1997), Field-scale evaluation of in situ cosolvent flushing for enhanced aquifer remediation, *Water Resour. Res*., 33(12), 2673–2686.

Rao, P. S. C., M. D. Annable, and H. Kim (2000), NAPL source zone characterization and remediation technology performance assessment: recent developments and applications of tracer techniques, *J. Contam. Hydrol*. 45, 63– 78.

Rao, P. S. C., J. W. Jawitz, C. G. Enfield, R. W. Falta, M. D. Annable, and A. L. Wood (2002), Technology integration for contaminated site remediation: Cleanup goals and performance criteria, in Groundwater Quality 2001, in *Natural and Enhanced Restoration of Groundwater Pollution, Proceedings of the 3rd International Conference*, S. Thornton and S. Oswald Eds., *IAHS Publ*., 273, 410– 412.

Rao, P. S. C., and J. W. Jawitz (2003), Comment on ‘‘Steady-state mass transfer from single-component dense non-aqueous phase liquids in uniform flow fields’’ by T.C. Sale and D. B. McWhorter, *Water Resour. Res*., 39(3), 1068.

Rivett, M. O., S. Feenstra, and J. A. Cherry (2001), A Controlled filed experiment on groundwater contamination by a multicomponent DNAPL: creation of the emplaced source and overview of the dissolved plume development. *J. Contam. Hydrol*., 49, 111-149.

Rivett, M. O., and S. Feenstra (2005), Dissolution of an emplaced source of DNAPL in a natural aquifer setting, *Environ. Sci. Technol*., 39, 447– 455.

Roy, J. W., J. E. Smith, & R. W. Gillham (2004), Laboratory evidence of natural remobilization of DNAPL pools due to dissolution. *J. Contam. Hydrol*., 74**,** 145-161.

Sale, T. C., and D. B. McWhorter (2001), Steady state mass transfer from single-component dense nonaqueous phase liquids in uniform flow fields, *Water Resour. Res*., 37(2), 393– 404.

Schwarzenbach, R. P., P. M. Gschwend, and D. M. Imboden (2002), *Environmental Organic Chemistry*, 2nd Ed., John Wiley & Sons, Inc., Hoboken, NJ. pp. 135-174, 277-324.

Setarge, B., J. Danzer, R. Klein, and P. Grathwohl (1999), Partitioning and interfacial tracers to characterize non-aqueous phase liquids (NAPLs) in natural aquifer material, *Phys. Chem. Earth (B),* 24(6) 501-510.

Sewell, G., S. C. Mravik, A. L. Wood, M. D. Annable, R. K. Sillan, and K. Warner (2006), Chlorinated solvent contaminated soils and groundwater: field application of the solvent extraction residual biotreatment technology, in *Bioremediation of Recalcitrant Compounds*, J. W. Talley Ed., CRC Press, Boca Raton, FL, pp. 59-136.

Sillan, R.K (1999), Field-scale evaluation of in-situ cosolvent flushing for enhanced aquifer remediation, Ph.D.Dissertation, University of Florida, Gainesville, Florida.

Sillan, R. K., M. D. Annaable, P. S. C. Rao, D. Dai, K. Hatfield, W. D. Graham, A. L. Wood, and C. G. Enfield (1998), Evaluation of in situ cosolvent flushing dynamics using a network of spatially distributed multilevel samplers, *Water Resour. Res*., 34(9), 2191–2202.

Soga, K., J. W. E. Page, and T. H. Illangasekare (2004), A review of NAPL source zone remediation efficiency and the mass flux approach, *J. Haz. Mat*., 110, 13–27.

Stroo, H. F., M. Unger, C. H. Ward, M. C. Kavanaugh, C. Vogel, A. Leeson, J. A. Marqusee, and B. P. Smith (2003), Remediating chlorinated source zones, *Environ. Sci. Technol*., 37(11), 224-230A.

U. S. Environmental Protection Agency (USEPA) (1999), Monitored natural attenuation of chlorinated solvents, Rep. EPA/600/F-98/022, Natl. Risk Manage. Res. Lab., Ada, Oklahoma.

USEPA (2003), The DNAPL remediation challenge: Is there a case for source depletion?, Rep. EPA/600/R-03/143, Natl. Risk Manage. Res. Lab., Cincinnati, Ohio.

Weidemeier, T. H., M. A. Swanson, D. E. Moutoux, J. T. Wilson, D. H. Kampbell, J. E. Hansen, and P. Hass (1996), Overview of the technical protocol for natural attenuation of chlorinated aliphatic hydrocarbons in groundwater under development for the U. S. Air Force Center for Excellence, in *Symposium on Natural Attenuation of Chlorinated Organics in Groundwater*, EPA/540/R-96/509, USEPA, Washington, DC, pp 335-359.

Wood, A. L., C. G. Enfield, F. P. Espinoza, M. D. Annable, M. C. Brooks, P. S. C. Rao, D. Sabatini, and R. Knox (2005), Design of aquifer remediation systems: (2) Estimating site-specific performance and benefits of partial source removal, *J. Contam. Hydrol*., 81, 148– 166.

Yang, Y. and P. McCarty (2000), Biologically enhanced dissolution of tetrachloroethene DNAPL, *Environ. Sci. Technol*., 34, 2979-2984.

Yang, Y. and P. McCarty (2002), Comparison between donor substrates for biologically enhanced tetrachloroethene DNAPL dissolution, *Environ. Sci. Technol*., 36, 3400-3404.

Zhang, Y., Khan, I. A., Chen, X., Spalding, R. F. (2006), Transport and degradation of ethanol in groundwater, *J. Contam. Hydrol*., 82, 183– 194.

BIOGRAPHICAL SKETCH

Gordon Hitchings Brown was born on June 19, 1969, in Rochester, NY. He was raised by two scientists and grew up in and around the Helmer Nature Center that his mother directed. After moving to Northern California in 1985, he graduated from Palo Alto Senior High School, Palo Alto, California, in 1987.

He returned to Upstate New York to play collegiate hockey at the State University of New York College at Cortland from 1987 to 1989. Not yet finding his scientific niche, he left collegiate studies to pursue a career in the sailing industry. He worked as a sailmaker and professional racing sailor from 1992-2002. He enrolled at the State University of New York College at Brockport in 1996 and received a Bachelor of Science degree in chemistry and earth science in 2003. He graduated as a departmental scholar in earth sciences, and received both analytical chemistry and sigma xi awards for excellence in undergraduate research at Brockport.

He continued his education at the University of Florida in the Department of Environmental Engineering Sciences pursuing a Master of Science degree from 2003 through 2006. Gordon was a graduate research assistant from August 2003 through August 2005. He was a National Science Foundation Science Partners In Collaborative Inquiry-based Education (SPICE) fellow from August 2005 through August 2006. He has served as an officer of the University of Florida's student chapter of the American Water Resources Association (AWRA) from 2003 to 2006, and was elected to the AWRA Florida Section Board of Directors for 2006.

In August 2006 he intends to pursue a Doctor of Philosophy in Environmental Engineering Sciences at the University of Florida.